U.PORTO

FEUP FACULDADE DE ENGENHARIA
UNIVERSIDADE DO PORTO

NUMERICAL MODELING OF EXCAVATIONS BELOW THE WATER TABLE

JOÃO BORLIDO FONTE

Dissertação submetida para satisfação parcial dos requisitos do grau de

MESTRE EM ENGENHARIA CIVIL — ESPECIALIZAÇÃO EM GEOTECNIA

Orientador: Professor Doutor António Joaquim Pereira Viana da Fonseca

Co-Orientador: Professor Doutor Marcos Arroyo Alvarez de Toledo

SETEMBRO DE 2010

MESTRADO INTEGRADO EM ENGENHARIA CIVIL 2009/2010

DEPARTAMENTO DE ENGENHARIA CIVIL

Tel. +351-22-508 1901

Fax +351-22-508 1446

✉ miec@fe.up.pt

Editado por

FACULDADE DE ENGENHARIA DA UNIVERSIDADE DO PORTO

Rua Dr. Roberto Frias

4200-465 PORTO

Portugal

Tel. +351-22-508 1400

Fax +351-22-508 1440

✉ feup@fe.up.pt

http://www.fe.up.pt

To my Parents, to my friends

ACKNOWLEDGMENTS

I would like to thank Professor Marcos Arroyo and Professor Viana da Fonseca, for providing this fabulous opportunity of making my thesis abroad, and for the orientation, patience, and experience which contributed for the achievement of the proposed objectives. This would not be possible without them.

To Professor Couto Marques, I wish to thank for always being available for me with his deep knowledge of the finite elements method.

I am grateful to all my family for their unconditional support in these five months. A special thanks to my father and mother for always advising me in the best way and for remembering me of my duties.

To all my friends and specially to the ones I met in Barcelona, I wish to express my profound gratitude for having contributed for the best times of my life. With them I shared experiences, joys and frustrations and they were always there for support and help whenever I needed, and I will never forget them.

ABSTRACT

This dissertation addresses the theme of excavations below the water table. The development of urban sites frequently requires the construction of deep excavations under retaining walls for deep basements, underground parking or tunnels. Deep excavations can carry major risks to nearby structures, equipments, and most important of all, persons. For this matter, extended studies are needed to assure that the risks are minimized, and major problems can be avoided.

When one is designing deep excavations, the main problem is often dominated by the water flow around the walls. The water flow, introduced by the excavation and consequently by the lowering of the ground water table influences the global stability of the wall and the stability of the excavation bottom where bulk heaving or boiling may occur.

There are many methods for controlling the bottom stability against seepage failure of soil, but even so failure occurs for this methods. Consequently, more profound study is needed to avoid this kind of situations.

In this work, it is being analysed the influence of seepage flows in the stability of deep excavations, and ways of achieving acceptable safety factors avoiding dangerous situations that may occur in the process. For this purpose, this thesis has the objective of defining a good 2D numeric model using the finite element program PLAXIS, as well as its complement, PLAXFLOW, which analyzes the water flow influenced by time, in terms of rising and lowering the groundwater level. From various series of numerical calculations, it is found that the failure mechanism shapes and the head loss at failure are significantly influenced by soil, interface characteristics, and very important, groundwater flow. This calculations will be then compared with other commercial software to evaluate the reliability of the achieved data.

KEYWORDS: excavations below the water table; finite-element analysis; bottom stability; heaving; boiling

RESUMO

Esta tese aborda o tema das escavações abaixo do nível da água. A construção de obras urbanas, requer, muitas vezes, a construção de escavações profundas, usando paredes de contenção para caves profundas, parques de estacionamento subterrâneo ou túneis. As escavações profundas podem trazer grandes riscos para estruturas vizinhas, para equipamentos, e o mais importante, para pessoas. Por este motivo, estudos exaustivos são necessários para assegurar que os riscos são minimizados, e para que problemas de maior possam ser evitados.

Quando alguém está a projectar uma escavação profunda, o problema principal passa muitas vezes pelo fluxo de água em volta da parede. O fluxo de água, introduzido pela escavação e consequentemente pelo rebaixamento do nível freático, influencia a estabilidade global da parede e a estabilidade do fundo da escavação, onde os fenómenos de levantamento hidráulico, ou erosão interna podem ocorrer.

Existem vários métodos para controlar a estabilidade de fundo contra a ruptura por percolação, mas mesmo assim, a ruptura acontece para estes métodos. Por consequência, estudos mais profundos são necessários para evitar este tipo de situações.

Neste trabalho, está a ser analisada a influência da percolação na estabilidade de escavações profundas e modos de se atingir factores de segurança aceitáveis, evitando situçações perigosas que possam ocorrer no processo. Deste modo, esta tese tem como objectivo a definição de um bom modelo 2D usando o programa de elementos finitos PLAXIS, bem como o seu complemento, PLAXFLOW, o qual analisa o fluxo de água influenciado pelo tempo, em termos de subida e descida do nível freático. Devido a vários cálculos numéricos, é descoberto que as formas dos mecanismos de ruptura e a perda de carga são bastante influenciados pelo solo, características de interface, e o mais importante, a percolação. Estes cálculos serão posteriormente comparados com outros programas comerciais para avaliar a fiabilidade dos dados atingidos.

PALAVRAS-CHAVE: escavações abaixo do nível freático; análise de elementos finites; ruptura de fundo; levantamento hidráulico; erosão interna

GENERAL INDEX

FIGURE INDEX

TABLE INDEX

1

INTRODUCTION

The development of urban sites frequently requires the construction of deep excavations under retaining walls for deep basements, underground parking or tunnels. Deep excavations can carry major risks to nearby structures, equipments, and most important of all, persons. Furthermore, an excavation failure occurs very quickly, giving a worker virtually no time to escape. For this matter, extended studies are needed to assure that risks are minimized so major problems can be avoided and lives can be saved.

Due to space limitations in urban areas, deep excavations are often constructed in close proximity to surrounding buildings and services. In the design of deep excavations, the design of the retaining structure and support system plays a very important role. The design of deep excavations is often dominated by the problem of the water flow around the walls. The water flow, introduced by the excavation and consequently by the lowering of the ground water table, influences the global stability of the wall and the stability of the excavation bottom where bulk heaving or boiling or piping may occur.

There are many methods for controlling the bottom stability against seepage failure of soil, but even so failure occurs, because soil is neither isotropic, nor homogeneous, and so there is a whole range of situations that cannot be predicted by models, and the only way to avoid dangerous conditions is to introduce a safety factor, which is the only way to prevent unsafe scenarios. Consequently, more profound study is needed to avoid this kind of situations.

In this work, is analysed the influence of seepage flows in the stability of deep excavations, aiming to achieve acceptable safety factors, avoiding dangerous situations that may occur in the process. For this purpose, this thesis has the objective of defining a good 2D numeric model using the finite element program PLAXIS, as well as its complement, PLAXFLOW, which is a finite element package intended for two-dimensional transient and steady state analysis of saturated and unsaturated groundwater flow problems in geotechnical engineering and hydrology. These calculations will then be compared with other commercial software to evaluate the reliability of the achieved data.

The study is primarily made for two types of soil, soft soils - or clays - and sands. These two types of soil are well known for having very different kinds of behaviour, in terms of strength, permeability and so on, so focalized study is needed in each one of them. In the analysis of the data, resultant pathologies will be described and commented to try to understand why do they happen and how can they be avoided.

Relatively to the soft soils, a comparison between two programs is going to be made. On one hand, we have a selfmade software created to evaluate the safety factor at the bottom of deep excavations in soft soils, influenced by the ratio of the depth to the width of the excavations, the thickness of the soft soil layer between the excavation base and hard stratum, the depth of the walls inserted below the excavation base, and the stiffness of the walls around the excavation. On the other hand, we have a

well known finite element commercial software, PLAXIS, which can also evaluate the safety factor of this type of excavations, and so a comparison will be made to see if the results are, indeed, the same and so, correct, and if this commercial software is a good choice when evaluating the risk of collapse in this kind of constructions, or, on the contrary, this situations are so specific, that it is better to create a new program which can correctly predict risk situations.

The sand analysis is different: it also is going to be evaluated the bottom failure of deep excavations, but in terms of the relation between the water head and the penetration depth of the sheet pile in the soil, and not by the safety factor as before. In this part, based in previous studies, where a powerful finite element software, FLAC^{-2D}, was used for better understanding of the seepage failure phenomena, a comparison will be made with PLAXIS, again to corroborate the results, and see if this software, more commercial and more interface friendly than the other, can also be used to calculate this type of bottom failures. These results are compared, not only by looking to the numerical data, but also to the final displacements, as well as the shear strength, total strength, and so on.

The third part addresses a different matter, but always inside the topic of seepage in excavations. This time, there's an old article, in which physical models were constructed to determine the type of failure occurring in strutted sheeted excavations in non-cohesive soils due to seepage water. An analysis is going to be made, to see if modern technologies, as finite element software, can be a reliable option for reproducing real excavations in these specific conditions. In summary, two already made investigations, one where a real scaled physical model was used with observations made with microscope, but by naked eye, and other using a commercial FEM software, FLAC^{-2D}, are going to be compared to see if, effectively, their results are consistent, and can be trusted.

Finally, the last part of this work comes in the sequence of the third part, where investigations in previous works were made to compare the non-homogeneous grounds with the correspondent homogeneous situation, but also using a simulated scaled physical model to analyze these conditions. This excavation is made under water and the water is subsequently pumped out from inside the cofferdam. Therefore, the objective of this part, is, once again, to try to reproduce the real conditions in a FEM software, PLAXIS, to see if, firstly, it can be done, and secondly, if the results are the same, and so if they can be corroborated.

2

STATE OF THE ART

Deep excavations under retaining walls are profoundly connected to urban sites, whether it is for basements construction, underground parking, or tunnels. Excavations construction, and corresponding walls and retaining situations, as all geotechnical construction in general,requires a lot of empiric knowledge, only possible to obtain through hard investigation and data analysis.

One of the main problems in this type of excavation is the water flow around the walls, which may cause instability problems, and consequently dangerous situations and, therefore, deep studies are needed to carry out excavations as safe as possible. These excavations are often near buildings, and sensitive zones, which implies that their design should be careful and well planned in order to make sure that no dangerous situations occur while and after excavations are made.

This work bases itself in a specific type of deep excavation failure known as bottom failure. This type of failure often occurs because of the water seepage from the highest water level to the lowest where the excavation bottom lies. This is a very complex issue, since the type of soils and soil parameters are never the same. The excavation phases are rather diverse, and also the wall stiffness and interface are variable.

With the objective of trying to prevent the problem of the bottom stability in deep excavations, several authors carried out studies for understanding how this type of failure works, of what it depends, and how can it be overcome. These studies involved different kinds of excavations, regarding the type of soil, soft soil or sand, homogeneous or not, dry excavation or submerged.

This research work has analysed those different kinds of situations and tries to establish a connection between them, evaluating if the results are effectively accurate and if they can safely be used in real excavations.

2.1. FAILURE MECHANISMS OF HYDRAULIC HEAVE AT EXCAVATIONS

Nowadays, building foundations are becoming deeper, and so the stability analysis of the bottom of the excavation is a very important issue. The uncertainty of extreme precipitation and expected rainfall leads simultaneously to an increasing importance of the limit states on dam and dike structures. When studying the influence of a hydraulic impact on a structure one has to be sure, that the applied limit state is relevant to the construction condition. In this part of the work, different types of failure mechanisms at the bottom of excavations are going to be explained.

2.1.1. HYDRAULIC HEAVE

When the local impact represented by the seepage pressure exceeds the available resistance, that is the dead load of the considered soil body, hydraulic heave occurs, as it may be seen in Fig. 1. If particle motion within the soil is possible the limit state in non cohesive soil is equal to the loss of the effective confinement ($\sigma' = 0$). Failure occurs as a sudden raising of the soil surface. The local seepage pressure has to be determinate using a flow net relevant for the building situation and under validity of Darcy's law applying Laplace's equation (Knaupe 1979). Safety against hydraulic heave is influenced by soil specific properties, the existing geological stratification and the type and extent of the structure.

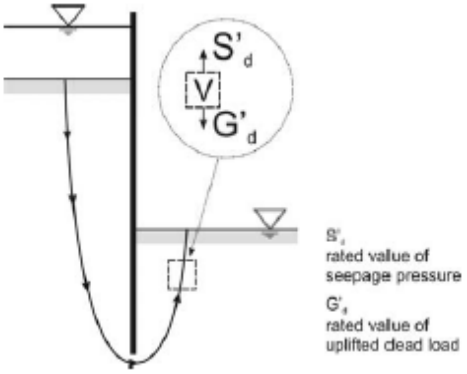

Fig. 1 - Schematic illustration of hydraulic heave on a building pit wall (Wudtke 2008)

2.1.2. PIPING

Piping is initiated by a flow causing particle transport on the free unloaded downstream soil surface (2), according to EAU (2004). This concept describes the failure as regressive particle erosion along the path of the maximum velocity or hydraulic gradient. Due to the proceeding reduction of the distance between upstream and downstream seepage pressure and the involved local increase of the hydraulic surface gradient the procedure features an incremental accelerated destruction of the soil continuum. Once the flow channel reaches the upstream soil surface the final failure of the construction occurs by extensive liquefaction of the soil.

During hydraulic uplift a continuous structure or soil layer with a low permeability compared to the surrounding soil loose its stability by a hydrostatic impact.

Every type of failure mentioned above lose their stability by water. The difference lies on the place of failure initiation, the course of failure and failure kinematics. Shear resistance or deformation energy are not considered by the limit states. Thus especially in cohesive soil an additional safety margin exists. In detail hydraulic heave and hydraulic uplift can be varied in the considered soil volume and the type of hydraulic impact. The limit state of hydraulic heave is characterised by a loss of effective stress inside the soil. Hydraulic uplift considers the limit state in the contact plane between soil and a massive structure or between permeable and much less permeable soil layers. Piping and hydraulic heave are induced by seepage pressure, however limit states are defined on different locations.

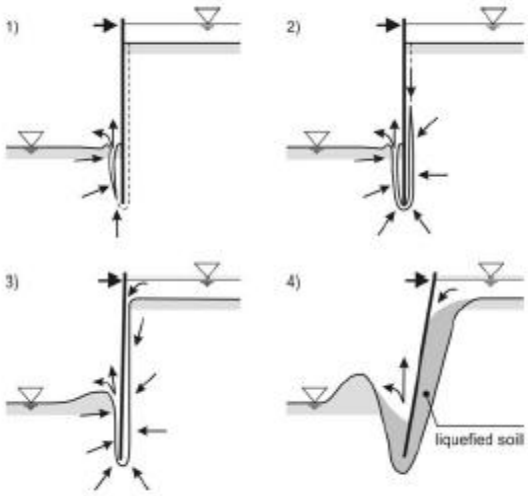

Fig. 2 - Piping on a sheet pile wall: 1) initiation and first deterioration, 2) regressive erosion, 3) formation of flow channel, 4) liquefaction and collapse according to EAU (2004) (Wudtke 2008)

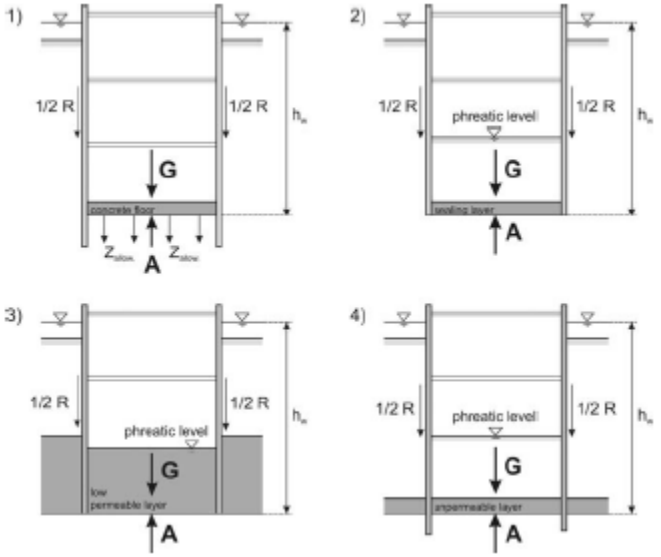

Fig. 3 - Different situations concerning hydrostatic uplift: 1) concrete floor, 2) deep sealing floor, 3) embedding in low permeable layer, 4) almost impermeable layer below bottom of excavation according to EAB 2006 (Wutke 2008)

2.1.3. HYDRAULIC HEAVE IN DESIGN PRACTICE

Stability against hydraulic heave is relevant for various building applications. The limit state is influenced by basic factors like geometrical constrains and the geological as well as hydrological periphery. In detail those are:

- Subsoil stratigraphy, permeability of soil layers;
- Flow net caused by structure, maximum hydraulic gradient, i_{max};
- Properties of flow impacted soil, weight and shear strength;
- Soil sensitivity against particle transport mechanisms, change of permeability.

2.2. BASE STABILITY IN EXCAVATIONS IN SOFT SOILS

Big excavations with large scale and depth are being used more often for underground space developments. For this purpose, safety factor analysis for base instability is needed for the design of excavations in soft soils. There are some methods proposed by Faheem (2003) to evaluate the safety factors. The undrained situation usually rules the stability of an excavation immediately after construction, and therefore a total stress analysis is considered necessary. Many limit equilibrium analysis methods are available to evaluate the base stability of excavations, and these safety factors vary with different methods. Until now, the safety factor of excavations has usually been obtained by the methods proposed by Terzaghi (1943) or Bjerrum and Eide (1956). However, Terzaghi (1943)'s method can only be used for shallow or wide excavation with $\frac{H}{B} \leq 1.0$, where *B* and *H* are the width and the depth of the excavation, respectively, as shown in Fig. 4. On the other hand, for Bjerrum and Eide (1956)'s method, modifications to the N_c values are needed when a hard stratum is present near the excavation base, for the reason that the failure will not extend fully across the base of the excavation, and a deep foundation rupture is no longer reasonable.

These two methods were created, when the stiffer retaining wall systems, such as diaphragm walls and secant piles, were not yet available. Therefore, the safety factors given by these methods do not consider the stiffness (*EI*) of the wall, which has significant influence on the base stability in soft soils. Furthermore, the depth of the wall penetration below the excavation base, *D*, is not considered as well.

In this work, to evaluate the 2D base stability of excavations, the finite element method with reduced shear strength is used, which is going to be explained next. The safety factor depends on the *H/B* ratio, the clay thickness under the base of the excavation (*T*), the wall stiffness (*EI*), the embedded depth of the wall (*D*), and, consequently, the net distance between the end of the wall and the hard stratum (*Tn)*. The consequences of strain softening and anisotropy have not been considered in the finite element method as well as in the limit equilibrium method.

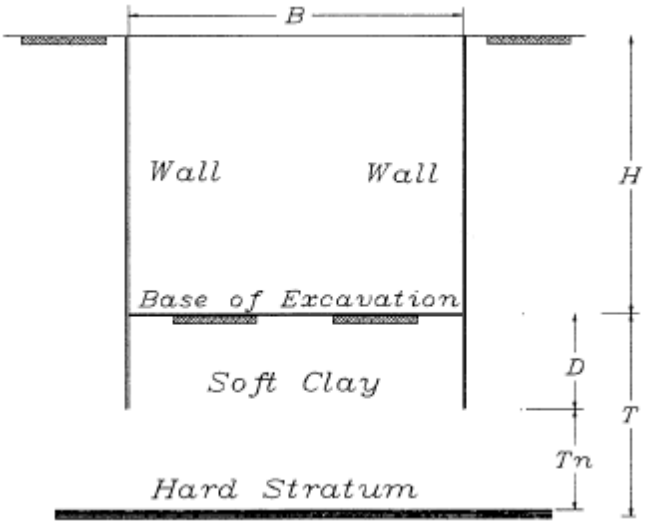

Fig. 4. Geometry of braced excavation

2.2.1. FEM WITH REDUCED SHEAR STRENGTH

The reduced shear strength parameters c'_f and ϕ'_f will replace the corresponding c' and ϕ' in the shear strength equation $\tau_f = c' + \sigma' tan\phi'$ with $c'_F = c'/F$ and $\phi'_F = tan^{-1}(\frac{\tan(\phi')}{F})$. Therefore, the equation with reduced shear strength can be written as $\tau_{fF} = c'_F + \sigma' tan\phi'_F$.

The initial value of *F* is assumed to be sufficiently small so as to produce a nearly elastic problem. Then the value of *F* is increased step by step until finally a global rupture occurs. This method is called the shear strength reduction FEM (SSRFEM). The numerical comparisons have shown that the SSRFEM is a reliable and robust method for obtaining the safety factor for the slope and the corresponding critical slip surface.

In Faheem's work, a 2D finite element program is used for the present analysis, where the return-mapping algorithm was used for stress integration, and the secant Newton method was used to accelerate the convergence of the modified Newton-Raphson scheme. The isoparametric elements with eight nodes are used to model the soil and wall elements. To obtain the precise results it is found that at least six rows of elements must be put below the bottom of the wall, where the soil failure should take place. The reduced integration is used to avoid the numerical difficulties, known widely as 'locking', arisen with modelling incompressible soft soils. The lower order techniques with reduced integration have been used with success in a wide range of geotechnical collapse problems including slope stability and earth pressures. The soil is modelled as linear elastic-perfectly plastic with the Mohr–Coulomb yield surface and the wall is assumed to behave linear elastically. The excavated depth (*H*) of all analysed excavations is 9 m, and the other geometrical parameters are changed case by case. The shear strength of the thin interface element was given as 0.01, 0.1, 0.5 times the shear strength of the clay and the obtained results were almost the same. The shear strength of the clay wall interface was found to have small influence on the base stability, and this is going to be tested.

The mechanical properties of the soft clay are shown in Table 1.

Table 1 – Mechanical properties of the soft clay

Parameters	Value
Undrained shear strength, s_u (kPa)	35.0
Young's modulus, E_u (kPa)	$E_U = 250\ s_u$
Poisson's ratio, ν	0.49
Unit weight, γ (kN/m^3)	20.0

In Faheem (2003)'s article, the base instability is indicated using the normalized maximum rebounding displacement on the excavation base, Δ, which is given by

$$\Delta = \frac{\delta_{max} E_u}{s_u (H+T)} \quad (2.1)$$

Where δ_{max} is the maximum nodal displacement at the base of the excavation. The location of the point is not fixed, but it depends on the geometry of the excavation. The maximum nodal displacement can be found at the middle of excavation if $T \geq T_c$, else it is located near the wall. T_c is called the critical depth and equal to B/$\sqrt{2}$. The normalized displacement Δ grows with the factor reduction of the shear

strength *F*, and dramatically increases when *F* approaches the safety factor of the excavation's base, as indicated in Fig. 5. On the other hand, for larger *H/B* ratios, or in case of increasing embedded wall depth with a few exceptions, the nodal curve did not indicate a well-defined asymptotic failure value, because the mesh was not sufficiently refined.

2.2.2. NUMERICAL MODELLING PROCEDURE

In the numerical model used in this study, the horizontal distance from the wall to the outer boundary of the excavation should not be less than at least 2H. The vertical distance in the mesh under the base of excavation must be refined as possible, which depends on the thickness of the clay under the base of excavation; for example, the vertical distance is 0.25 m, in case of T = 3.0 m, and 0.5 m in the case of T = 4.5 m.

2.2.3. EFFECT OF *H/B* (D = 0, $T \geq T_c$)

The values obtained of the FEM with reduced shear strength show that the location of hard stratum has influence on the N_c-value, when the thickness of the soft soil layer below the excavation base is less than the critical depth, $T \leq T_c = B/\sqrt{2}$. When $T \geq T_c$, and D = 0, the influence of *H/B* in the base stability is indicated in Fig. 6, where N_c is given by

$$N_c = Fs\gamma H/s_u \qquad (2.2)$$

where *Fs* is the safety factor of excavation base. The value of *Fs* can be obtained in the next figure, and when it is substituted in the previous equation, *Nc* can be obtained. *Nc* is a dimensionless coefficient depending on the geometry of the excavation.

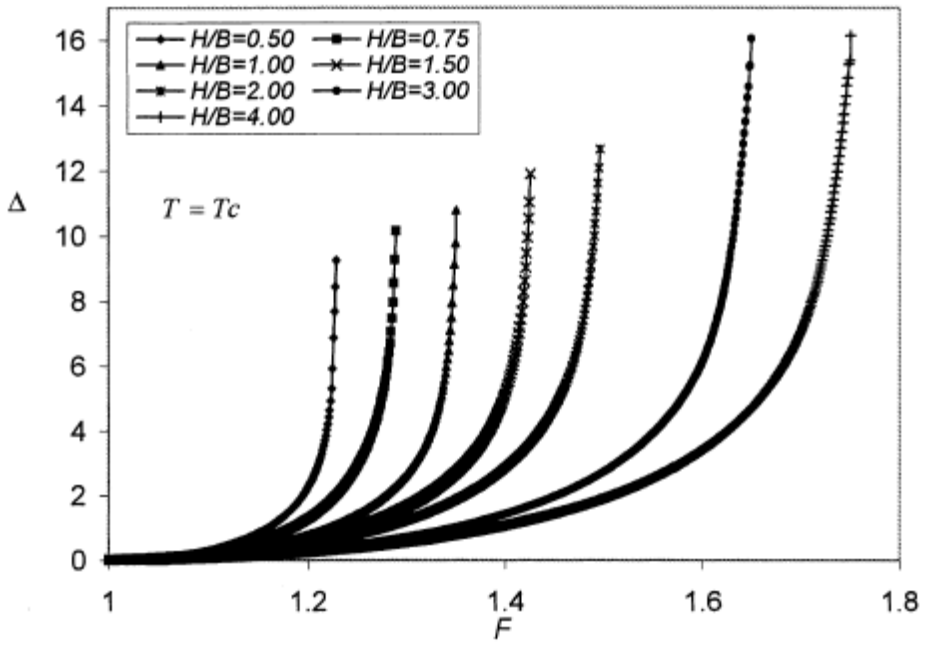

Fig. 5 - Normalized displacement versus shear strength reduction factor, F (D = 0.0) (Faheem, 2003)

The next figure indicates various types of Nc predictions from different types of approaches, as the FEM results of Faheem (Faheem,2003), and models considered by Terzaghi (1943) , Eq. (1), and

Prandtl, Eq. (2). From Fig. 6 it can be seen that the Nc-value, obtained using the FEM with reduced shear strength, is close to Eq. (1) for the shallow or wide excavation with $H/B \leq 1.0$. On the other hand, when $H/B > 1.0$, the Nc-value increases with the ratio of H/B is higher than Bjerrum & Eide's method. The failure mechanism by the FEM can be indicated using nodal displacement vectors induced by the shear strength reduction, just before the failure takes place. The failure mechanism of H/B = 1.0 with T = Tc is shown in Fig. 6 with D = 0.0.

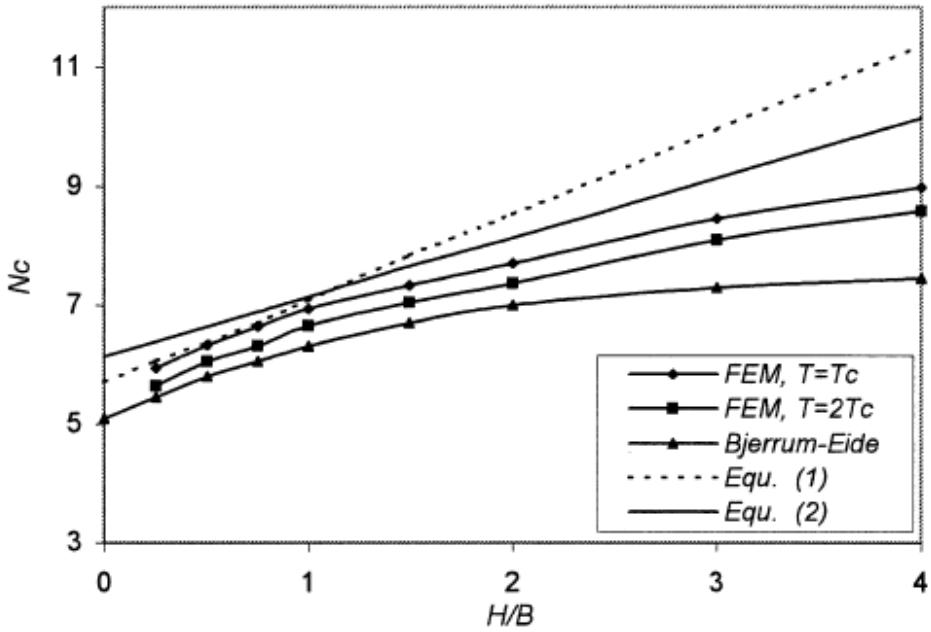

Fig. 6 - Effect of H=B on Nc-value (D=0 and T=Tc) (Faheem, 2003)

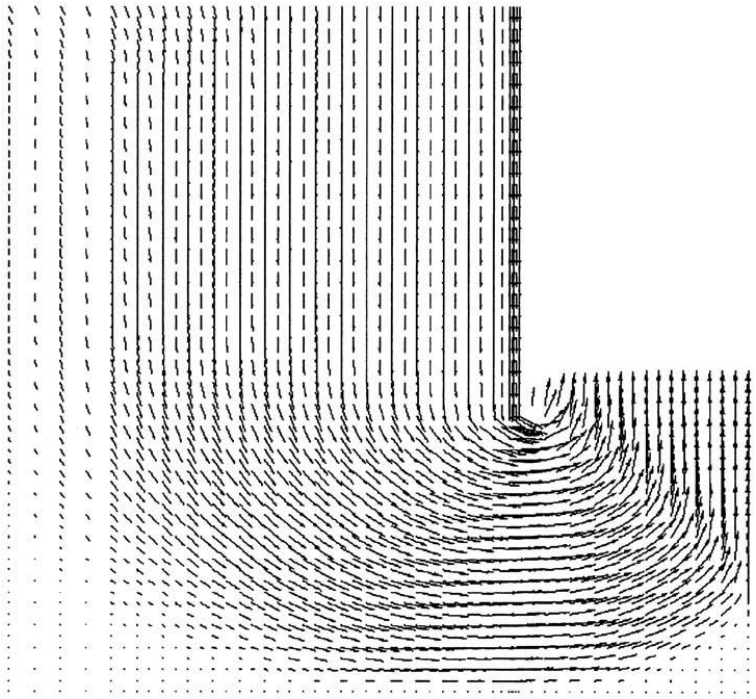

Fig. 7 - Nodal displacement vectors for H/B = 1.0, D = 0.0; and T = Tc (Faheem, 2003)

2.3. NUMERICAL STUDIES OF SEEPAGE FAILURE IN SANDS

The design of deep excavations is frequently dominated by the water flow around the walls. The seepage flow given rise by lowering of the groundwater table inside the excavation influences the global stability of the wall and the stability of the excavation bottom where bulk heaving or boiling or piping may occur.

There are many published methods for the assessment of bottom stability against seepage failure of soil. However, the catastrophic rupture still occurs even in deep excavation designed by these methods. Consequently, more precise analysis is required to better understand the failure mechanisms.

2.3.1. ELEMENTAR HYPOTHESIS TOWARDS NEW ANALYSIS APPROACHES

The influence of seepage flow on the stability of retaining excavations was first investigated by Terzaghi (1943). From model tests he has discovered that within an excavation, the zone of danger of bottom heave is confined to a soil prism adjacent to the wall. He assumed, from experimental evidence, that the body of sand, which is lifted by water, has the shape of a prism with a width equal to the half of the wall penetration *D/2* and the horizontal base at some depth D_0 below the surface ($0 \leq D_0 \leq D$). It is assumed that at the instant of failure, the effective horizontal stresses on the prism vertical sides and the corresponding frictional resistance are zero.

Consequently, the prism rises up and collapses as soon as the total value of water pressure U_e on the bottom of the prism *IJ* becomes equal to the submerged weight of the prism *W'*.

The safety factor against bulk heave is obtained by the ratio of the submerged weight of the prism to the excess water force on the prism base:

$$F_s = W'/U_e = i_c/i_m \quad (2.3)$$

where i_m is the average hydraulic gradient between IJ and EF.

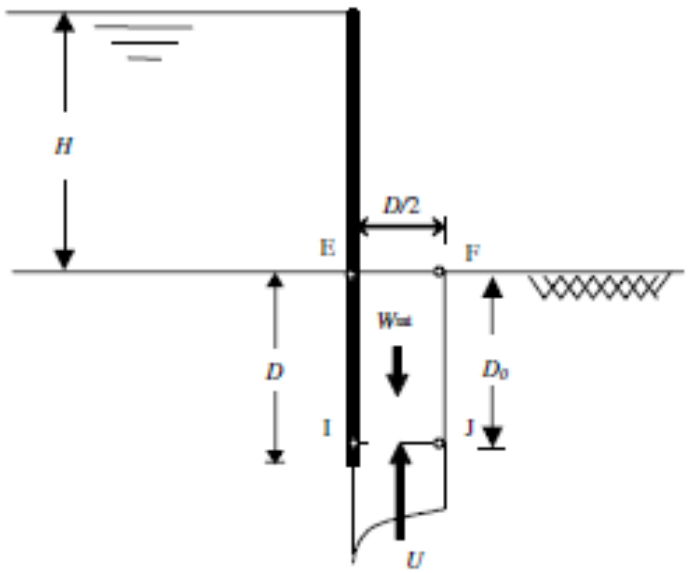

Fig. 8 – Failure by heaving (Benmebarek et al., 2005)

McNamee (1949) identified two main types of failure:

- Local failure as “piping” or “boiling” is most likely to begin at a point on the surface adjacent to the sheet pile as it lies within the shortest seepage path.
- General upheaval “heaving”, which involves a greater volume of soil.

Piping or boiling occurs when a small prism of soil at the excavation level is not sufficiently heavy to resist uplift forces due to upward flow. Terzaghi (1943) defined the concept of critical hydraulic gradient (or flotation gradient) i_c that controls the phenomenon of piping or boiling.

McNamee defined the safety factor against boiling as the ratio of the critical gradient to the exit gradient i_e at the excavation level, hence

$$F = i_c/i_e \quad (2.4)$$

This author presented charts enabling the determination of the corresponding safety factor for a range of dimensions of the excavation.

Marsland (1953) carried out extensive model tests using both dense and loose homogeneous sand in an open water excavation. He has concluded that in loose sand, rupture occurs when the pressure at the sheet pile tip is enough to lift the column of submerged sand near the wall of the cofferdam. In dense sand, failure occurs when the exit gradient at the excavation surface reaches a critical value.

By examining the equilibrium conditions with respect to excess pore pressures, Davidenkoff (1954) showed that bulk heave of a rectangular prism is possible only if the shear forces at vertical faces are neglected and its width is smaller than noted by Terzaghi (1943). He has concluded that the prism rises up as soon as the mean gradient calculated over the embedment length of the wall becomes equal to the critical gradient and the failure prism begins from the wall toe for homogeneous soils.

Soubra et al. (1999), published results of the passive earth pressure coefficients in the presence of hydraulic gradients using the variation approach applied to the limit equilibrium method. Their results (Fig. 9) showed a quasi linear decrease in the passive earth pressure K_p for the hydraulic head loss (*H/D*) values, varying from 0 to 2.5, for the case of a single sheet pile wall driven into a homogeneous and isotropic semi infinite soil medium. The passive earth pressures are sensitive to the soil-structure, has no effect on the *H/D* against seepage failure by heaving equal to 2.82, while the boiling phenomenon, which appears for a critical hydraulic gradient at point *E* (Fig. 8), occurs with a theoretical value of the hydraulic head loss equal to $H/D = 3.14 = \pi$. From these overviews, it appears that seepage failure at the excavation bottom can arise from different failure mechanisms.

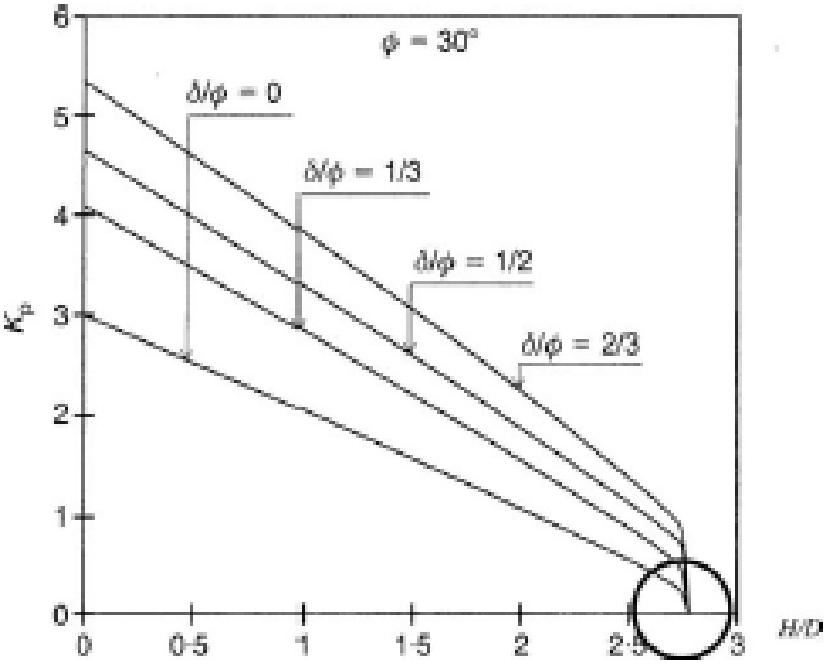

Fig. 9 - Kp versus H/D for ϕ = 30º and δ/ϕ = 0,1/3,1/2 and 2/3 in the case of a homogeneous isotropic semi-infinite medium (Soubra et al. (1999))

2.3.2. BENMEBAREK ET AL'S NUMERICAL MODELLING OF BOTTOM STABILLITY

Benmebarek et al. (2005) deal with the numerical study of bottom stability against seepage failure of sand within a cofferdam. A sheet pile with penetration depth equal to *D* in homogeneous isotropic semi-infinite soil, which is subjected to hydraulic head *H*, is considered as shown in Fig. 10.

This problem involves many parameters: excavation or cofferdam width, penetration of retaining wall in the soil, thickness of permeable soil, wall flexibility, strut rigidity, wall translation and rotation, etc.

The objective of the paper was not to consider the influence of all these parameters but to check if a numerical analysis using the finite difference or the finite element approach could describe correctly the various failure mechanisms observed due to upward seepage flow into a cofferdam. Consequently, the problem had been simplified by referring to some model test observations of failures and to the classical approaches where the action of the wall on the soil was not directly considered, but the wall has been considered as fixed.

An infinite rigid wall fixed by struts was considered in that study. This was a simplification of the real problem where the wall flexibility leads to a limited partial support of the soil on the wall embedment. This allowed showing the presence of the supposed fixed wall effect on the failure mechanisms as well as the comparison of the results with the classical approaches where the wall is taken into account from the hydraulic point of view only.

The analysis was carried out using the computer code FLAC^{-2D} (Fast Langrangian Analysis of Continua) which is a commercially available finite difference explicit program.

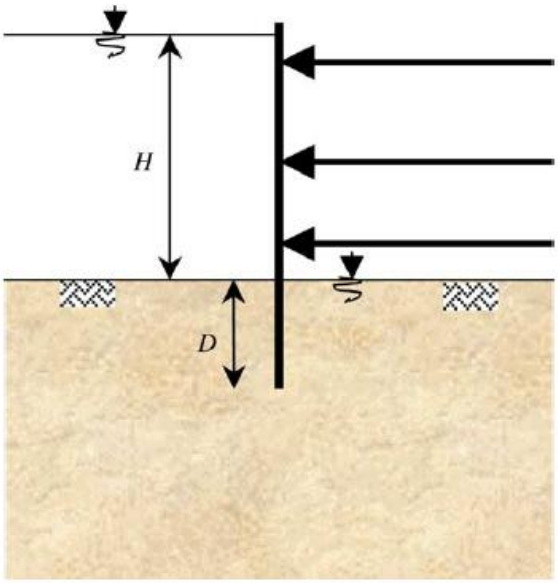

Fig. 10 – Case study (Benmebarek et al., 2005)

In this article the soil behaviour was modelled by the elastic-perfectly plastic nonassociative Mohr-Coulomb model encoded in the FLAC^{-2D} code. All results were given for $\gamma_{sat}/\gamma_w = 2$, elastic bulk modulus K = 30 MPa and shear strength modulus G = 11.25 MPa. Four values of internal friction angle were considered ϕ = 20º, 30º, 35º, 40º, four values of the friction angle at the soil/wall interface δ/ϕ = 0, 1/3, 2/3, 1, and three values of the dilation angle ψ/ϕ = 0, 1/2, 1 are considered in the analysis.

In the case of a rough wall, modelling the interface between the soil and the wall is an integral part of the analysis. The material properties, particularly stiffness assigned to an interface, depend on the way in which the interface is used. In the case of soil-structure interaction, the interface is considered stiff compared to the surrounding soil, but it can slip and may be open in response to the loading. Joints with zero thickness are more suitable for simulating frictional behaviour at the interface between the wall and the soil.

In this paper the interface has a friction angle δ, a cohesion c' = 0 kPa, a normal stiffness $K_n = 10^9$ Pa/m. These values of K_n and K_s, interface shear stiffness, are selected to approximate the results for the case where the wall is rigidly attached to the grid. The results showed the difficulty in capturing the failure mechanisms for coarse meshes and prove the requirement of refined mesh to capture it clearly. As an illustration, Fig. 11 shows the failure mechanism presented by the displacement fields and the corresponding distribution of maximum shear strain rates at steady state plastic flow for course mesh 40 × 20 (horizontal by vertical) and fine mesh 80 × 40 elements.

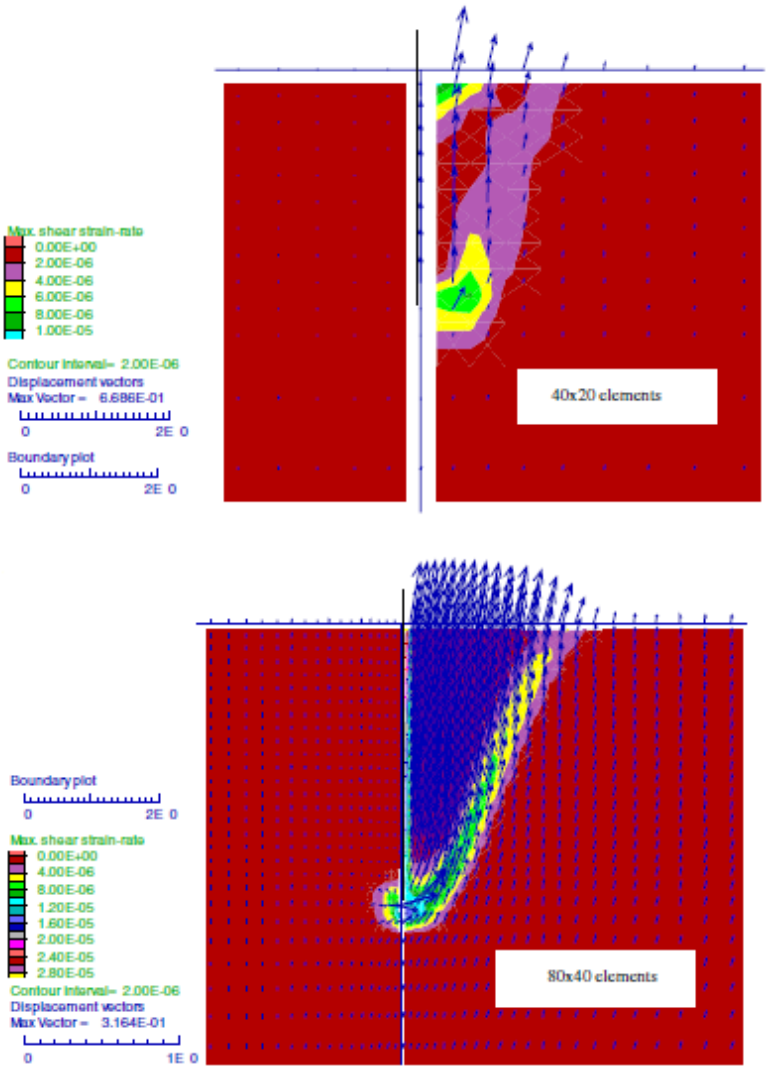

Fig. 11 - Capture failure mechanisms when ϕ = 35º, δ/ϕ = 2/3, ψ/ϕ = 1/2, H/D = 3.00 for: (a) coarse mesh 40 x 20; (b) fine mesh 80 x 40 (Benmebarek et al., 2005)

Results also confirm that variation in practical range of the elastic soil parameters and earth pressure coefficient at rest K_0 do not have any significant influence on the critical hydraulic pressure loss, as the numerical estimation of the bearing foundation capacity factor N_γ. In this analysis, the mesh size is fine near the wall where deformations and flow gradients are concentrated, as it can be seen in Fig. 12. In order to minimize boundary effects, the length from the wall and the depth of the mesh are respectively located at six and five times the wall penetration. The bottom boundary was considered fixed; the right and left lateral boundaries are fixed in the horizontal directions. The sheet piles wall is modelled by structural beam elements connected to the soil grid via interface elements attached on both sides of the beam elements, and the wall acts as an impermeable member.

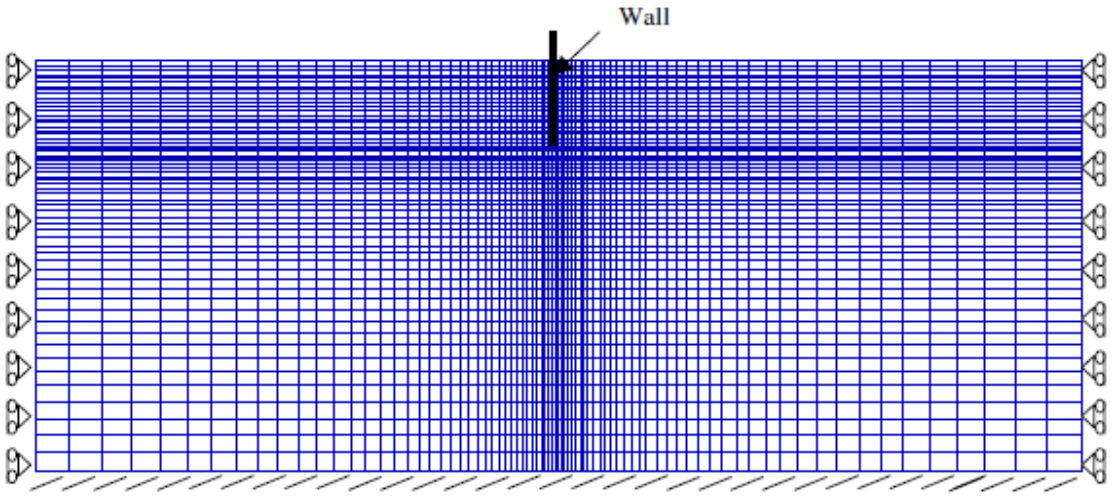

Fig. 12 - Mesh used and boundary conditions (Benmebarek et al., 2005)

To identify the limiting cases corresponding to zero passive earth pressures and seepage failure by heaving or boiling, the following three procedures were adopted:

- The material is assumed to be elastic. The initial pore pressure and effective stresses are established using the fish library function assuming that the ratio of effective horizontal stress to effective vertical stress at rest is taken 0.5, or in other words $K_0 = 0.5$. The groundwater level is assumed to be located at the ground surface.
- The field describing the distribution of the pore water pressure due to a hydraulic head loss H is calculated under hydraulic limit conditions shown in Fig. 13.
- The mechanical response is investigated for the pore pressure distribution established in the previous step.

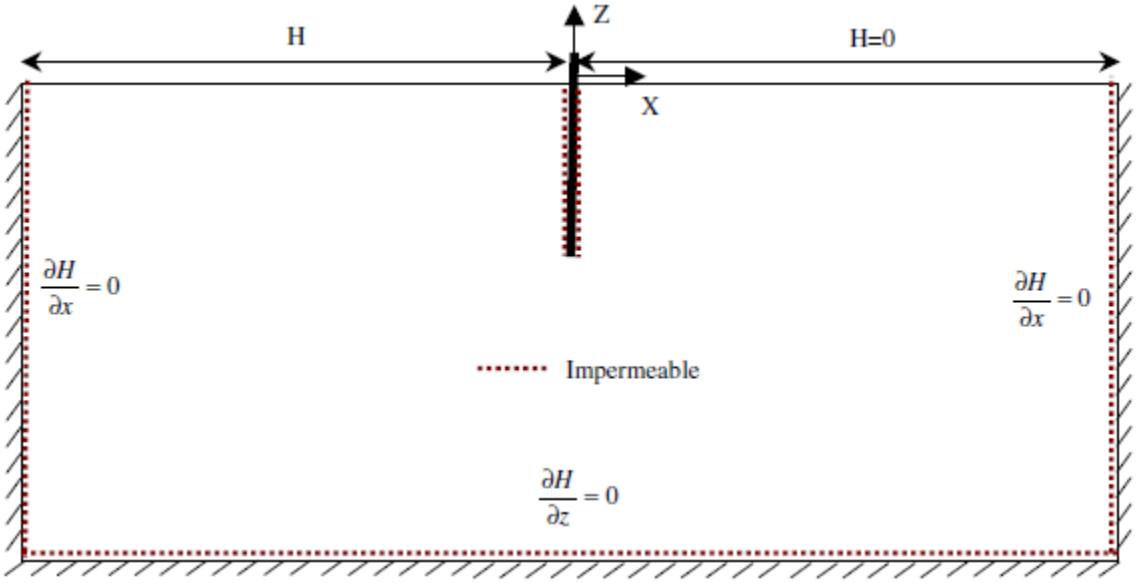

Fig. 13 - Hydraulic boundary conditions

2.3.3. RESULTS AND DISCUSSION

In this paper numerical studies were performed for different soil friction angles and the results presented in Table 2 for ϕ = 20º, 25, 30º, 35º and 40º. Results for failure by heaving are denoted by one asterisk or two and failure by boiling by three. The results indicate that the bottom stability against seepage failure always correspond to a bulk heave except in the case of a dense sand $\phi \geq 40^0$, a dilating material $\psi/\phi > 1/2$ and a rough wall $\delta/\phi \geq 2/3$ where boiling would occur. It can be seen that boiling starts from a hydraulic pressure loss of *H/D* = 3.16. This value is very close to the theoretical critical head loss value *H/D* = 3.14. In this case, the exit hydraulic gradient attains the critical hydraulic gradient value. For ψ/ϕ = 0, a rectangular soil prism similar to that proposed by Terzaghi (1943) is observed. Fig. 14 shows the failure mechanism in the case of ϕ = 35º, ψ/ϕ = 0, δ/ϕ = 2/3, and *H/D* = 3 where bulk heave of a rectangular soil prism with a width smaller than that ofTerzaghi (1943)'s method is observed. On the other hand, for dilating material$\psi/\phi \geq 1/2$, a triangular soil prism is obtained and as an example, Fig. 15 shows the case of ϕ = 35º, ψ/ϕ = 1/2, δ/ϕ = 2/3, *H/D* = 3 where bulk heave of a triangle soil prism is observed. This simulation has shown that the soil dilation angle has a significant influence on the failure mechanism shape.

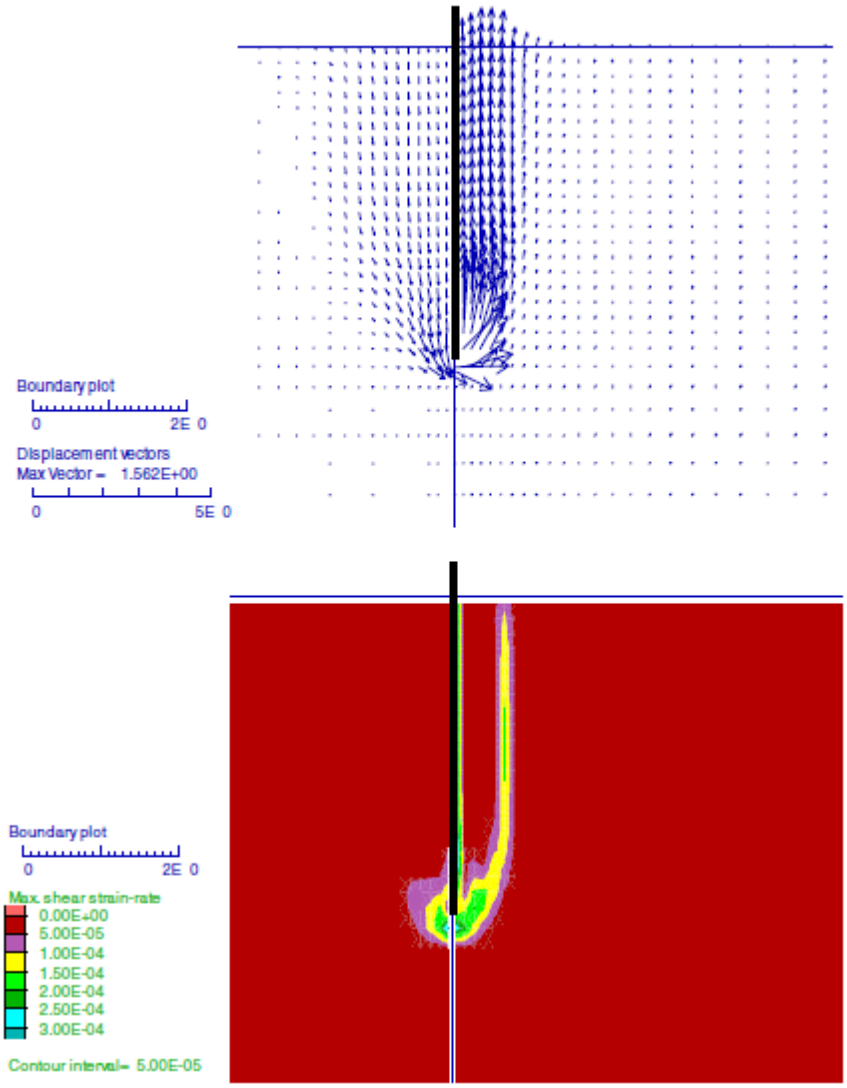

Fig. 14 - Displacement field and the corresponding distribution of maximum shear strain rates when ϕ = 35º, δ/ϕ = 2/3, ψ/ϕ = 0, H/D = 3 (Benmebarek et al., 2005)

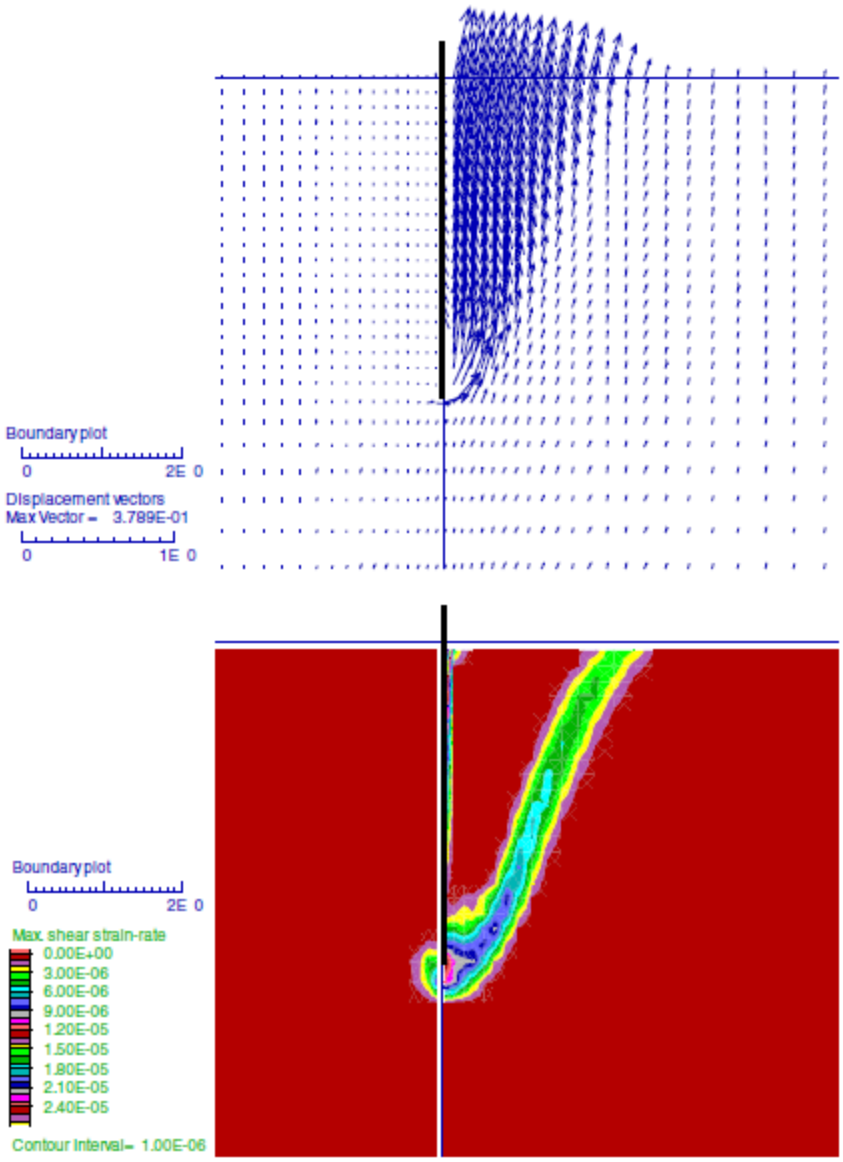

Fig. 15 - Displacement field and the corresponding distribution of maximum shear strain rates when ϕ = 35º, δ/ϕ = 2/3, ψ/ϕ = 1/2, H/D = 3 (Benmebarek et al., 2005)

From Table 2, for $\delta/\phi = 0$, $\psi/\phi = 1$ and ϕ vsrying from 20º to 40º, the critical value of *H/D* lies in the range of 2.64 – 2.93. It was noted that for various values of ϕ Terzaghi (1943)'s solution is *H/D* = 2.82 whereas the Soubra et al. (1999)'s solution gives rise to *H/D* = 2.78. These results show that the critical hydraulic pressure loss *H/D*, corresponding to the zero effective passive pressures, depends on the soil friction angle and the soil/wall interface friction.

Table 2 – Critical hiydrulical head loss *H*/*D* for various governing parameters ϕ, ψ/ϕ and δ/ϕ

δ/ϕ	ψ/ϕ	*H*/*D* limit				
		$\phi = 20^0$	$\phi = 25^0$	$\phi = 30^0$	$\phi = 35^0$	$\phi = 40^0$
0	0	2.63*	2.68*	2.74*	2.77*	2.8*
	1/2	2.64**	2.70**	2.79**	2.82**	2.90**
	1	2.64**	2.71**	2.82**	2.84**	2.93**
1/3	0	2.67*	2.78*	2.84*	2.90*	2.93*
	1/2	2.73**	2.83**	2.92**	2.97**	3.12**
	1	2.73**	2.84**	2.93**	3.04***	3.16***
2/3	0	2.72*	2.81*	2.90*	2.92*	2.97*
	1/2	2.73**	2.83**	2.92**	2.97**	3.12**
	1	2.73**	2.84**	2.93**	3.04***	3.16***
1	0	2.73*	2.84*	2.90*	2.93*	2.99*
	1/2	2.73**	2.87**	2.94**	3.03**	3.13**
	1	2.73**	2.90**	2.98**	3.05***	3.16***

Failure by bulk heave of rectangular (*) or triangular (**) soil prisms, or by boiling (***)

This behaviour was explained as follows: when the soil adjacent to the wall expands by dilation at failure, the shear forces induced on the vertical faces of the prism block the rising of the rectangular prism. Therefore, a triangular failure prism appears instead. For higher values of φ and ψ, shear forces on the wall embedment and horizontal soil expansion by dilation, delay the triangular prism failure. Therefore, the surface exit gradient becomes critical before the bulk heave of the triangular prism and initiates the boiling. This case may also occur for a flexible wall partially supported by the soil.

2.3.4. CONCLUSIONS

In Benmebarek et al. (2005)'s article it was concluded that although there are several methods to assess the risk of seepage failure at the excavation bottom of a braced cofferdam by heaving or boiling, sometimes this methods lead to great differences on the hydraulic head loss inducing failure and, for that matter, more precise analysis was completed to clarify the real cause of the failure. The results of these simulations showed the following:

- The critical hydraulic loss *H/D* against failure by seepage flow depends on the soil friction angle and the interface soil/wall friction.

- Piping and boiling appears only for dense and dilatant sand in which ϕ = 35º, $\psi/\phi > 2/3$ and a rough wall $\psi/\phi \geq 2/3$. In this case the exit gradient becomes equal to the critical hydraulic gradient, whereas heaving occurs for the other cases.
- The soil dilation angle has a significant influence on the failure mechanism shape. For a dilating material, a triangular prism failure by heaving is obtained, whereas a rectangular prism for other cases.
- The rectangular prism obtained has a smaller width than the one obtained in Terzagui's method.

Finally, the obtained results in this paper validate the simulation procedure using FLAC^{-2D} code to estimate the risk of failure due to seepage flow. Such approaches can thus be used to estimate the risk of failure for more complex works rather than the example presented in this study, such as layered soils and deep excavations strongly penetrating underneath the ground water table.

2.4. STRENGTH AND DILATANCY OF SANDS

Bolton (1986), collected extensive data about the strength and dilatancy of 17 different sands in axisymmetric or plane strain at different densities and confining or pressures. In this article it was said that the critical state angle of shearing resistance of soil, which is shearing at constant volume, is mainly a function of mineralogy, being usually 33º for quartz and 40º for feldspar. The extra angle of shearing of 'dense' soil is related to its rate of dilatation and hence to its relative density and mean effective stress, which can be combined in a specific relative dilatancy index.

The objectives of the paper were, primarily, to clarify the concepts of friction and dilatancy in relation to the selection of strength parameters for design; secondly, to introduce a relative dilatancy index and demonstrating its use in relation to the available published data; and thirdly to consider the implications of the new correlations to the procedures of laboratory and field testing.

2.4.1. RELATION BETWEEN THE ANGLE OF SHEARING RESISTANCE, Φ', AND THE DILATION ANGLE, Ψ

The stress-dilatancy theory of Rowe proved to be a good explanation, of the relation between ϕ and ψ. Suppose that the critical friction angle, ϕ'_{crit} is the angle of shearing observed in a simple shear test on loose soil that is to be in a critical state, with no dilation. Now suppose, following Fig. 16, that the same soil is tested dense, so that overriding in points of contact must, occur unless the particles crush, and that the particles above the overall zero-extension line ZZ form one rigid zone sliding upwards at ψ over the rigid zone beneath, in accordance with the external observation of a dilatancy angle ψ. Assume that the angle of shearing resistance developed on the inclined microfacets SS, on which there is no dilation, remains at ϕ'_{crit}. Since all the sliding now occurs on surfaces parallel to SS it is allowable to view the observed angle of shearing ϕ' on the rupture surface as comprising the two components ϕ'_{crit} and ψ as shown in Fig.16. In these conditions,

$$\phi' = \phi'_{crit} + \psi \quad (2.5)$$

which is an elementary friction-dilatancy relation where no attempt has been made either to optimize the failure mechanism or to correlate the directions.

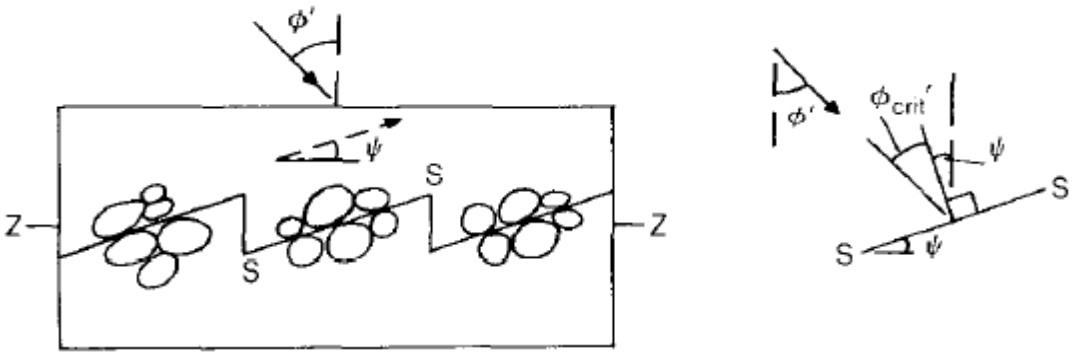

Fig. 16 - The saw blades model of dilatancy (Bolton, 1986)

By means of comparison, it was observed that the previous equation overestimates φ by 20%, so a more suited equation could be expressed. Rowe's stress dilatancy relationship for plane shear, over the range of ψ is operationally indistinguishable from

$$\phi' = \phi'_{crit} + 0.8\psi \quad (2.6)$$

2.4.2. Effects of density and confining stress

The general definition for the state of compaction of granular materials is

$$I_D = \frac{e_{max} - e}{e_{max} - e_{min}} \quad (2.7)$$

where e_{max} is defined as the void ratio achieved in quickly inverting a measuring cylinder containing the dry soil and e_{min} is that achieved under optimal vibration of a compactive mass under saturated conditions and without causing crushing.

If soil particles were perfectly strong and rigid, the tendency towards dilation would be solely a function of the density and arrangement of the particle structure. However, other experiments have proven that increased confining pressure leads to reduced angle of shearing (Bishop, 1972).

Bolton (1936) made various investigations and calculations on the sands showed in Table 3 to analyse the behaviour of the dilation angle. Hence, he created a definition for a relative dilatancy index, I_R, which offered a unique set of correlations for the dilatancy-related behaviour of each of the sands in laboratory element tests due to the feeling that the above definition was not enough to represent most of the several behaviours.

$$I_R = I_D(10 - \ln p') - 1 \quad (2.8)$$

being p' the mean effective stress at failure.

Therefore, for plane strain,

$$\phi'_{max} - \phi'_{crit} = 0.8\psi_{max} = 5{I_R}^0 \quad (2.9)$$

Table 3 – Sand data (Bolton 1986)

Identification	Name	d_{60}: mm	d_{10}: mm	e_{min}	e_{max}	ϕ'_{crit}	Reference
A	Brasted river	0·29	0·12	0·47	0·79	32·6	Cornforth (1964, 1973)
B	Limassol marine	0·11	0·003	0·57	1·18	34·4	Cornforth (1973)
C	Mersey river	≈0·2	≈0·1	0·49	0·82	32·0	Rowe (1969) Rowe & Barden (1964)
D	Monterey no. 20	≈0·3	≈0·15	0·57	0·78	36·9	Marachi, Chan, Seed & Duncan (1969)
E	Monterey no. 0	≈0·5	≈0·3	0·57	0·86	37·0	Lade & Duncan (1973)
F	Ham river	0·25	0·16	0·59	0·92	33·0	Bishop & Green (1965)
G	Leighton Buzzard 14/25	0·85	0·65	0·49	0·79	35·0	Stroud (1971)
H	Welland river	0·14	0·10	0·62	0·94	35·0	Barden *et al.* (1969)
I	Chattahoochee river	0·47	0·21	0·61	1·10	32·5	Vesic & Clough (1968)
J	Mol	0·21	0·14	0·56	0·89	32·5	Ladanyi (1960)
K	Berlin	0·25	0·11	0·46	0·75	33·0	De Beer (1965)
L	Guinea marine	0·41	0·16	0·52	0·90	33·0	Cornforth (1973)
M	Portland river	0·36	0·23	0·63	1·10	36·1	Cornforth (1973)
N	Glacial outwash sand	0·9	0·15	0·41	0·84	37·0	Hirschfield & Poulos (1964)
P	Karlsruhe medium sand	0·38	0·20	0·54	0·82	34·0	Hettler (1981)
R	Sacramento river	0·22	0·15	0·61	1·03	33·3	Lee & Seed (1967)
S	Ottawa sand	0·76	0·65	0·49	≈0·8	30·0	Lee & Seed (1967)

2.5. MODEL EXPERIMENTS TO STUDY THE INFLUENCE OF SEEPAGE ON THE STABILITY OF A SHEETED EXCAVATION IN SAND

Marsland (1953) made a series of experiments, using scaled physical models to observe the influence of water flow in the stability of sheeted excavations in sand. Despite of the rough techniques used to analyze the results, these experiments were innovative and led the way to new investigations with more updated technologies.

Marshland's article describes model experiments to determine the type of failure occurring in strutted sheeted excavations in non-cohesive soils due to seepage water, having been taken observations to determine the flow net, following the mode of failure of the soil under different conditions. In these models, a significant number of factors were varied, such as the width of the cofferdam, the depth of penetration of the sheet-wall and the soil conditions.

2.5.1. DESCRIPTION OF APPARATUS AND TEST PROCEDURE

The investigations were carried out in a tank with dimensions of 2.75 m long, by 0.61 m deep, and 0.1525 m wide. By various type of tubes and recipients with an adjustable constant head over flow, as it can be seen in Fig.17 the tank was fitted with water pressure points fixed on the bottom of the tank. For tracing the flow lines, as an indicator fluid in manometer tubes - fluorescein-sodium dye - was used.

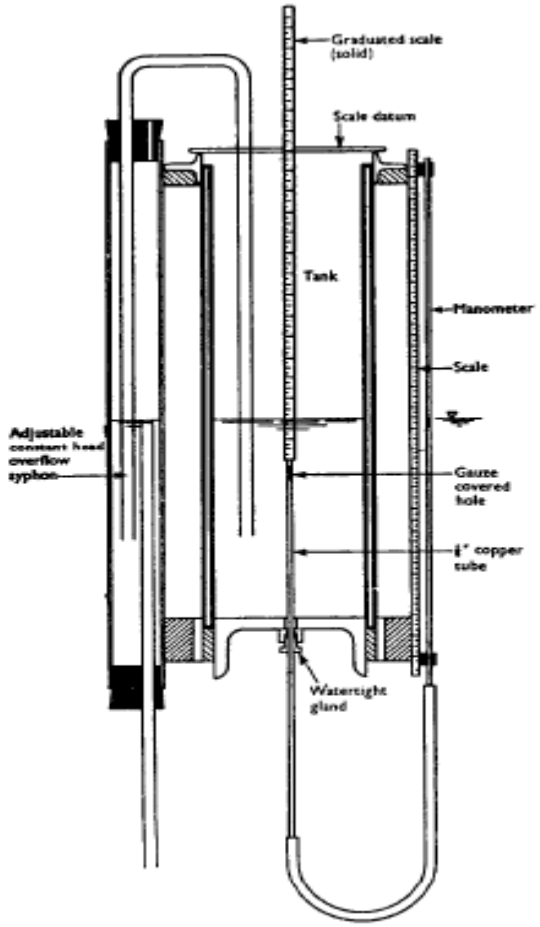

Fig. 17 - Diagramatic sketch showing position of syphon (Marsland 1953)

After sealing the tank, it was filled with water and sand, making sure that the soil and the auxiliary tube and the pressure points were free from air. Then, the water level was lowered to a level that did not produce failure. Pressure readings were then taken in various points, and flow lines were obtained by marking the paths of spots of dye, introduced at various distances from the sheeting, in the glass borders of the tank. The latter were then traced off and in conjunction with the pressure readings the flow net was obtained. Afterwards, the water level was slowly lowered until it produced failure, observed by means of photographs and motion film strips.

2.5.2. EXPERIMENTS USING HOMOGENEOUS SANDS

2.5.2.1. Effect of width of cofferdam and degree of penetration of the sheet-wall

With the objective of studying the effect of width, it was decided to compare very deep narrow cofferdams with both infinitely wide or single wall case. Two types of sand were used, one especially loose (n = 42%), and other very dense (n = 37-38%). After determining which sand to use on the construction of the flow net, the water level was lowered until failure occurred, registering the correspondent failure head as well as the mode of failure. Once again, this was obtained by taking pictures and making film strips of the failure. In the next figure it can be seen the type of symbology used.

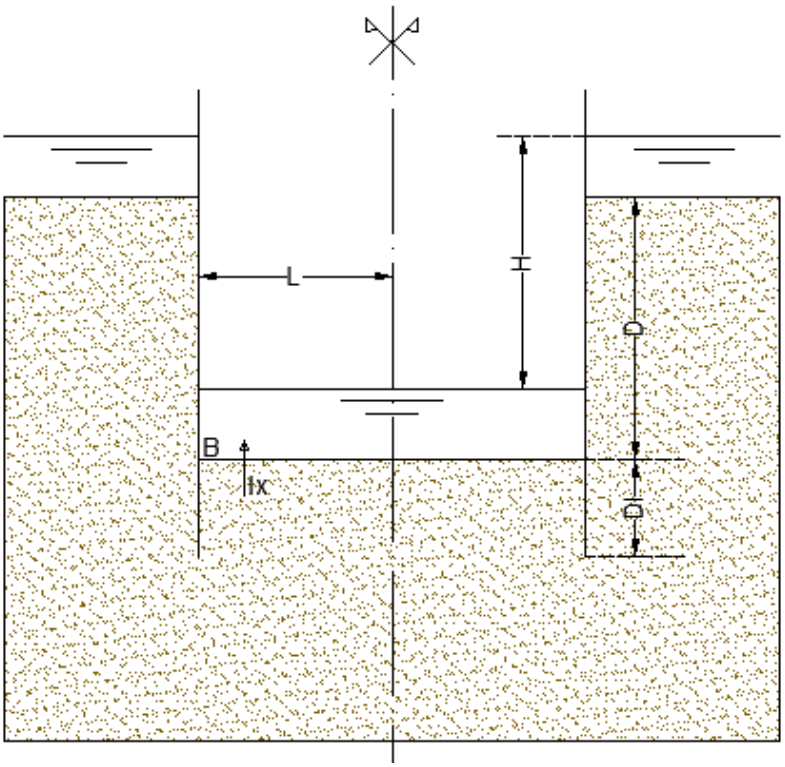

Fig. 18 – Diagram of sybols used

2.5.2.2. Development of instability in loose sand

Previously, the failures were observed by naked eye, and the first indication of movement was usually the formation of small eruptions about a quarter of an inch (≈ 6.35 mm) across on the surface of the excavation. The failure occurred in narrow excavations, for example, those in which the depth of penetration of the sheet-wall D1 was greater than the width (2L). This event was characterized by eruptions over the entire excavation base in addition to general heaving of the formation. On the other hand, in the case of wide excavations, as those in which the depth of penetration was less than the width, the eruptions only occurred near the sheet-wall and the total head had to be raised by about 10% before the collapse took place.

The results of the experiments on loose sand are given in Table 4. The observation of the flow nets in Fig. 19 shows that the upward gradient in any horizontal plane inside the excavation is higher near the sheet-wall and when the pile tips are approached.

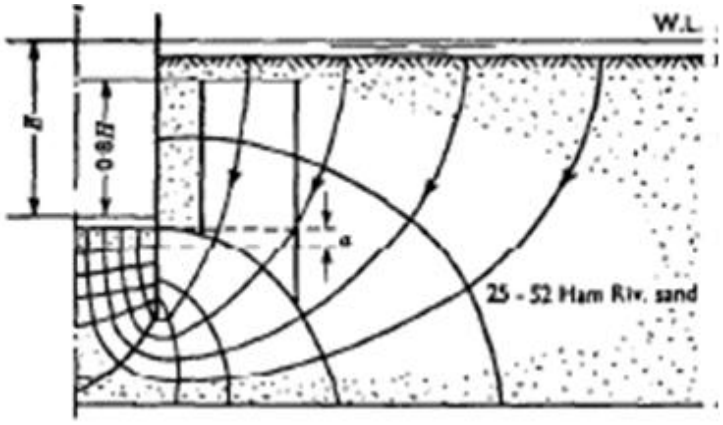

Fig. 19 – standard case (Marsland 1953)

Table 4 – Values of the failure heads in homogeneous loose sand (Marsland 1953)

Values of the failure head in homogeneous loose sand

Porosity, $n = 42$ per cent : $i_c = 0{\cdot}97$
All lengths in centimetres

Details of cofferdam		Failure head (H_c) (cm. of water)				Remarks
$2L$ Width (1)	D_1 Penetration (2)	Experimental failure head (3)		As calc. from U_e (4)	As calc. from I_x (5)	
7·6	2·5	7·75 ± 0·5		5·5	8·6	Column (3) values taken are for initial movement observed by eye.
	5·1	11·6 ± 0·4		9·5	12·4	
	7·6	14·5 ± 0·3		11·8 (12·7)	14·5 (15·3)*	
	10·2	17·0 ± 1·0		16·7	20·0	
15·2	2·5	9·5 ± 0·4		6·2	12·3	Columns (4) and (5) are obtained from experimental flow net.
	5·1	15·3 ± 0·3		11·7	16·0	
	7·6	19·1 ± 1·2		14·4 (16·1)	18·7 (23·7)*	
	10·2	20·0 ± 1·3		17·0	21·9	
		Initial movement	Total failure			Initial movement column (3) observed with microscope. Columns (4) and (5) obtained from measured values of U_e and I_x in the model.
Single wall	2·5	10·0	11·3	10·4 (9·5)	12·5 (15·0)	
	5·1	18·0	20·8	15·4 (15·9)	20·0 (22·8)	
	7·6	23·9	29·0	20·0 (20·0)	32·5 (31·0)	

* The values in brackets are obtained from theoretical flow nets.

2.5.2.3. Development of instability in dense sands

Experimental results of dense sand are summarized in Table 5. The analysis of these results indicates that failure usually occurs when the exit gradient I_x becomes equivalent to i_c, the critical floatation gradient. The failure appears to take place suddenly and to be of a very well defined well shape, and so closer observation appears to be needed.

Preceding experiments, where a uniform upward gradient was applied to densely packed sample of length in a circular tube, showed that for complete failure the critical failure head (H_c) exceeded li_c, where i_c denotes the critical gradient for flotation based on the overall porosity.

Supposedly, i_c reduces as the porosity, n, increases so failure should become more aggressive with an enhancement in the quantity of water flowing. When a sample in a confined tube is studied, side friction must be considered as well, and this cannot be reduced until expansion has taken place through the main body of the model, which cannot happen before expansion has taken place at the surface. Consequently, this requires more quantities of water to flow through the material, which requires a higher value of H.

Same actions were assumed to happen in the cofferdam, so microscopic observations were made through the glass sides of the tank, having indicated that expansion took place before failure occurred and that in wide cofferdams, wedge type failures were more probable to happen. On the other hand, for narrow cofferdams, numerous boils occurred over the entire excavation base.

Table 5: Values of the failure head in homogeneous dense sand

Porosity = 37 per cent : $i_c = 1{\cdot}05$
All dimensions in centimetres

Details of cofferdams		Failure head (H_c) (cm. of water)		
$2L$ Width (1)	D_1 Penetration (2)	Experimental failure head (3)	Failure head calculated from flow net exit gradient I_x*	
			(4)	(5)
7·6	2·5 5·1 7·6 10·2 12·7 15·2	11·4 ± 0·4 13·8 ± 0·3 17·3 ± 0·3 20·5 ± 0·4 22·5 ± 0·4 25·1 ± 0·2	16·0	16·2
15·2	2·5 5·1 7·6	12·3 ± 0·8 19·0 ± 0·5 24·7 ± 0·5	22·5	24·8
Single wall	2·5 5·1 7·6	15·5 ± 0·2 24·7 ± 0·4 36·5 ± 0·5	13·5 22·0 31·8	16·2 24·6 33·4

* Flow net value based on $I_x = i_c$.

2.5.2.4. General conclusions

(1) The water head increases with increasing width and penetration;

(2) Rupture, in loose sands, occurs when $U_c = D_1 * i_c$, which meaning that failure occurs when the pressure at the wall tip is sufficient to lift the column of submerged sand near the wall of the cofferdam;

(3) In dense sands, failure occurs when the exit gradient at the excavation surface becomes equal to

$$i_c = (G_8 - 1)(1 - n) \quad (2.10)$$

(4) The water head values from the model concur with the ones obtained numerically.

2.5.3. EXPERIMENTS WITH NON-UNIFORM SITE CONDITIONS

The objectives of these investigations were to compare non-homogeneous site with homogeneous site. Therefore, four broad conditions were considered for this purpose:

(a) a fine soil overlying a coarse soil;

(b) a course soil overlying a fine soil;

(c) a fine horizontal layer in a homogeneous mass;

(d) fine material inside an excavation replaced by coarse material as a construction expedient.

2.5.3.1. Fine layer over a coarse layer

The materials used in these experiments were the following:

- Upper fine layer: 25-52 B.S.S. Ham River sand packed loosely at a porosity of 42%, having a permeability (K) of 6.8 cm/min and having a critical flotation gradient (i_c) of 0.97.

- Lower coarse layer: 7-14 B.S.S. Ham River sand packed loosely at a porosity of 48%, and having a permeability (K) of 78 cm/min and a critical flotation gradient, $i_c = 0.86$.

A sequence of tests was performed with the sheetpile tips at 15.2 cm above the bottom of the tank. Again, water level was lowered until failure was observed, and some differences were noted. This was observed changing the level of the boundary between the coarse and the fine layer. The results are given in the next figure.

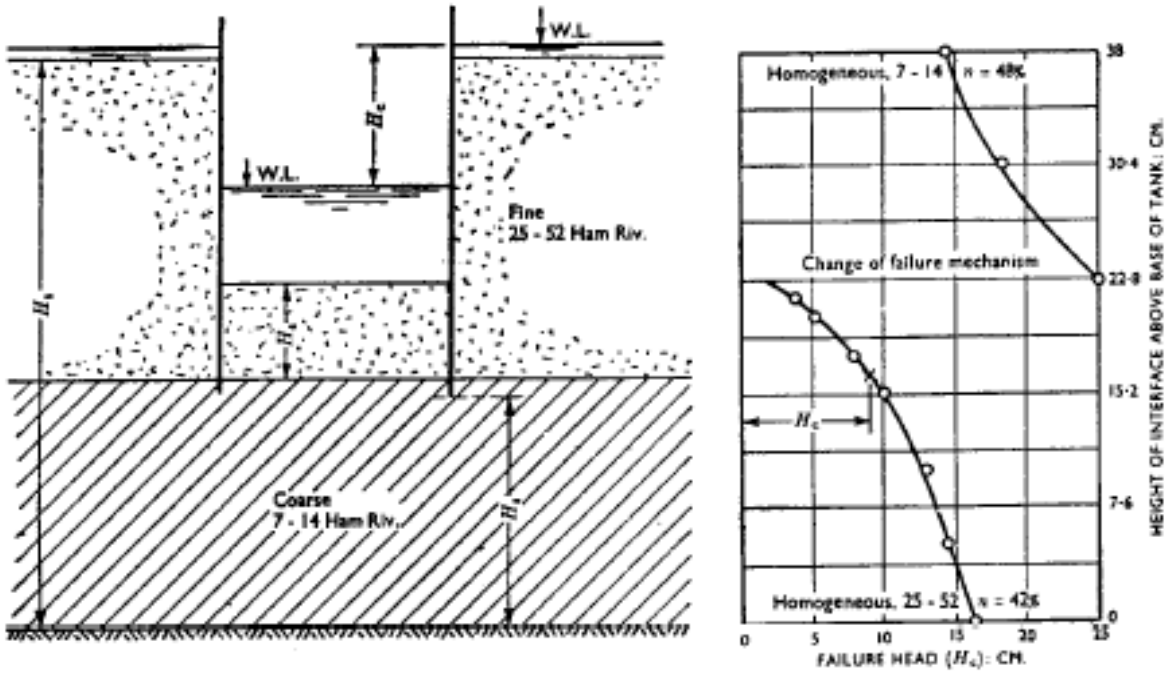

Fig. 20 – Fine over coarse: variation of failure head with position of interface (Marsland, 1953)

These models simulated an excavation made under water, and, consequently, water was pumped out of the cofferdam, indicating the value of failure head of the bottom. Some conclusions can be taken from these experiments:

- The coarse layer existence makes the water flow more vertically and more concentrated in the fine layer;
- When the coarse layer appears at a depth, below the sheet-pile tips, greater than the width, homogeneous values can be considered;
- If the excavation needs to be carried to the coarse layer, then the failure head will be greater than for the homogeneous case by an amount depending of the permeability ratio of the two layers. It must be pointed that at some stage of the excavation, the fine material will become completely unstable and dangerous conditions will be created;
- If the division line between the fine and coarse material lies between the proposed excavation level and a depth below the sheet-pile tips less than the width of the excavation, cautious study is required, since the failure head can have very low values.

2.5.3.2. Coarse layer over a fine layer

The results of this experiment show that the critical head changes as the interface of the two layers is moved vertically depending of the excavation. Prior investigations had shown that when a coarse layer is over a fine layer, careful analyses must be done, so in this case a microscope was used, and general motion at the surface was taken as failure head. Some conclusions can be drawn from these investigations:

- If the interface is anywhere between the points A and B, then the value of the water head may lie between the values for the corresponding homogeneous case and the homogeneous case with an impermeable base at the level of the interface;
- When the interface lies between the sheet-pile tip and the end of the excavation, between B and D, usually failure occurs by heaving of the excavation;
- On the other hand, for the cases where no coarse material exists below the excavation base, the failure head occurs between the one corresponding to the homogeneous case and when the coarse material is neglected altogether.

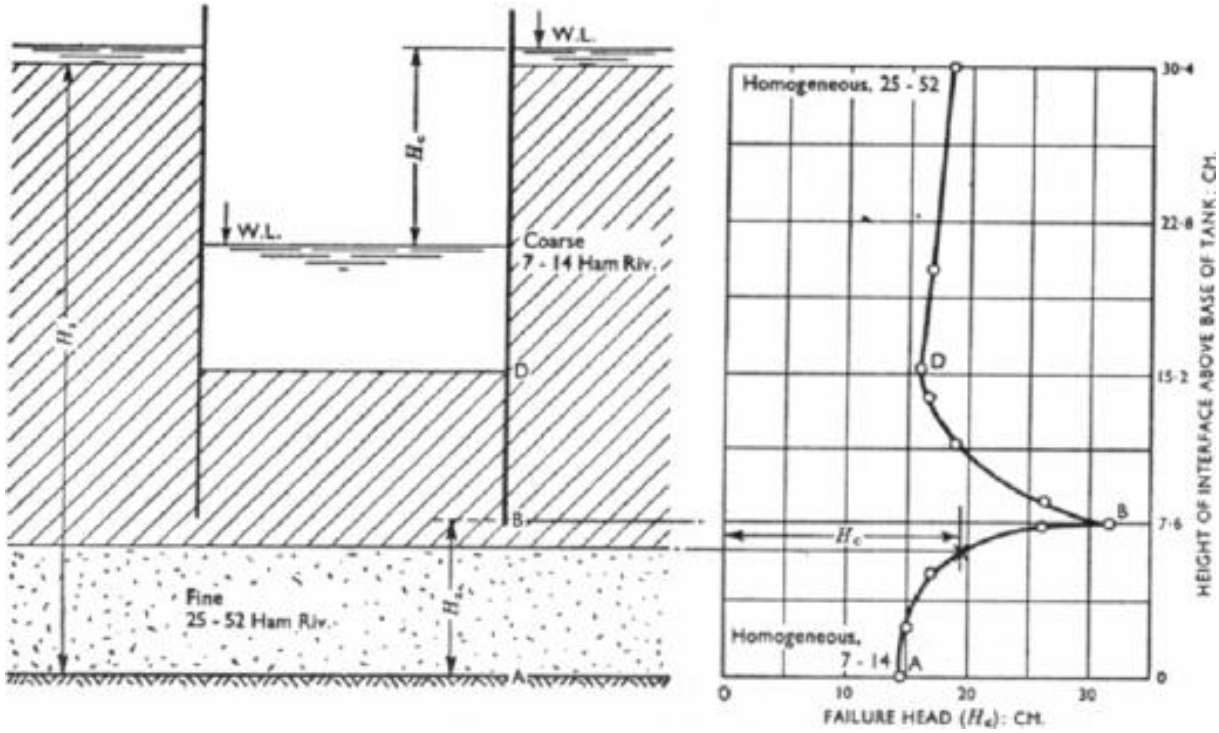

Fig. 21 – Coarse over fine: variation of failure head with position of interface (Marsland, 1953)

2.5.3.3. The effect of a single fine layer in homogeneous coarse sand bed

In this series of experiments, the material used was 25-36 B.S. sieve Leighton Buzzard sand packed loosely at a porosity of 41.5% and with a permeability of 47.5 cm/min, together with Ham River sand passing 100 sieve at a porosity of 44% with a permeability of 0.55 cm/min that was used for the 1.25 cm thick fine layer. The following observations can be made:

- When the impervious layer is distant from the sheet-pile tips, the thin layer will act as an impervious base and will give values of the H_c slightly higher than in the homogeneous case. As the thin layer approaches the pile tips, the rupture results of a mix of a wedge and heave. When the thin layer is near the pile tips the failure results in a heave type;
- If the low permeability layer exists between the level of excavation and the sheet-pile tips, a very dangerous condition is ought to happen, characterized by a rupture by heaving. This failure needs only a small rise of the water head level, H_c, to take place, and it is represented by a lift of a column of soil between the bottom of the fine layer and the level of the excavation formation;
- If a fine layer exists above the excavation base, a dangerous situation may occur while the soil is being excavated as the layer is being reached.

2.5.3.4. The effect of replacing sand inside the excavation with coarser material

The purpose of these experiments was to become aware of how replacing sand below the level of the excavation would improve its stability. For that purpose, the homogeneous 25-52 B.S.S. Ham River sand was replaced by 7-14 B.S.S. Ham River sand in varying depths. The same way, photos of the failure were taken, and one could see that this case was very similar to the one of a coarse soil on a

fine soil. In the end, it will be concluded that the replacement of the coarse material will result in an improvement in the stability of the excavation.

There are two reasons for this to happen: firstly, the replacing of the coarse material lowers the pressure at the sheet-pile tip; secondly, there's a spreading of the upward seepage drag. In an ultimate analysis, the gain comes mostly from the reduction of the water pressure gradient within the coarse material, which means that a lower safety factor can be used.

2.5.4. CONCLUSIONS

For studying mechanisms of failure due to seepage in sheet-wall excavations, sand-water models can be used, but careful observation is needed. The author recurred to microscopes to observe the failure mechanisms, as well as the time exposure photographs and slow speed films.

These experiments have shown that the stability of the excavation depend both upon dimensions and soil conditions of the model. It was proved that the safety factor diminishes as the excavation becomes narrower, and increases as the penetration of the sheeting becomes deeper. In a case where high pressure exists in pervious strata underlying fine material, the level of safety can be increased by relieving the excess pressure by means of relief wells or carry out the excavation and possibly the construction under water or substituting the coarse material by less coarse sand.

3

PLAXIS AND PLAXFLOW

After a review of the State of Art, and other proper literature about the seepage problem in underwater excavations, much more studies about this complex subject were needed, with the use of more updated technologies, such as commercial geotechnical software. These studies will help to learn more properly the behaviour of bottom failure in deep excavations, and that will bring increased safety to their design and construction.

Consequently, a way of studying this soil behaviour was imagined by trying to correlate the results of previous works with the use of a finite element method (FEM) geotechnical software. The chosen program was PLAXIS, which is a very powerful and well-known geotechnical software, with a friendly interface.

The aim of this study is to try a new approach to the bottom stability problem in deep excavations, and therefore to have a better knowledge of that important subject, because deep excavations are increasing with the rehabilitation of urban sites. Nowadays, underground parking is becoming a great concern, in an attempt of getting rid of public parking, which occupies large areas.

To apply PLAXIS program to this study, some modifications are needed to achieve the proper results. In addition, different programs have different features, and, as it was said, different input parameters should be introduced. In FEM software application, the mesh generator works in different ways, which means that the final result may not be exactly the same. Therefore, proper result analysis is needed, so the data can be compared and studied appropriately.

On the other hand, physical models are a different subject: they are much harder to reproduce in software, because there are a lot of variables which may not be considered in the physical model, or are not very accurate, which may lead to different results. Therefore, this part of the work will take more time than any of the other ones, because it is also very hard to reproduce the exact same conditions, in terms of stress, strain and water conditions, such as permeability and constant water head.

3.1. DEVELOPMENT OF PLAXIS

The development of PLAXIS began in 1987 at Technical University of Delft, as an initiative of the Dutch Department of Public Works and Water Management. The initial goal was to develop an easy way to use 2D finite element code for the analysis of river embankments on the soft soils of the lowlands of Holland. In the subsequent years, PLAXIS was extended to cover most other areas of geotechnical engineering. Because of continuously growing activities, a company named PLAXIS b.v. was formed in 1993.

The main objectives of this program are intended to provide a tool for practical analysis to be used by geotechnical engineers who are not necessarily numerical specialists. Many engineers frequently consider non-linear finite element computations which take a lot of time and effort. On the contrary, PLAXIS has robust and theoretically sound computational procedures, which have a friendly interface.

Development of PLAXIS would not be possible without worldwide research at universities and research institutes. To ensure that the high technical standard of PLAXIS is maintained, the development team is in contact with a large network of researchers in the field of geomechanics and numerical methods.

There are many PLAXIS versions, but in this study was only used the *2D Version 9.0* and PLAXFLOW, which will be described later.

3.2. PLAXIS 2D

PLAXIS 2D is a finite element package intended for the two dimensional analysis of deformation and stability in geotechnical engineering. Geotechnical applications require advanced constitutive models for the simulation of the non-linear, time dependent and anisotropic behaviour of soils and/or rock. In addition, since soil is a multi-phase material, special procedures are required to deal with hydrostatic and non-hydrostatic pore pressures in the soil. Although the modelling of the soil itself is an important issue, many tunnel projects involve the modelling of structures and the interaction between the structures and the soil. PLAXIS is equipped with features to deal with various aspects of complex geotechnical structures.

The input of soil layers, structures, construction stages, loads and boundary conditions is based on convenient CAD drawing procedures, which allows for a detailed modelling of the geometry cross-section. From this geometry model, a 2D finite element is generated. PLAXIS allows for automatic generation of unstructured 2D finite element meshes with options for global and local mesh refinement, and the 2D mesh generator is a special version of the Triangle generator.

In this program, it can be used quadratic 6-node and 4^{th} order 15-node triangular elements to model the deformations and stresses in the soil. Many elements can be inserted in the model such as plates, anchors, geogrids, tunnels, with a lot of definition options available.

In this software, special beam elements are used to model the bending of retaining walls, tunnel linings, shells, and other slender structures. The behaviour of these elements is defined using a flexural rigidity, a normal stiffness and an ultimate bending moment. Plates with interfaces may be used to perform realistic analysis of geotechnical structures. In addition, joint elements are available to model soil-structure interaction. Values of interface friction angle and adhesion are generally not the same as the friction angle cohesion of the surrounding soil. To model anchors and struts, elastoplastic spring elements are used. The behaviour of these elements is defined using a normal stiffness and a maximum force. A special option exists for the analyses of prestressed ground anchors and excavation supports.

The PLAXIS program offers a convenient facility to create circular and non-circular tunnels using arcs and lines. Plates and interfaces may be used to model the tunnel lining and the interaction with the surrounding soil. Fully isoparametric elements are used to model the curved boundaries within the mesh. Various methods have been implemented to analyse the deformations.

PLAXIS uses various soil models such as the well-known Mohr-Coulomb model, which is based on notorious soil parameters in engineering practice. In addition, it has advanced soil models of many types as elastoplastic hyperbolic models, and time-dependent models. This program has a soil test

option, which permits to check the behaviour of the selected soil material model with the given material parameters.

With the help of the *Staged construction* feature, it is possible to make a realistic simulation of construction and excavation processes by activating and deactivating clusters of elements, application of loads, changing of water tables, etc. In this study, this feature is very helpful, because in every calculation the excavations or the rise of the water level is phased. The decay of excess pore pressure with time can be computed using a consolidation analysis, which requires the input of permeability coefficients in the various soil layers. Automatic time stepping procedures make the analysis robust and easy to use.

The safety factor is usually defined as the ratio of the failure load to the working load. This definitions is suitable for foundation structures, but not for sheet-pile walls or embankments. For this latter type of structure it is more appropriate to use the soil mechanics definition of a safety factor, which is the ratio of the available shear strength to the minimum shear strength needed for equilibrium. PLAXIS can be used to compute this factor of safety using a *phi-c reduction* procedure, which will be explained later.

The PLAXIS postprocessor has enhanced graphical features for displaying computational results. Values of displacements, stresses, strains and structural forces can be obtained from the output tables. Plots and tables can be sent to output devices to export them to other software. A special tool is available for drawing load-displacement curves. The visualisation of stress paths provides a valuable insight into local soil behaviour which allows a detailed analysis of the results of a PLAXIS calculation.

In summary, PLAXIS is an excellent tool for a lot of geotechnical problems, with various features which allow a good and safe evaluation of the majority of the geotechnical constructions, and because it has a friendly interface, not hard to use, and for that matter there is not so much chance for error.

3.3. PLAXFLOW

PLAXFLOW is one of PLAXIS products. In 1999 the Road and Hydraulic Engineering division of Rijkswaterstaat took the initiative for development of a new Groundwater flow program, compatible with the 2D deformation and stability analysis software. The main goal was to improve the analysis software for the evaluation of river dike stability in the case of time-dependent groundwater flow during high water on the Dutch rivers.

The PLAXIS Groundwater flow program is an independent program for the analyses of steady-state and transient groundwater flow. PLAXFLOW incorporates sophisticated models for saturated/unsaturated groundwater flow, using the well-known “Van Genuchten” relations between pore pressure, saturation and permeability. This program is numerically stable and provides state-of-the-art facilities to incorporate time-dependant boundary conditions. It also enables you to combine results with the PLAXIS 2D professional version for deformation and stability analysis.

This software is a finite element package intended for two-dimensional transient and steady state analysis of saturated and unsaturated groundwater flow problems in geotechnical engineering and hydrology. Groundwater flow applications require advanced models for the simulation of the unsaturated, time-dependent and anisotropic behaviour of soils. PLAXFLOW is equipped with features to deal with various aspects of complex geotechnical flow problems. The input of soil layers, structures, construction stages and boundary conditions is similar to PLAXIS 2D, since it is based on convenient CAD drawing procedures, which allows for a detailed modelling of the geometry cross-section. From this geometry model, a 2D finite element mesh is easily generated. It also allows for

automatic generation of unstructured 2D finite element meshes composed of 3-node triangular elements, with options for global and local mesh refinement. For compatibility with PLAXIS 2D, 6-node and 15-node elements can also be chosen. Screen elements are used to simulate an impermeable screen. An active screen is fully impermeable and of course an inactive screen is fully permeable. Other features of this program are drains and wells: these ones are used to prescribe points inside the geometry model where a specific discharge is subtracted from (source) or added to (sink) the soil; drains are used to prescribe lines inside the geometry model where pore pressures are set to zero.

General groundwater heads or pore pressures and external water pressures can be conveniently generated on the basis of water levels. Groundwater head and pore pressures can also be specified directly in individual boundary lines. PLAXFLOW allows for conditions that are gradually changing in time. Time-dependent conditions can be defined by a linear or harmonic function or by means of an input table.

4

APPLICATIONS

4.1. SOFT SOILS

4.1.1. OBJECTIVES

The objective of this part of the work is to reproduce the some conditions of Faheem (2003)'s paper, explained in 2.1., but with another FEM software, PLAXIS, to see if it can be used, to corroborate the results obtained in the paper and to see if they are realistic. The geometric data and the mechanical properties of the clay are the same used in the paper and therefore some cases were tested to have a general view of the program reliability. It was only tested the effect of H/B, so *T* was considered with the same value of *Tc*, which was obtained by the function $B/\sqrt{2}$, *D* is equivalent to 0, and the ratio H/B took the values 0.5, 1, 2, 3. For these calculations the value of *H* was considered constant and equal to 9 m. The values obtained are in the next table.

Table 6 – Model dimensions

H/B	0.5	1	2	3
B (m)	18	9	4.5	3
B/2 (m)	9	4.5	2.25	1.5
T=Tc (m)	12.73	6.36	3.18	2.12

Other important issue is how the excavation procedure is going to be done. To analyse this topic, two types of excavation procedures were consider:

- One, where the 9 m of excavation are done at once;
- Another, where the excavation takes place in three phases of 3 m each.

4.1.2. MODELLING PROCEDURE

To begin with the model procedure, in PLAXIS, first the material must be defined. This program has a whole range of material models, as it was explained before, as *Linear elastic* or *Soft-soil model*, but in this case the common model, *Mohr-coulomb* was chosen. To consider an undrained condition, a value of 0.49 was considered to the Poisson's ratio. The SI unit weight was taken as 20 kN/m^3 and a permeability of 0.01m/day was considered, as it is a common value for clays. For the Young's modulus, E_u, a value of 8750 kN/m^2 was considered since $E_U = 250\ s_u$. Finally, to enter the s_u value in PLAXIS, the undrained shear strength is called c_{ref}, and in this case has a value of 35 kN/m^2, so the

friction angle, ϕ, and the dilatancy angle, ψ, are considered null. In this program, the interface is represented by R_{inter}, which is the same as δ/ϕ.

The next step is to define the plate. In this analysis, the plate was considered rigid, so its stiffness has a great value to make sure it does not deform itself, since this is not being studied in this work. In addition, the plate is fixed, so the option *Total fixities* were applied, to make sure that the sheet-pile does not move at all. To the whole model *Standard fixities* were applied too, which means that in the bottom of the model horizontal and vertical fixities were applied, and in the sides only vertical fixities. Another feature that had to be taken in consideration was the application of the interfaces in both sides of the plate.

After the application of the material to all the clusters, the mesh is ready to run. It was consider a medium *global coarseness* as a good choice for the mesh, but close to the plate and its tip it was refined, since it is close to those locations that the failure will take place. In Fig. 21 a global view of the model with the mesh generated can be seen. As it was said before, the mesh is much finer close to the plate and tip.

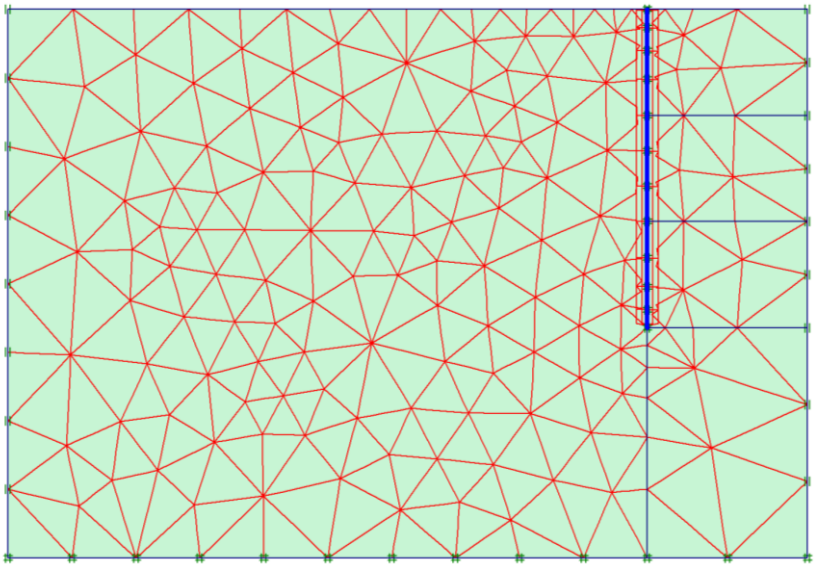

Fig. 22 – General view of the model with mesh generated

Following this, the *Initial conditions* can be entered. The ground water level was considered in the bottom of the excavation, because the water load does not enter in this study. One phase of the *Calculation Program* was the introduction of the plate in the soil, so in the *Initial conditions* only the soil appeared. Now, the model is ready for the *Calculation program* where the different stages are going to be introduced.

For the phased model, 5 stages were made:

- Phase 1: introduction of the plate;
- Phase 2: excavation of the first layer;
- Phase 3: excavation of the second layer;
- Phase 4: excavation of the third layer;
- Phase 5: *phi-c reduction.*

4.1.3. PHI-C REDUCTION

In the software PLAXIS, the shear strength reduction procedure is called *phi-c reduction*, and is used to compute safety factors. This option can be selected as a separate Calculation Type in the General tab sheet. In the *phi-c reduction* approach the strength parameters *tan ϕ (phi)* and *c* of the soil are successively reduced until failure of the structure occurs. The strength of the interfaces, if used, is reduced in the same way. The strength of structural objects like plates and anchors is not influenced by *phi-c reduction*.

The total multiplier $\sum Msf$ is used to define the value of the soil strength parameters at a given stage in the analysis:

$$\sum \mathrm{Msf} = \frac{\tan\varphi_{\mathrm{input}}}{\tan\varphi_{\mathrm{reduced}}} = \frac{c_{\mathrm{input}}}{c_{\mathrm{reduced}}} \qquad (5.1)$$

where the strength parameters with the subscript 'input' refer to the properties entered in the material sets and parameters with the subscript 'reduced' refer to the reduced values used in the analysis. $\sum Msf$ is set to 1.0 at the start of a calculation to set all material strengths to their unreduced values.

A phi-c reduction calculation is performed using the Load advanced number of steps procedure. The incremental multiplier *Msf* is used to specify the increment of the strength reduction of the first calculation step. This increment is by default set to 0.1, which is generally found to be a good starting value. The strength parameters are successively reduced automatically until all Additional steps have been performed. By default, the number of additional steps is set to 100, but a larger value up to 1000 may be given here, if necessary. It must always be checked whether the final step has resulted in a fully developed failure mechanism. If that is the case, the factor of safety is given by:

$$\mathrm{SF} = \frac{\text{available strength}}{\text{strength at failure}} = \text{value of } \sum \mathrm{Msf} \text{ at failure} \qquad (5.2)$$

If a failure mechanism has not fully developed, then the calculation must be repeated with a larger number of additional steps.

To capture the failure of the structure accurately, the use of Arc-length control in the iteration procedure is required. This feature enables accurate computations of collapses loads and failure mechanisms to be carried out. In conventional load-controlled calculations the iterative procedure breaks down as soon as the load is increased beyond the peak load. With arc-length control, however, the applied load is scaled down to capture the peak load and any residual loads. The use of a Tolerated error of no more than 3% is also required. Both requirements are complied with when using the Standard setting of the Iterative procedure.

4.1.4. RESULTS

Before the calculation starts, a point of the mesh is chosen to know its displacements. This point, as it was said before, is the one located in the middle of the excavation. When the calculation is finished there are many possible results that can be examined but the ones which are more pertinent to this study are the *Deformed mesh*, and the *Total Displacements*, to know how the soil behaves in the moment just before its failure. In Fig. 22 it can be seen a rupture of the case when *H/B* = 1.0 and *T* =

T_c. It can be noticed, as it was said before, that the most sensitive part of the model is the tip of the plate, and this constructive element, because it is fixed, effectively does not move.

Another figure that needs to be analysed carefully is the Fig. 24 where the *Total displacements* are displayed. It can be seen that the arrows have the same direction as the ones in Fig.7, but there's a specificity that appears not to be equal to this figure and that is the direction of the arrows next to the plate. Eventually these arrows seem to be not so linear in that location, which could mean that the interface has a more important role than the one mentioned in Faheem (2003)'s paper in terms of obtaining the safety factor.

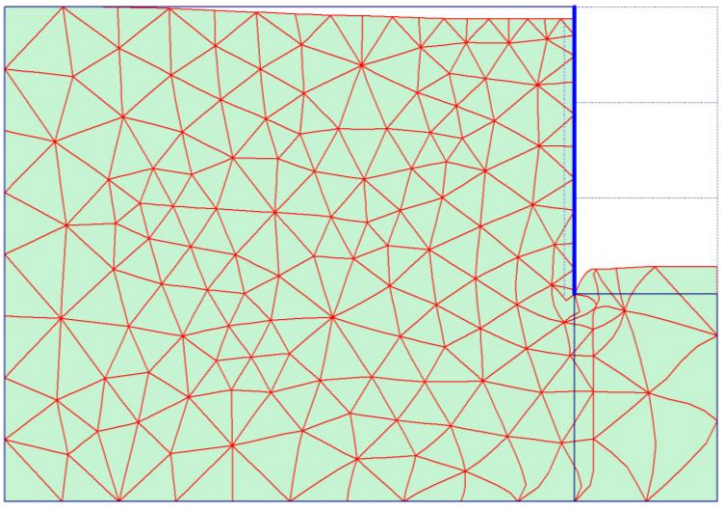

Fig. 23 – Rupture when H/B = 1.0 and $T = T_c$

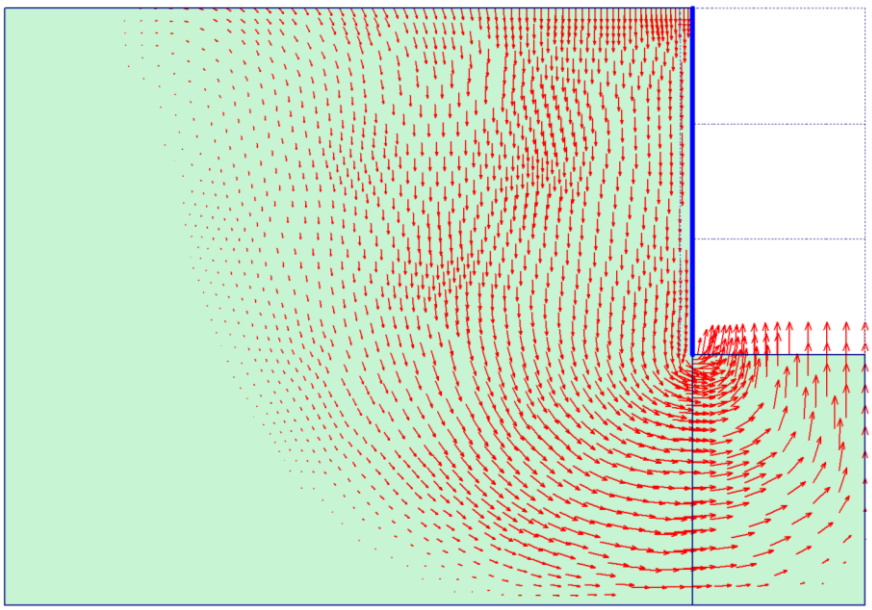

Fig. 24 – Total displacements of Fig. 22

The point selected before the *Calculation* was made can be analysed in the *Curves program*. This program shows the evolution of the Safety Factor since the shear strength reduction starts until the soil

fails. The *Curves program* can display a graphic representation which shows the evolution of the Safety Factor, but for a better understanding and editing of the chart it was chosen to extrapolate the data of that point to *Microsoft Excel*. In Fig. 25, it can be seen a chart which represents the evolution of the Safety Factor in the model where *H/B* = 1.0, and the relation δ/ψ is equivalent to 0.01, 0.1 and 0.5. As it can be seen, the relation δ/ψ, represented by 'R' in the chart, does not have such a minor role as the one mentioned in Faheem (2003)'s analysis.

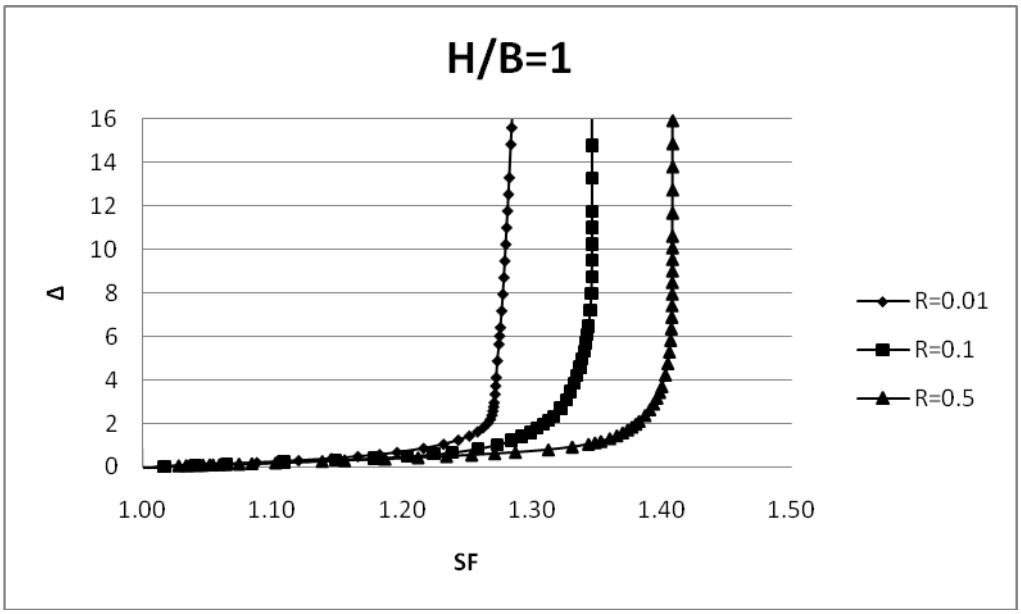

Fig. 25 - Evolution of the Safety Factor in the model where *H/B* = 1.0

Another important issue regards the choice of the excavation being phased or not. In this study was discovered that if the excavation is phased the Safety Factor stays the same. On the other hand, what does change a little is the safety factor evolution curve shape, being the phased case more close to the curve in Faheem (2003)'s paper. This means that in the phased excavation the displacements don't start so soon as the total excavation.

Relatively to the δ/ψ issue, it was analysed that effectively this had a major role in the safety factor for theoretical purposes, as it can be seen in Fig.25. In this chart are represented the safety factors of the different cases studied with a δ/ψ, or (*R*), equivalent to 0.01 and the results are not the same of Faheem (Faheem, 2003)'s article, and the same happens with the cases where 'R' is equal to 0.5.

Only for the cases where R = 0.1 was chosen, were the safety factors almost identical to the ones showed in the article, which means that these results were in fact obtained for R = 0.1. Fig. 27 shows the results obtained using this interface value and the comparison with the previous results is very satisfactory indeed.

In addition, the nodal displacements indicate a well-defined asymptotic failure value, better defined than the ones obtained in the paper, and this situation is more intense as the *H/D* relation increases. The reason this happens is due to the used mesh in Faheem (2003)'s software being coarse and rectangular and the one used in PLAXIS is automatic and can be finer where it is needed, in this case in the plate and bottom tip of the plate.

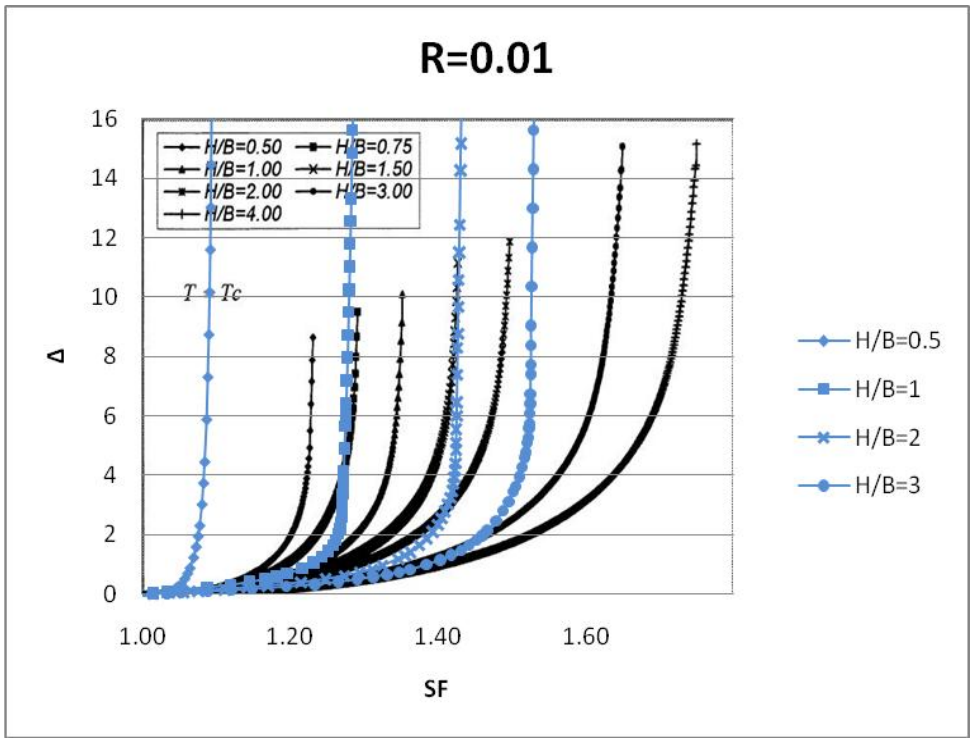

Fig. 26 – Comparison between the evolution of the safety factor obtained in PLAXIS (blue) and in Faheem's paper, when R = 0.01

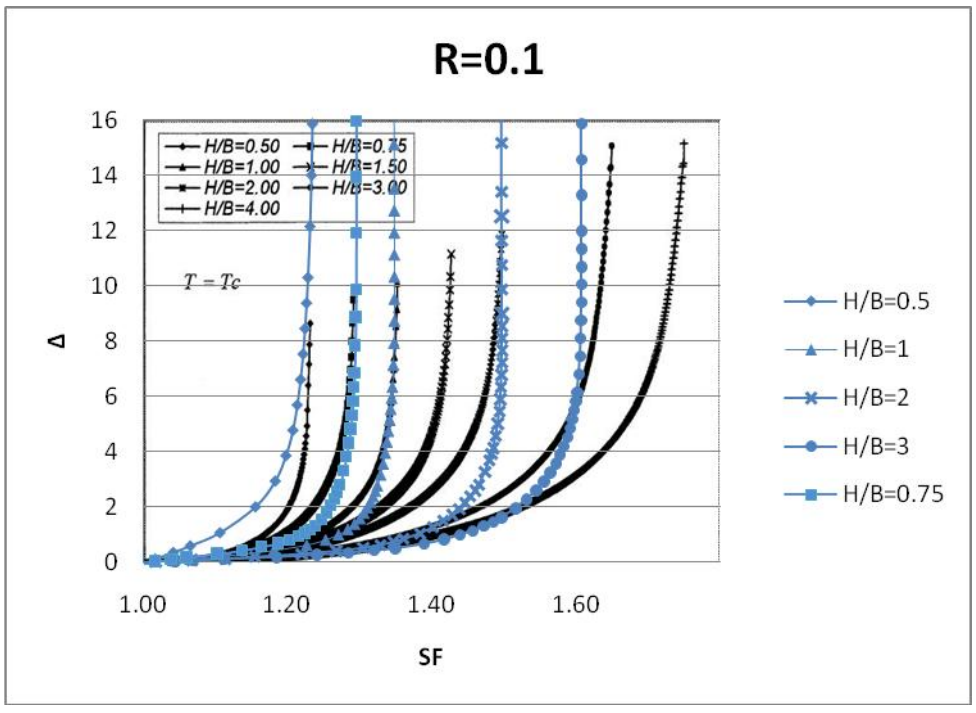

Fig. 27 - Comparison between the evolution of the safety factor obtained in PLAXIS (blue) and in Faheem's paper, when R = 0.1

Regarding the Nc-value, the results were very satisfactory, being the trend line very close to the case T = Tc, which is the one being analysed in this part of the work. These results can be seen in Fig. 27.

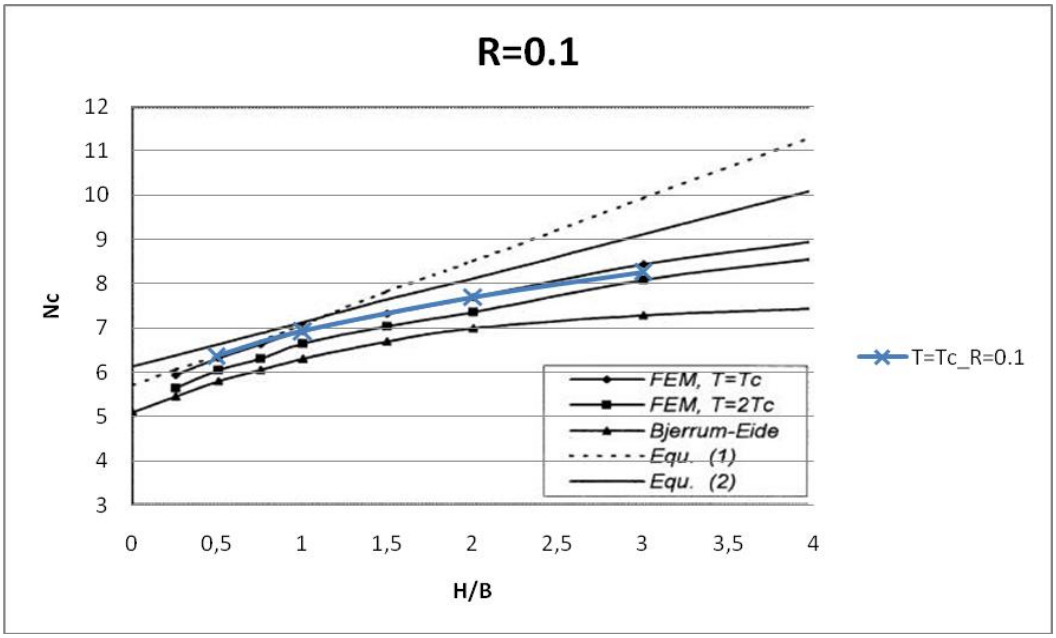

Fig. 28 - Comparison between the evolution of the N_c parameter obtained in PLAXIS (blue) and in Faheem's paper, when R = 0.1

4.1.5. H/B = 0.5 CASE STUDY

Throughout this work, all the data obtained in PLAXIS was similar to the one obtained in Faheem (2003)'s article, which meant that all the calculations were correct. However, one case never seemed to achieve similar results, no matter what was done to try to correct it. The safety factor obtained in the case *H/B* = 0.5 was always lower than the others and the graphic representation did not seem to fit within the others, as it can be seen in Fig. 29. This specific case was the only thing keeping this part of the work from corroborating Faheem (2003)'s article, so it was a very frustrating issue for a long time.

Finally, this issue was overcome when a closer look was given to the *Total displacement* output, of this case, with the *arrows* option on, as showed in Fig. 31. This figure shows that the arrows at the left side of the model are completely vertical and the plastic flow seems constrained too early into that direction,. It was then when it was thought to expand the horizontal distance from the wall to the outer boundary, and the results were outstanding.

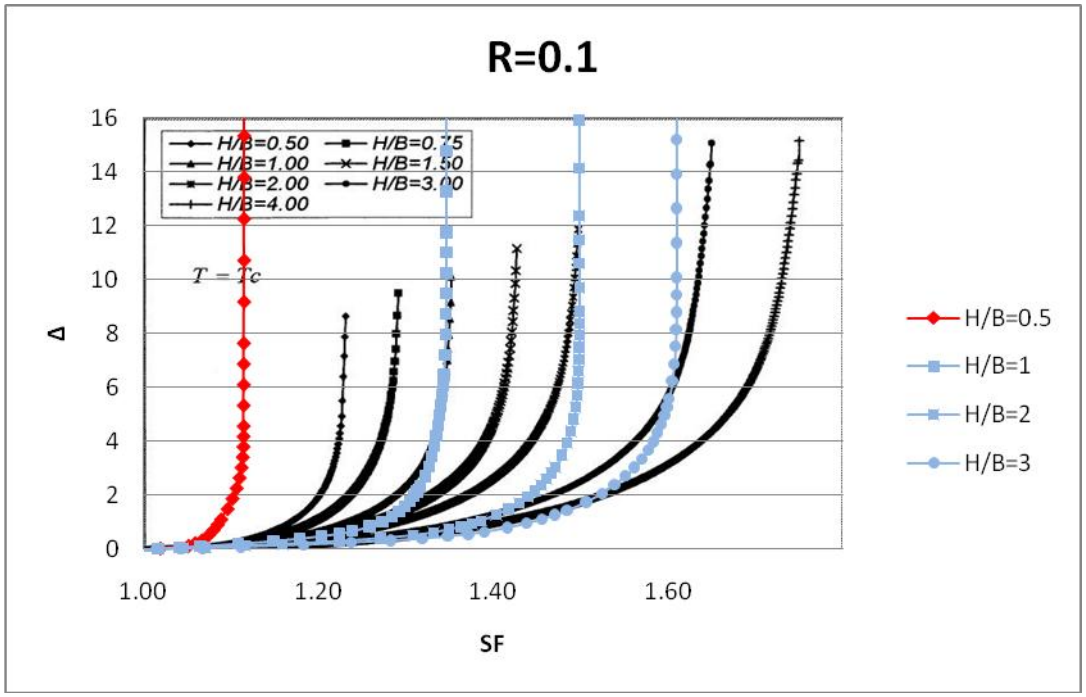

Fig. 29 – Specific analysis of the case when H/B = 0.5 (red)

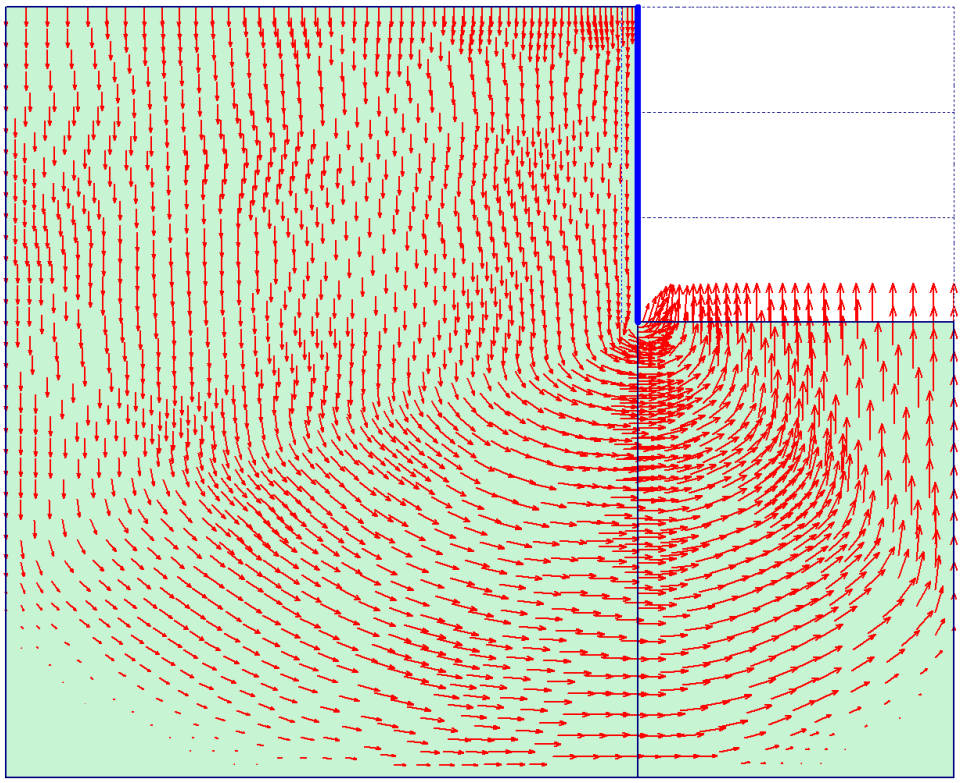

Fig. 30 – *Total displacements* of the case when H/B = 0.5

After this, a general view was given to all other cases and a pattern was noticed. Since the wall was considered constant with 9 m, the horizontal distance from the wall to the outer boundary was always at least 18 m (2*H*), as it was said in Faheem (2003)'s article. However, as the *T*, the distance from the

tip of the wall to the hard stratum, increases, or in other words, as the relation *H/B* decreases, the volume of displaced soil grows, and for this theoretical exercise infinite side boundaries are considered, so the soil has to have space to move freely. Therefore, a relation between the width of soil displaced, in the various cases studied, and the distance from the tip of the plate to the hard stratum, *T*, was made. As it can be observed in Fig. 30 the correlation of the trend line with the chart is very good ($R^2 = 0.99$). Consequently, a good equation for obtaining the horizontal distance from the wall to the outer boundary should be,

$$H.W. = 1.5T + 7 \quad (5.3)$$

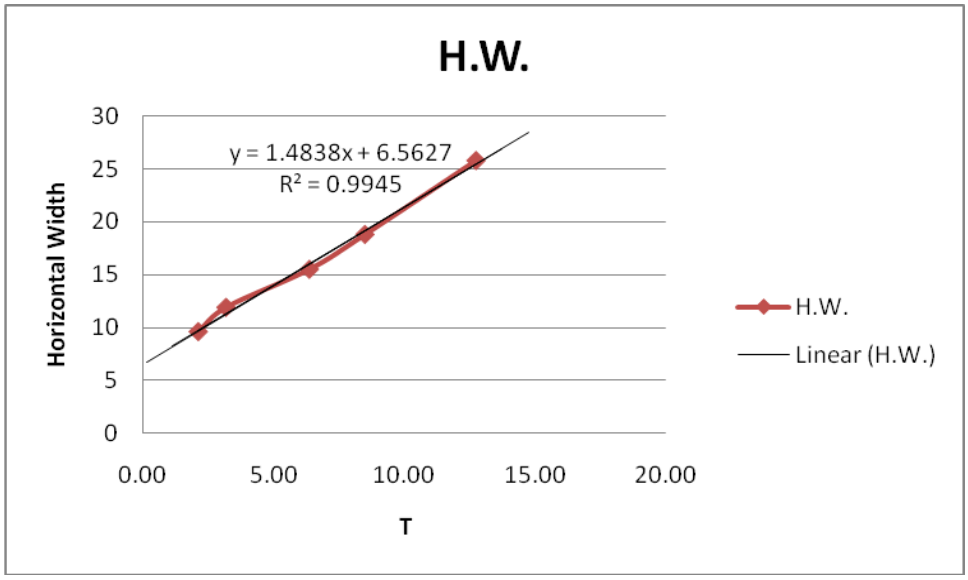

Fig. 31 – Correlation between the horizontal distance from the wall to the outer boundary and the thickness of the layer of soft sand between the tip of the pile and the hard stratum

After this correction, the safety factor of the case H/B = 0.5 increased by 8% from 1.1 to 1.24, which means that if the soil it is confined it is more unstable, and more careful and planned the design of the excavation must be. In Fig. 32 it is visible the enhancement of the safety factor.

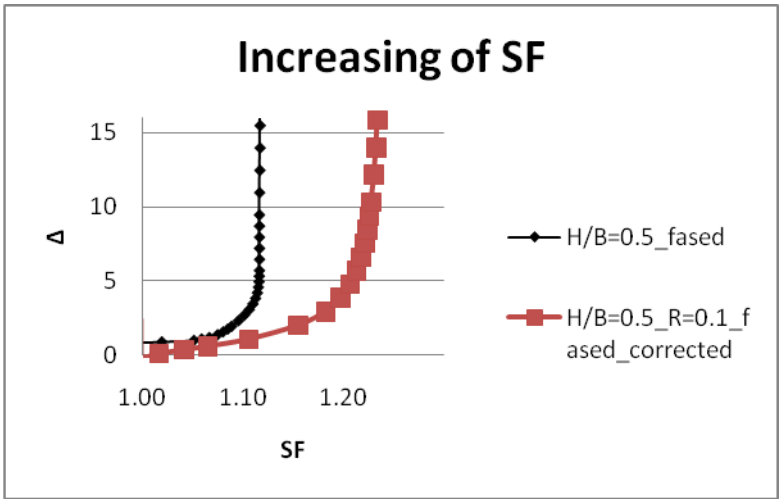

Fig. 32 – Increasing of the safety factor when the horizontal distance from the wall to the outer boundary is augmented

4.1.6. CONCLUSIONS

The study of the base failure in soft soils revealed itself very productive. In the end, it was proven that PLAXIS can, indeed, be used without problem in this type of analysis. All the results turned out to be very satisfactory, sometimes even better than in previous literature analysis.

The *phi-c reduction* is a very good tool to calculate safety factors in geotechnical constructions, as it can be seen in the output data showed before. Besides, PLAXIS has a better and easier way to generate meshes. Using the *mesh generator*, the mesh can quickly be created and refined wherever one wants. This is very useful, because the results can be better, and that can be seen in the charts above.

It was also proven that of the safety factor in this type of models depends also on the distance from the outer boundary to the wall. Moreover, such a dependency is related to the *H*/*B* ratio, or in other words, of the distance between the pile tip and the bottom of the model. This dependency expresses the need of enough space to achieve conditions of unconstrained plastic flow. When the failure surface is constrained by the model boundaries the models behave differently.

4.2. SAND

In this part of the work, we will try to reproduce the results obtained by Benmebarek *et al.* (2005) in their paper. As explained in chapter 2.3. they were using the software FLAC^{-2D}, and we will see if their results can be corroborated using PLAXIS.

4.2.1. GEOMETRY OF THE MODEL

The first step was trying to obtain the same results of Fig.11, to see if these are right, and if PLAXIS can be effectively used in the same study. This was a huge problem, and a lot of time was spent trying to get accurate results.

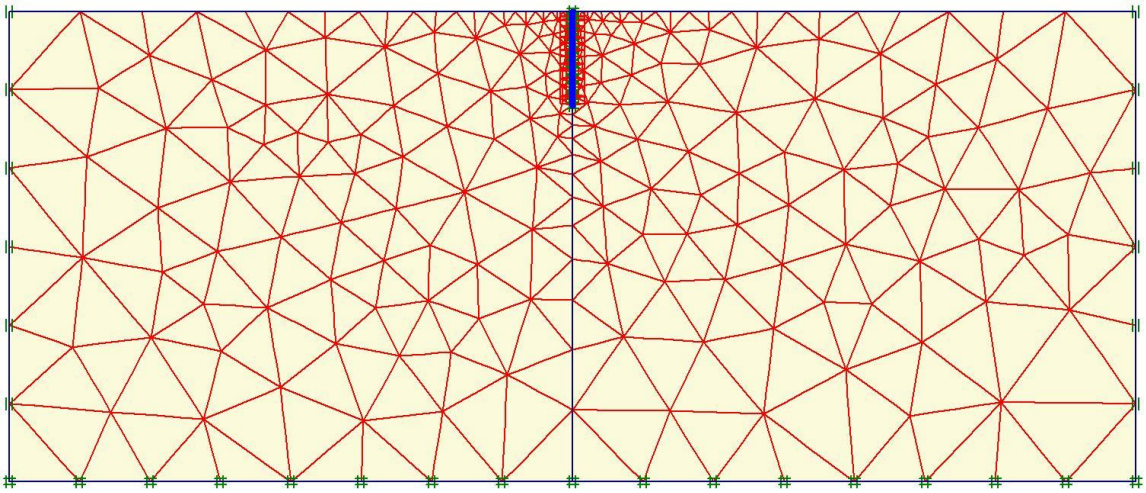

Fig. 33 – Model design with generated mesh

In the PLAXIS Input program, the first thing to do is to draw the model, as it is shown in Fig.32. As it was said before, the mesh size is fine near the wall where deformations and flow gradients are concentrated, and to minimize boundary effects, the length from the wall and the depth of the mesh are respectively located at six and five times the wall penetration, so the model should be 30 m deep, and 72 m long.

The material described in the referred paper was used in this investigation. However, some values had to be changed in order to be input in PLAXIS, because the given characteristic values of the soil are the elastic bulk modulus K = 30 MPa and shear modulus G = 11.25 MPa. The problem is that in PLAXIS, for the Mohr-Coulomb model type of soil, the input values for soil stiffness are the Young's modulus, E, and the Poisson's ratio, ν, and for that matter a transformation must occur.

4.2.2. DEFINITION OF MATERIAL CONSTANTS

4.2.2.1. *G*, *K*

When a specimen made from an isotropic material is subjected to pure shear, for instance, a cylindrical bar under torsion in the xy sense, σ_{xy} is the only non-zero stress. The strains in the specimen are obtained by,

$$\begin{bmatrix}\varepsilon_{xx}\\ \varepsilon_{yy}\\ \varepsilon_{zz}\\ \varepsilon_{yz}\\ \varepsilon_{zx}\\ \varepsilon_{xy}\end{bmatrix} = \frac{1}{E}\begin{bmatrix}1 & -\nu & -\nu & 0 & 0 & 0\\ -\nu & 1 & -\nu & 0 & 0 & 0\\ -\nu & -\nu & 1 & 0 & 0 & 0\\ 0 & 0 & 0 & 1+\nu & 0 & 0\\ 0 & 0 & 0 & 0 & 1+\nu & 0\\ 0 & 0 & 0 & 0 & 0 & 1+\nu\end{bmatrix}\begin{bmatrix}0\\ 0\\ 0\\ 0\\ 0\\ \sigma_{xy}\end{bmatrix} \quad (5.4)$$

The shear modulus G, is defined as the ratio of shear stress to engineering shear strain on the loading plane,

$$G = \frac{\sigma_{xy}}{\varepsilon_{xy}+\varepsilon_{yx}} = \frac{\sigma_{xy}}{2\varepsilon_{xy}} = \frac{\sigma_{xy}}{\gamma_{xy}} = \frac{E}{2(1+\nu)} \quad (5.5)$$

where

$$\gamma_{xy} = \varepsilon_{xy} + \varepsilon_{yx} = 2\varepsilon_{xy} \quad (5.6)$$

The shear modulus *G* is also known as the rigidity modulus, and is equivalent to the 2nd Lamé constant μ mentioned in books on continuum theory.

Common sense and the 2nd Law of Thermodynamics require that a positive shear stress leads to a positive shear strain. Therefore, the shear modulus *G* is required to be nonnegative for all materials, $G > 0$

Since both *G* and the elastic modulus, *E*, are required to be positive, the quantity in the denominator of *G* must also be positive. This requirement places a lower bound restriction on the range for Poisson's ratio, $\nu > -1$.

When an isotropic material specimen is subjected to hydrostatic pressure s, all shear stress will be zero and the normal stress will be uniform, $\sigma_{xx} = \sigma_{yy} = \sigma_{zz} = \sigma$. The strains in the specimen are given by,

$$\begin{bmatrix} \varepsilon_{xx} \\ \varepsilon_{yy} \\ \varepsilon_{zz} \\ \varepsilon_{yz} \\ \varepsilon_{zx} \\ \varepsilon_{xy} \end{bmatrix} = \frac{1}{E} \begin{bmatrix} 1 & -\nu & -\nu & 0 & 0 & 0 \\ -\nu & 1 & -\nu & 0 & 0 & 0 \\ -\nu & -\nu & 1 & 0 & 0 & 0 \\ 0 & 0 & 0 & 1+\nu & 0 & 0 \\ 0 & 0 & 0 & 0 & 1+\nu & 0 \\ 0 & 0 & 0 & 0 & 0 & 1+\nu \end{bmatrix} \begin{bmatrix} \sigma \\ \sigma \\ \sigma \\ 0 \\ 0 \\ 0 \end{bmatrix} \quad (5.7)$$

In response to the hydrostatic load, the specimen will change its volume. Its resistance to do so is quantified as the bulk modulus *K*, also known as the modulus of compression. Technically, *K* is defined as the ratio of hydrostatic pressure to the relative volume change (which is related to the direct strains),

$$K = \frac{\sigma}{\Delta V/V} = \frac{\sigma}{\varepsilon_{xx}+\varepsilon_{yy}+\varepsilon_{zz}} = \frac{E}{3(1-2\nu)} \quad (5.8)$$

Common sense and the 2nd Law of Thermodynamics require that a positive hydrostatic load leads to a positive volume change. Therefore, the bulk modulus *K* is required to be nonnegative for all materials, $K > 0$.

Since both *K* and the elastic modulus *E* are required to be positive, the following requirement is placed on the upper bound of Poisson's ratio by the denominator of *K*, $\nu < 1/2$.

4.2.2.2. *E*, *v*

When a specimen made from an isotropic material is subjected to uniaxial tension, say in the x direction, xx is the only non-zero stress. The strains in the specimen are obtained by,

$$\begin{bmatrix}\varepsilon_{xx}\\ \varepsilon_{yy}\\ \varepsilon_{zz}\\ \varepsilon_{yz}\\ \varepsilon_{zx}\\ \varepsilon_{xy}\end{bmatrix} = \frac{1}{E}\begin{bmatrix}1 & -\nu & -\nu & 0 & 0 & 0\\ -\nu & 1 & -\nu & 0 & 0 & 0\\ -\nu & -\nu & 1 & 0 & 0 & 0\\ 0 & 0 & 0 & 1+\nu & 0 & 0\\ 0 & 0 & 0 & 0 & 1+\nu & 0\\ 0 & 0 & 0 & 0 & 0 & 1+\nu\end{bmatrix}\begin{bmatrix}\sigma_{xx}\\ 0\\ 0\\ 0\\ 0\\ 0\end{bmatrix} \quad (5.9)$$

The modulus of elasticity in tension, also known as Young's modulus *E*, is the ratio of stress to strain on the loading plane along the loading direction,

$$E = \frac{\sigma_{xx}}{\varepsilon_{xx}} \quad (5.10)$$

Common sense (and the 2nd Law of Thermodynamics) indicates that a material under uniaxial tension must elongate in length. Therefore the Young's modulus *E* is required to be non-negative for all materials, $E > 0$.

A rod-like specimen subjected to uniaxial tension will exhibit some shrinkage in the lateral direction for most materials. The ratio of lateral strain and axial strain is defined as Poisson's ratio ν,

$$\nu = -\frac{\varepsilon_{yy}}{\varepsilon_{xx}} \quad (5.11)$$

The Poisson ratio for most metals falls between 0.25 and 0.35. Rubber has a Poisson ratio close to 0.5 and is therefore almost incompressible. Theoretical materials with a Poisson ratio of exactly 0.5 are truly incompressible, since the sum of all their strains leads to a zero volume change. Cork, on the other hand, has a Poisson ratio close to zero. This makes cork function well as a bottle stopper, since an axially-loaded cork will not swell laterally to resist bottle insertion.

The Poisson's ratio is bounded by two theoretical limits: it must be greater than -1, and less than or equal to 0.5,

$$-1 < \nu \leq \frac{1}{2} \quad (5.12)$$

The proof for this stems from the fact that *E*, *G*, and *K* are all positive and mutually dependent. However, it is rare to encounter engineering materials with negative Poisson ratios. Most materials will fall in the range,

$$0 \leq \nu \leq \frac{1}{2} \quad (5.13)$$

4.2.2.3. Transformation of *G*, *K* in *E*, *v*

The relationships between these 4 elastic constants are given by,

$$E = \frac{9KG}{3K+G} \quad (5.14)$$

$$\nu = \frac{3K-2G}{6K+2G} \quad (5.15)$$

Hence, the values of the elastic bulk modulus, *K*, and the shear strength, *G*, were transformed in Young's modulus and Poisson's ratio, and the values are displayed in the next table, Table 6.

Table 7 – Parameters for sand resistance

K (MPa)	30
G (MPa)	11.25
E (MPa)	33
v	0.33

4.2.3. INITIAL CONDITIONS

After defining the model's geometry and generating the mesh, the *Initial conditions* are going to be established. As it can be seen in Fig. 34 the phreatic level is situated on the top of the model. It can be also noted that a *closed flow boundary was specified* in the bottom and side boundaries to restrict the water flow only to the model's dimensions.

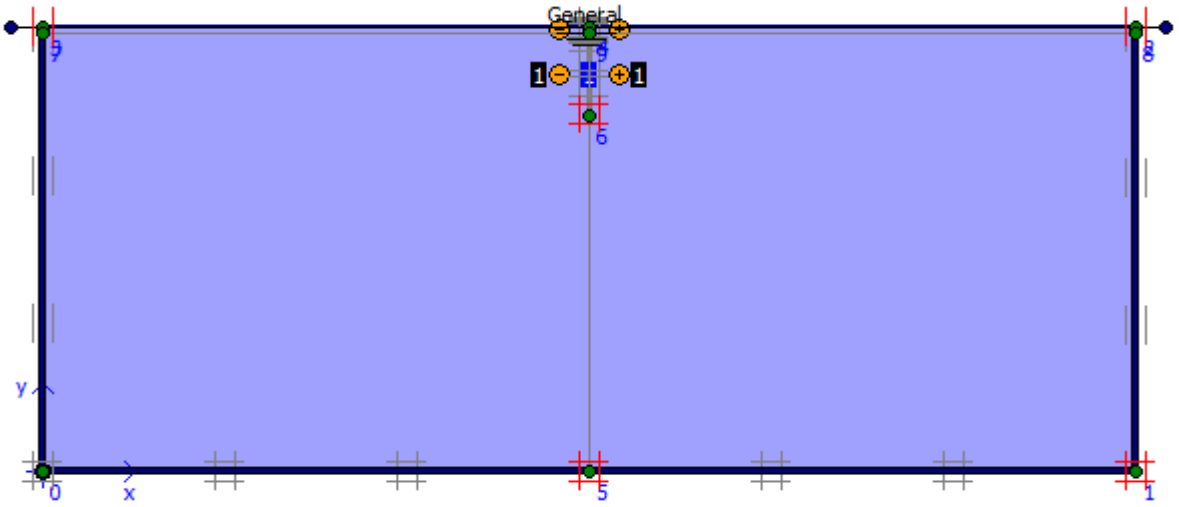

Fig. 34 – Initial water conditions of the model

After generating the initial pore pressures by means of the phreatic level, one has to generate the initial stresses. In Benmebarek et al. (2005)'s study it was assumed that the ratio of effective vertical stress at rest is 0.5, or K_0 = 0.5, and that is what's going to be input in PLAXIS. Once the initial stresses are generated, the model is ready to be calculated.

4.2.4. CALCULATION

Next step is calculating the model. This is done by specifying 14 different phases. The first one is a gravity loading phase, where the soil consolidates; in the other phases the water level rises in the upstream part of the model. In each groundwater rising phase the hydraulic time-dependent program, PLAXFLOW, is used, and the upstream water level takes 1 day to rise in each phase, but the time variation was proven not to have much influence in the final results. In Fig. 35 it can be seen the

PLAXFLOW input in the ultimate phase, where the limit values are reached, of the case where ϕ = 40º, ψ/ϕ = 1 and δ/ϕ = 1. The rupture phase is the final phase, when the water level variation is so great that the soil fails in the downstream next to the wall.

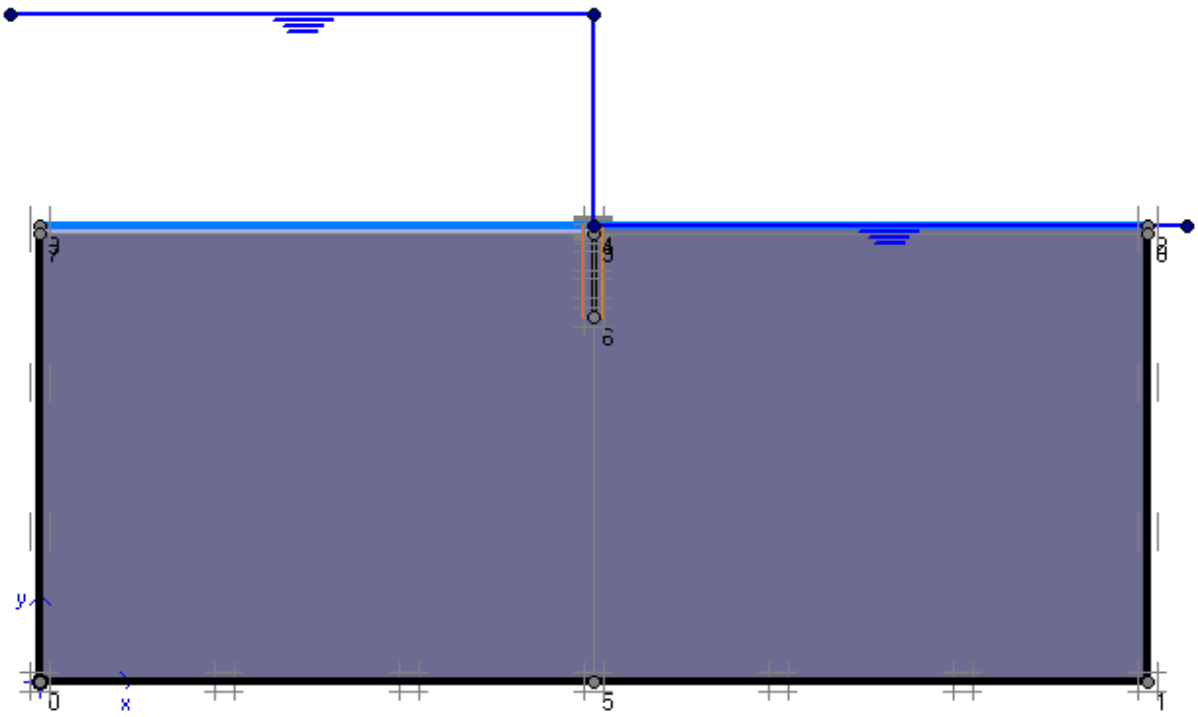

Fig. 35 - PLAXFLOW input in the rupture phase of the case where ϕ = 40º, ψ/ϕ = 1 and δ/ϕ = 1

It can be observed that the groundwater level rising was all made by means of the modification of the water level line, which is not always the best choice as it is going to be explained in what follows.

After a lot of time spent and a lot of attempts, nothing seemed to result in good values, or at least, similar to the ones obtained by Benmebarek et al. (2005) The same always happened: a point of the chosen grid, the one next to the sheet pile in the bottom of the excavation, plastified before the rupture by heaving or boiling could occur, as it can be seen in Fig. 36, so it has resulted in an error that took some time to overcome. It could be guessed that there was some kind of numerical error related to the software, but none of the ways to correct it seemed to work. The first attempts to overcome this error, without getting to any good result were the following:

- refine the grid close to the wall;
- include more clusters in the model, next to the wall, instead of the basic two, and try to input phreatic levels in each cluster, instead of a global one;
- increase the time of the water table rising phases.

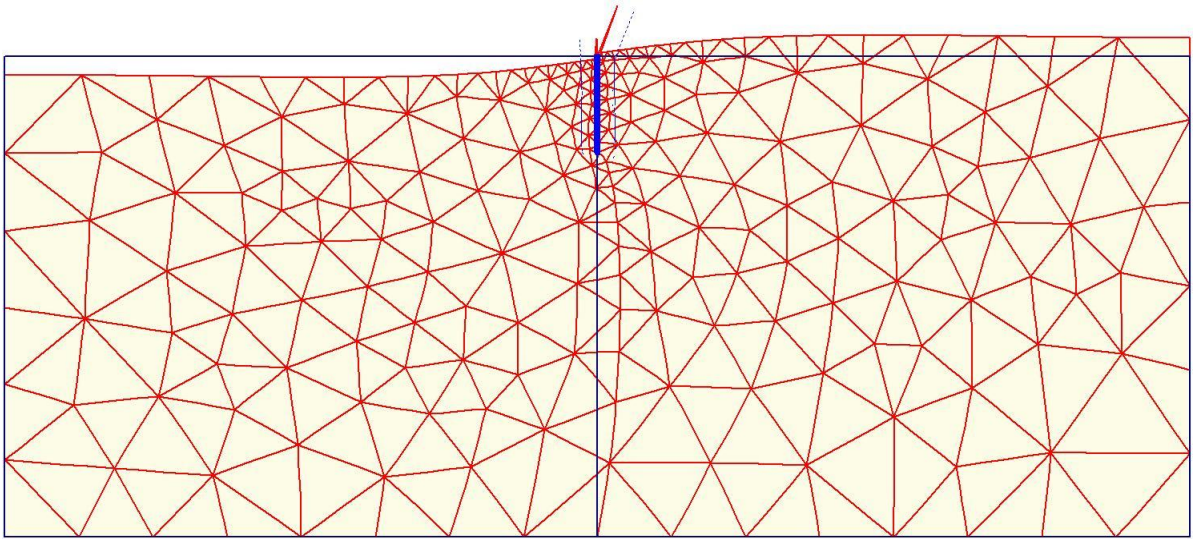

Fig. 36 – Rupture of the model not caused by heaving or boiling

In the end, and after several attempts, it was agreed that the best way to attain good results was to include an elastic material, with the same elastic properties of the sand considered in the model, in an extra cluster of small thickness at the bottom of the excavation. This way, the upper point could not plastify, and the calculation would proceed as it was planned. However, even after these modifications, the results did not seem to be the same as the ones obtained in the referred paper. Therefore, a numerical approach was attempted: it was noticed that the number of iterations was limited to 60. When this number was increased to 100, the results were outstanding. The next figure, Fig. 37, shows the output of the shear strength of the mechanism capture when ϕ = 35º, δ/ϕ = 2/3, ψ/ϕ = 1/2 and H/D = 3.0, the same as Fig.11, but using PLAXIS.

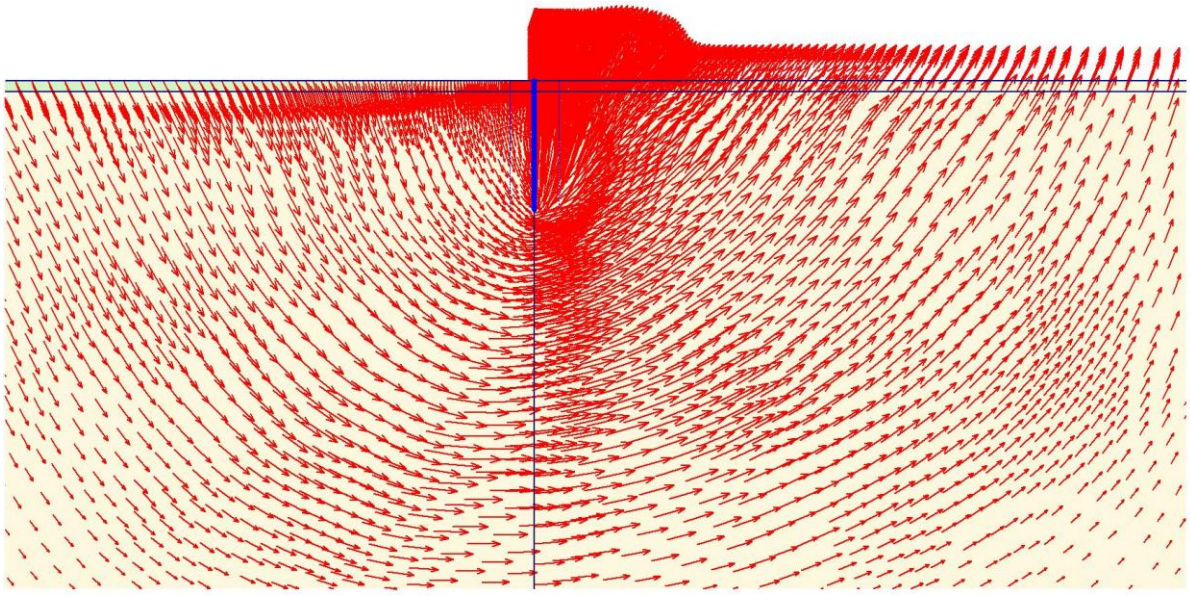

Fig. 37 – Displacements in failure of the model when ϕ = 35º, δ/ϕ = 2/3, ψ/ϕ = 1/2 and H/D = 3.0

As it can be observed in the Fig. 37, the failure by bulk heave, with the conditions said above, is triangular, and there is a localized rupture, which corroborates the Benmebarek et al. (2005)'s paper, in some part. An example of a failure by bulk heave in a rectangular prism form is showed in Fig. 38, where ϕ = 35º, δ/ϕ = 2/3, ψ/ϕ = 1/2 and H/D = 3.0and it is equivalent to the paper too. In these two

particular cases the failure was of the same type and occurred at the same H/D ratio than the described paper. However, that was not always the case.

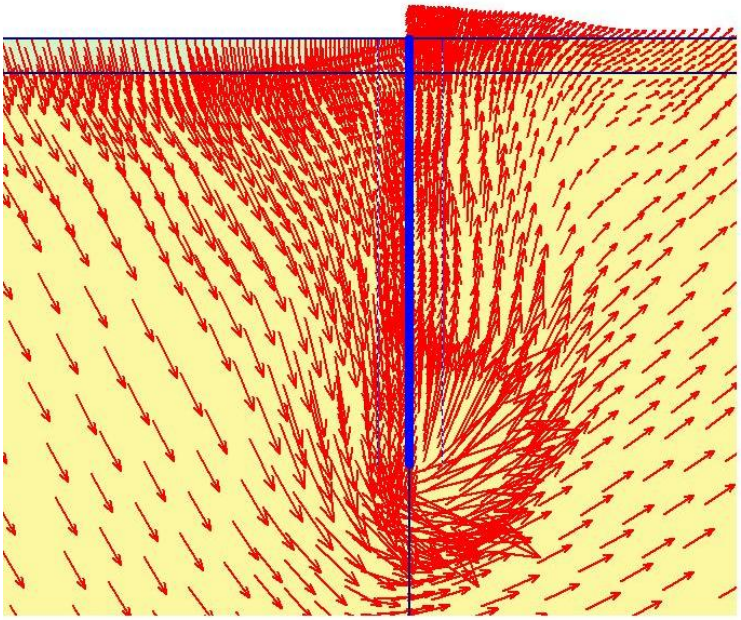

Fig. 38 – Zoom of the rupture when ϕ = 35º, δ/ϕ = 2/3, ψ/ϕ = 1/2 and H/D = 3.0

The shear strength outputs did not seem to be exactly the same, even when the *Total displacements* were. The reason for this occurrence is because PLAXIS does not show the maximum shear strain, like the other software FLAC^{-2D}, but only the shear strain at the moment of rupture, that is, at this level of the ultimate state, some elements may have dropped the strain level values. For that reason, the shear strength results are not presented in this part, but it can be seen in the *Total displacements* output the well designed soil prism. The next figure, Fig.38, shows the *Total displacements* at failure by hulk heave in a triangular shape of a sand that ϕ = 25º, δ/ϕ = 1/3, ψ/ϕ = 1 and H/D = 2.84.

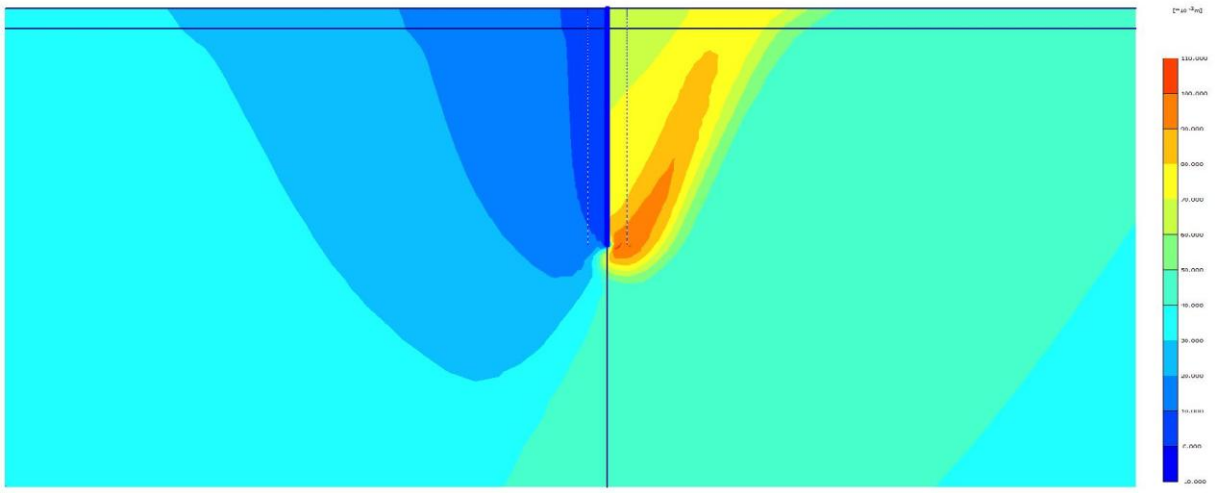

Fig. 39 – *Total displacements* when ϕ = 25º, δ/ϕ = 1/3, ψ/ϕ = 1 and H/D = 2.84

As it was said before, not always the results attained in PLAXIS were the same as the ones obtained by the program used by Benmebarek et al. (2005) In the next table it may be seen the comparison between the two programs in terms of the *H*/*D* ratio. The correct results, or in other words, the results which have the same *H*/*D* ratio and the same shape are shown with no background colour; the results having the same *H*/*D* ratio but apparently showing a different failure shape are displayed in yellow, and finally the results which neither have the same value neither the same shape are displayed in red.

Table 8 - Critical hydraulic head loss H/D for various governing parameters of ϕ, δ/ϕ and ψ/ϕ

δ/ϕ	ψ/ϕ	*H*/*D* limit				
		ϕ = 20º	ϕ = 25º	ϕ = 30º	ϕ = 35º	ϕ = 40º
0	0		1			2.8
	1/2			2.33		
	1	1				
1/3	0	2.67*		2.67		
	1/2					2.98**
	1		2.84**			
2/3	0	2.67				
	1/2				3**	
	1				3.04***	3***
1	0	2				
	1/2		2.87			
	1					2.67

It can be seen that results that have the relation ψ/ϕ equivalent to 0 are the ones more likely to end up with wrong results. It has to be noticed that is not easy to achieve accurate results: it takes a considerable time to calculate, because there is a large number of phases, and if some detail is forgotten, even in just one of the phases, the calculation should be repeated all over again with the corrected input parameters.

The cases where the results come out better are the ones where the δ/ϕ ratio is 2/3 and the range of friction angles are over 30º. In these cases the results come out perfect either in *H*/*D* ratio and in failure form as it can be seen in the next image, Fig. 40, which is the case where ϕ = 40º, δ/ϕ = 2/3 and ψ/ϕ = 1.

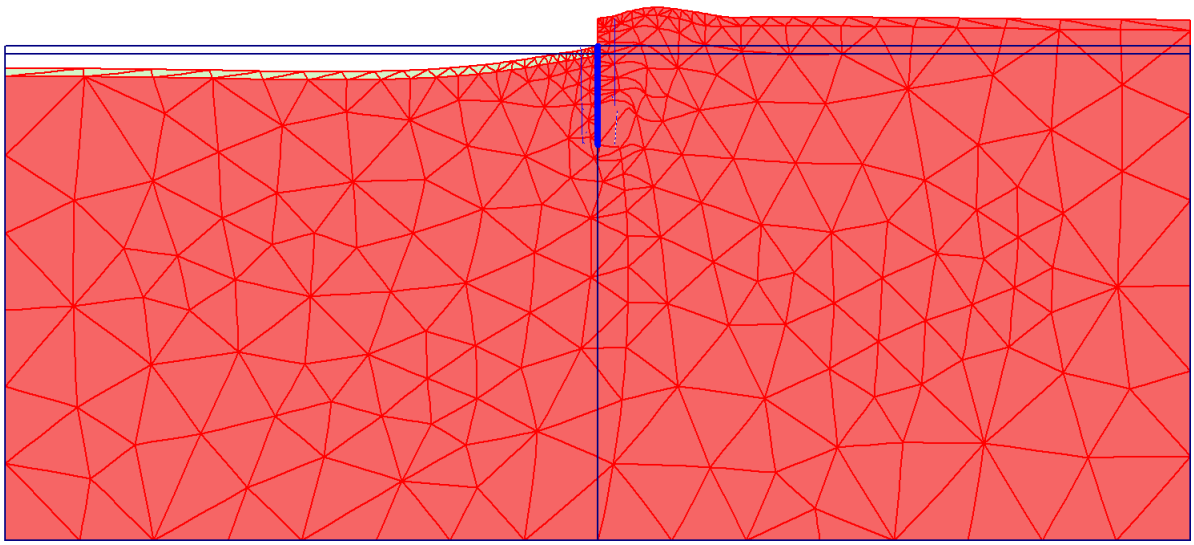

Fig. 40 – Failure when ϕ = 40º, δ/ϕ = 2/3 and ψ/ϕ= 1

In this rupture, it can be noted the triangular shape of the failure which shows that the calculation is indeed correct, and the results are acceptable.

On the other hand, when one analyses the output results of, for example, the case when ϕ = 40º, ψ/ϕ = 1 and δ/ϕ = 1, the results are pretty strange. Neither the H/D ratio is correct, neither the final form of the soil, as it can be seen in Fig.41.

The obtained value of 2.67 in the H/D ratio is not the same obtained by Benmebarek et al. (2005) and it can be observed in the output result that the final failure is not localized, but general, because it is noted a general heaving of the downstream part of the model.

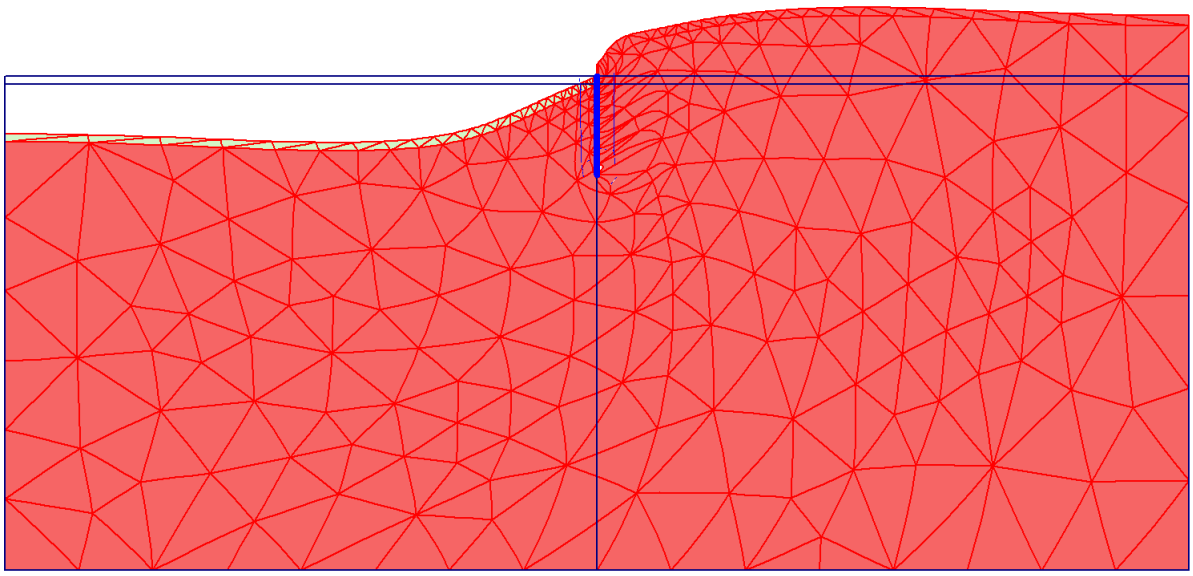

Fig. 41 – Failure when ϕ = 40º, ψ/ϕ = 1 and δ/ϕ = 1

4.2.5. NULL INTERFACE RATIO'S CASE STUDY

Another thing was noticed: when the interface ratio, δ/ϕ, was close to zero (0.01 is the lowest possible value in PLAXIS), to simulate the absence of interface friction, the results were really bad. In other words, when δ/ϕ was close to 0, PLAXIS did not seem to respect the *Total Fixities* option input in the wall in the beginning of the calculation, which supposedly does not let any kind of movement to happen. As it can be seen in Fig. 41 all movements of the wall are restrained by imposed fixities. What did occur, in the early phases, was a great movement of the wall that does not make any sense, since the sheet pile is allegedly fixed, and therefore such results could never be produced. In Fig. 43 the *Deformed mesh* of the case with $\delta/\phi = 0$, $\psi/\phi = 0$ and $\phi = 25^{o}$ can be observed.

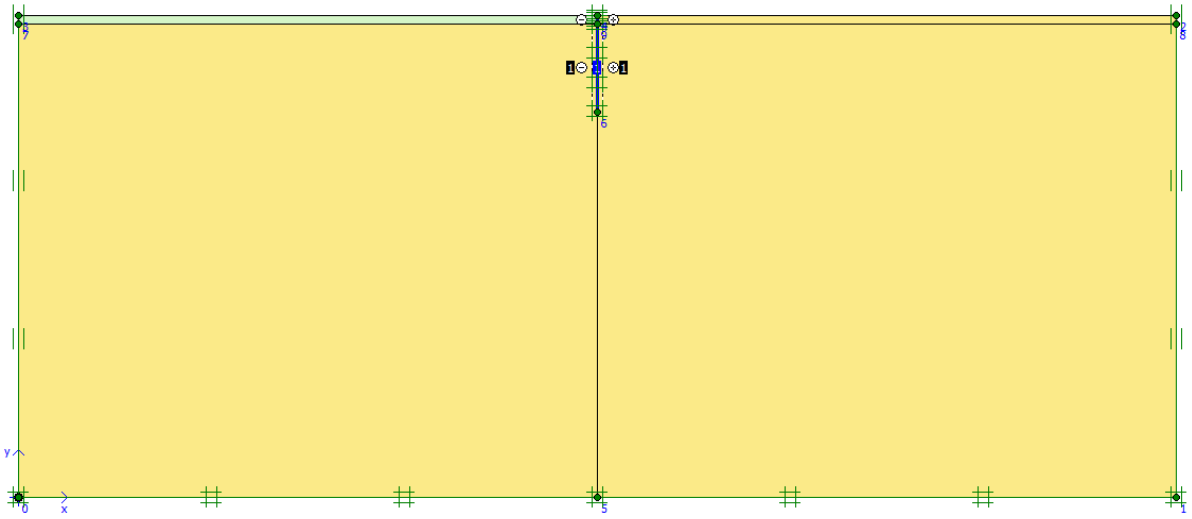

Fig. 42 – Geometry of the model with the applied fixities

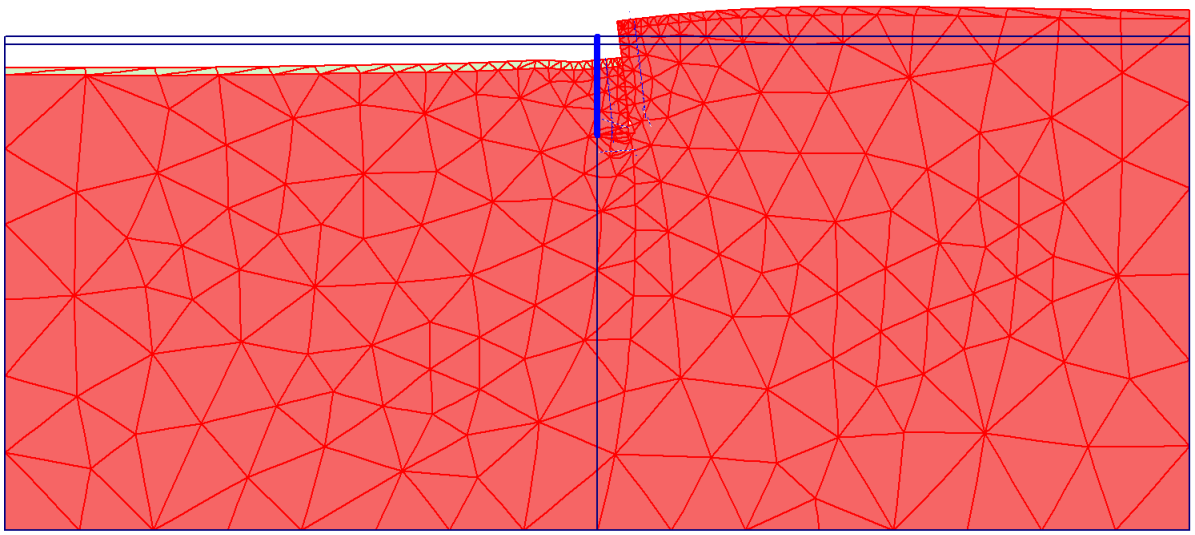

Fig. 43 – Rupture of the model

As it can be seen in this example the wall moves, making the soil to collapse in a strange form, which is not the wanted one. In other words, this type of displacements does not give any type of knowledge about bottom failure because all of the analysis is supposed to be with a fixed wall, so only the soil can have displacements. Obviously, the results are not the expected ones, and a whole variety of possible solutions were tried but with no success. One of the attempted solutions was not to include the

interfaces on the wall as usual, to simulate the δ/ϕ equivalent to zero. The result was even worse because the soil failed with a H/D ratio of just 1.2.

4.2.6. CONCLUSIONS

After closely studying the seepage failure of sand within a cofferdam with PLAXIS and PLAXFLOW, some conclusions can be taken.

It is not easy to obtain fine results with these programs in this type of analysis. Even though the input data is correct and the model has the proper dimensions, the final result is not always the expected one, because some errors may occur and a lot of time was spent trying to fix them.

The use of the complementary program, PLAXFLOW, to input the hydraulic time-dependent data, it is not always very simple to use. One has to be patient and perseverant in order to achieve proper results, because otherwise it can be a very frustrating task.

It was proved in this part of the work, that indeed the critical head loss against failure by seepage flow depends on the soil friction angle, and the interface friction angle. On the other hand, it could not be proven that all the values of the H/D ratio were right, because not all the attained values from PLAXIS were very accurate. All the number of phases were the same with the same groundwater variation, only changing the final water head for each case, and even so, the final results were not always very good.

Some results were fairly correct, with a perfectly defined failure prism, and the right H/D ratio of failure, but others were completely nonsense, with a H/D ratio of 1 and a very strange failure shape.

The causes of these discrepancies are not clear. Some possible intervening factors may be:

- the elements used in PLAXIS are different from the one used in Benmebarek et al. (2005). While this one is rectangular, the other one is triangular;
- it is not stated in Benmebarek et al. (2005)'s paper the amount of time used to rise the groundwater level and that can be a possible cause for not all the results being the wanted ones;
- it is not clear if the soil-structure interface model employed in both programs is fully equivalent. Since most divergent results between the two programs correspond to extremes of the interface friction values the detailed definition and operation of the interface elements in both programs might be a root cause of the observed discrepancies.

4.3. REPRODUCTION OF PHYSICAL MODELS IN NUMERICAL MODELS

After studying Marsland (1953)'s paper closely, it was decided to make a comparison between this article and the Benmebarek et al. (2005)'s. Both papers study failure in strutted sheeted excavations in non-cohesive soils due to seepage water. The big difference is that the first one is a real physical model at a small scale and the last one is a numerical analysis using a finite element software. Therefore, an analysis between this two investigations should be a good way to see if the modern technologies can reproduce well the real cases, or if they are even better than the physical models. After this, a more extensive analysis will be made to try to reproduce the same physical model in an alternate software to, once more, analyse the results, and compare the non-uniform site conditions.

4.3.1. HOMOGENEOUS SAND COMPARISON

In this comparison only the part of the homogeneous sands will be studied, since Benmabarek et al's study does not analyse models with different sand layers.

There are several problems to make this comparison because in Marsland (1953)'s paper the specification of sand properties is not done in a way that is directly comparable with the elasto-plastic Mohr-Coulomb parameters employed by Benmebarek et al. (2005).

Although the parameters of the soils of the two papers are different, one thing can be said: in Benmebarek et al. (2005)'s paper the ratio *H*/*D*, ratio between the ground water head and the wall penetration, is in a range between 2.63 and 3.16. This range encompasses a whole variety of friction angles, from 20º to 40º; dilation angles with ψ/ϕ equivalent to 0, 1/2 and 1; and interface angles with δ/ϕ equivalent to 0, 1/3, 2/3 and 1. On the other hand, when one looks at Marsland (1953)'s article, although the parameters are not the same, the same type of *H*/*D* ratio calculation can be made.

Since in Benmebarek et al. (2005)'s investigation, no excavation width is considered, it will be only compared the single wall case. In Marsland (1953)'s paper, as it was said before, the study was made for two types of sand: homogeneous loose sand with a porosity, *n*, of 42%, and a critical gradient for flotation, i_c equal to 0.97; and homogeneous dense sand with a porosity, *n*, of 37%, and a critical gradient for flotation, i_c equal to 1.05. In each case the *H*/*D* ratio was calculated to see if the data was reasonable, and the values appear in Tables 8 and 9.

Table 9 – Failure head in homogeneous loose sand

Failure Head in homogeneous loose sand			
Details Cofferdam	D1 Penetration (cm)	Experimental failure head (Hc) (cm)	H/D
Single Wall	2.5	10	4.00
	5.1	18	3.53
	7.6	23.9	3.14
		Mean	3.56

Table 10 – Failure head in homogeneous dense sand

Failure Head in homogeneous dense sand			
Details Cofferdam	D1 Penetration	Experimental failure head (Hc)	H/D
Single Wall	2.5	15.5	6.20
	5.1	24.7	4.84
	7.6	36.5	4.80
		Mean	5.28

When analysing the attained results, it was noticed that the values are not very similar to the ones obtained by Benmebarek et al. (2005), or in other words, the data is almost never in the range between 2.63 and 3.16. On the contrary, the values obtained with the physical models are almost always above

that range. Therefore, either the sand in the physical models has some parameters that are outside the range of those employed in the numerical calculations, or the numerical model does not represent effectively the real conditions in the physical model. A combination of these two explanations might be more reasonable, because the level of stress at the small scale models is far below that explored in the numerical studies. At very low stresses the curvature of the Mohr Coulomb failure envelope is important and, if approximated by a tangent value, would result in very high friction angles, above those explored numerically. A similar argument can be made for dilatancy. Therefore it is likely that a non-linear strength envelope will be needed to reproduce correctly both types of results.

Finally, it can be noted that the results attained by the numerical procedures are in this case more conservative than the numerical ones, which means that programs can be indeed used, without much concerns in this type of analysis, and are a good way of preventing accidents, so it can be said that they are a safer option.

4.3.2. PHYSICAL MODEL'S REPRODUCTION IN PLAXIS

In this part of the investigation the physical models studied in Marsland (1953)'s paper are going to be reproduced in a geotechnical FEM software. Once again, the parameters and geometry are input by the same sequence as before: geometry of the model, materials, initial conditions, calculations and output, so only parts of this sequence different than previous will be explained.

4.3.2.1. Materials

There are only two sands used in Marsland (1953)'s investigation, which are the *Ham river* and the *Leighton Buzzard*, both of them catalogued in Bolton (1986)'s paper. In this paper, the obtained sand's data is given in terms of d_{60}, d_{10}, e_{min}, e_{max} and ϕ'_{crit}, and this parameters have to be transformed to obtain input values for the material models in Plaxis. The obtained data of these two sands may be seen in Table 10, in which *p'* is the mean effective stress, and because this is a small model, 30 kN/m^2 was thought as a good value for *p'*.

Table 11 – Characteristics of the sands

Name	d_{60} (mm)	d_{10} (mm)	e_{min}	e_{max}	ϕ'_{crit} (º)	p' (kN/m²)
Leighton Buzzard	0.85	0.65	0.49	0.79	35	30
Ham River	0.25	0.16	0.59	0.92	33	30

As it was said before, these values have to be converted in other parameters so they can be input in FEM software. The first case studied was the *Effect of a single fine layer in homogeneous coarse sand bed*. As it was previously described, the porosity of the basic material, Leighton Buzzard sand, is 41.5%, and the porosity of the constituent material of the fine layer, Ham River sand, is 44%. With these site parameters, the current voids ratio, *e*, can be determined with the relation,

$$e = n/(1-n) \quad (5.16).$$

After this, also the relative density can be calculated by the expression,

$$I_D = \frac{e_{max}-e}{e_{max}-e_{min}} \quad (5.17),$$

where the e_{max} and e_{min} are, respectively, the maximum and minimum void ratios measured in laboratory.

In Bolton (1986)'s paper, after a series of calculations, it was found out that the maximum dilation angle, ψ_{max}, was a function of a relative dilatancy index, I_R, according to the expression,

$$I_R = I_D(10 - \ln p') - 1 \quad (5.18)$$

Finally, the relation between ψ_{max} and I_R is given by the next expression, and the results (obtained using a mean stress value p' = 30 kPa as indicated in the previous table), are displayed in Table 11.

$$0.8\psi_{max} = 5I_R \Leftrightarrow \psi_{max} = \frac{5}{0.8} I_R \quad (5.19)$$

Table 12 - relation between ψ_{max} and I_R

Fine layer in homogeneous course sand					
Parameter	n	e	I_D	I_R	ψ_{max} (º)
Leighton Buzzard	0.415	0.71	0.27	0.77	4.83
Ham River	0.44	0.79	0.41	1.69	10.53

4.3.3. HOMOGENEOUS CASE

Now, these material characteristics can finally be input in PLAXIS. The first model considered was the homogeneous case with an excavation width of 15.2 cm and a wall penetration of 7.6 cm, and a step by step procedure will be explained.

Firstly, the model has to be drawn. Only half of the model will be analysed, because it is symmetrical. As it was said before, the pile tip is 15.2 cm above the model base, the excavation is 15.2 cm wide, so only 7.6 cm will be represented. The wall penetration is 7.6 cm and the sand level outside the cofferdam was maintained at 38 cm above the pile tips, or 53.2 cm above the hard stratum. With the purpose of not having confinement problems the model has a total width of 52.6 cm at the base.

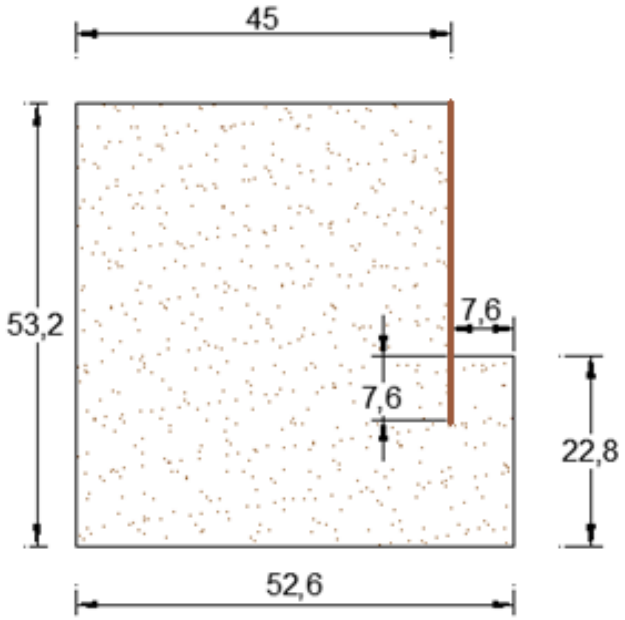

Fig. 44 – Model geometry

After all the model is drawn, the material parameters must be inserted. As it was calculated in Bolton (1986)'s paper the Ham River sand has a ϕ = 33º, and a ψ_{max} = 10.53º. The specific weight was a common one for sands, γ_{sat} = 20 kN/m^2, and the permeability was considered 47.5 cm/min, as in the non-homogeneous cases. Because nothing was said about the Young's module, Poisson's ratio and interface angle, these values were considered 33000 kPa and 0.33 for the first two. For the interface angle, the starting value was 0 and then it was raised.

In this model the ground water level is on top of the soil, which means that the ground water head is constant and equal to 53.2 cm. Then, in the excavation, the water level will be lowered until failure occurs by water flow.

When this experiment, firstly was made by the usual way, considering a lowering using the phreatic level feature in PLAXIS, it was noticed that when the calculation was done the phreatic level was not constant outside the cofferdam as it was in the experiments Therefore, boundary conditions had to be input manually to make sure the water level was constant. This has a major problem, which is taking a lot more time calculating the water conditions in PLAXFLOW, and that means that less numerical experiments could be done.

In the *Calculations* program two attempts were made:

- the first one, without using PLAXFLOW, only inputting boundary conditions in PLAXIS without time dependence. These boundary conditions are applied by inputting the same groundwater head in each border line of the model;
- the second one, using PLAXFLOW.

Actually, an unexpected result was obtained. In the first attempt, although the water flow field was correct and the displacements were high, the soil did not fail no matter what water head lowering was input or friction angle. The water flow and the displacements can be seen in Fig. 45. After this, a safety factor calculation was attempted to see how far from the rupture this model was but it was not possible because an error occurred.

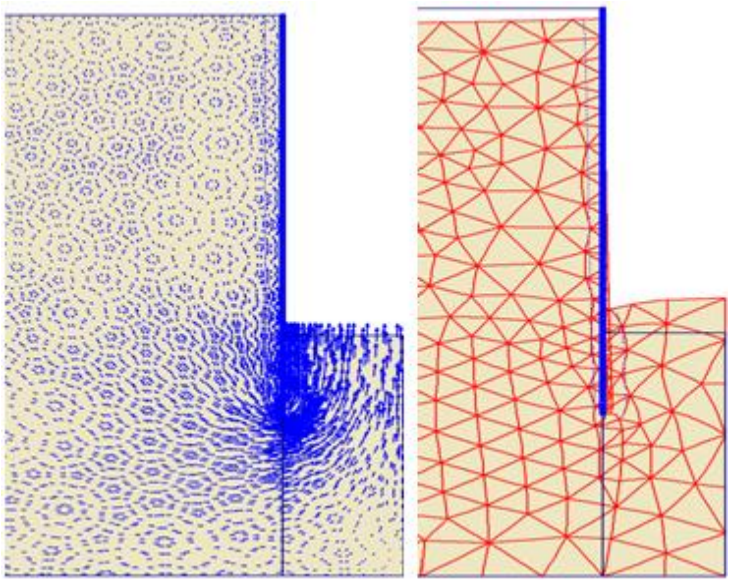

Fig. 45 – Water flow and soil displacements of the model

Then, when the second attempt was made another strange thing happened. In the end of the calculation of PLAXFLOW with only a lowering of 3.2 cm in one minute the displacements seemed to be large. So, a calculation of the safety factor was made using the *phi-c reduction* feature and weirdly it was 0.07 which seems a complete contradiction. This is utterly unusual, since it can be observed the water flow arrows going in the right direction, from the highest water head to the lowest, with a large concentration below the excavation bottom, which seems to be correct. Furthermore, the deformed mesh passes the idea that the soil is going to fail, but apparently it does not. In the next figure, Fig. 46, it can be seen what was explained before: the safety factor calculated by the *phi-c reduction* feature of PLAXIS, characterized by the $\sum M_{sf}$ parameter is equal to 0.07 and the previous phases are all OK, or in other words, they don't originate failure in the model, as it can be seen by the green checkmarks in the identification column. It would seem that the phi-c reduction feature does not work properly when a combined PLAXIS PLAXFLOW model is run.

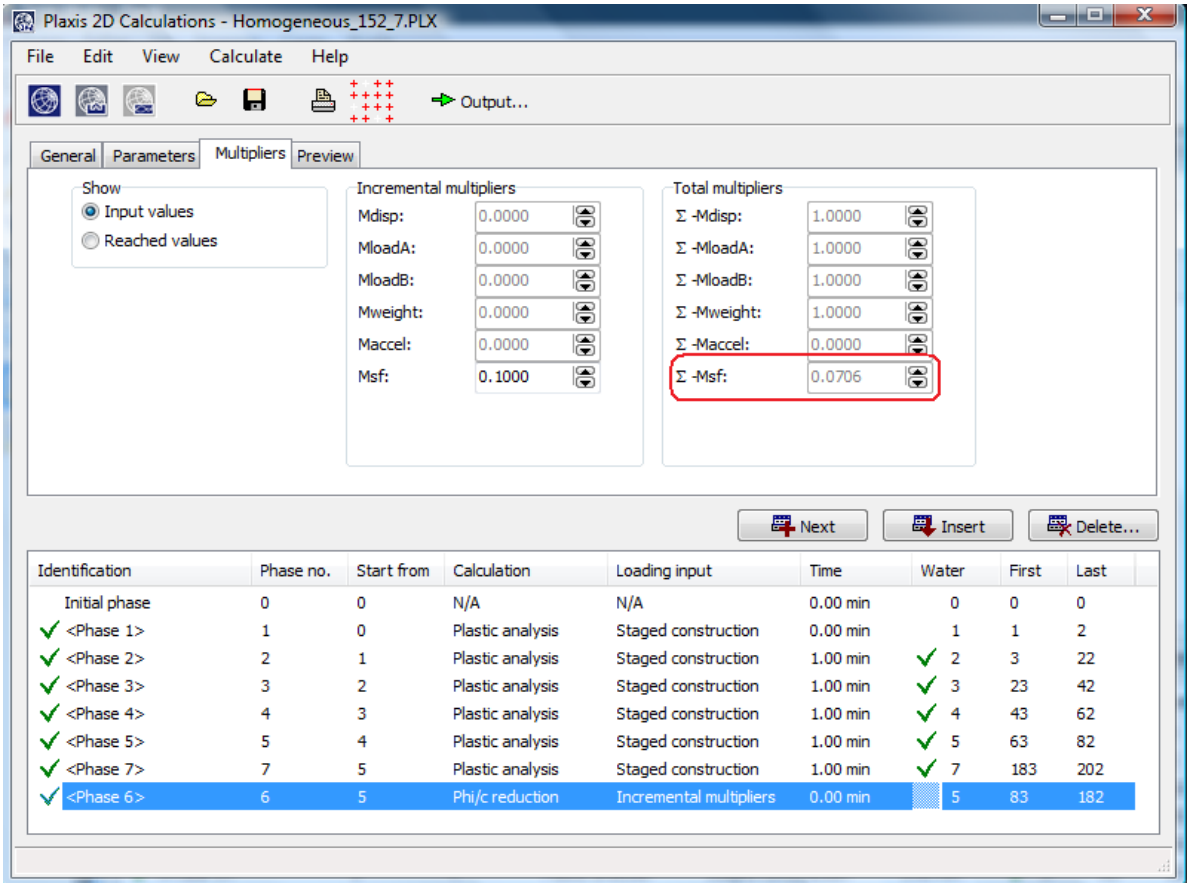

Fig. 46 – PLAXIS calculations program of the homogeneous case

4.3.4. NON-UNIFORM SITE CONDITIONS

The purpose of these experiments, as it was said before, was to compare the non-homogeneous site with the corresponding homogeneous site. In this particular work, once again, PLAXIS is going to be used to reproduce the physical models of Benmebarek et al. (2005)'s paper. The same geometric measures used in the homogeneous case were used in this investigation for comparison.

The same type of method was used: firstly not using PLAXFLOW, only inputting boundary conditions in various phases, and secondly using PLAXFLOW in phases of one minute each. The same thing happened again. No matter what Young's modulus, or friction angle, or dilation angle, or cohesion was input the result was always the same: when not using PLAXFLOW, and only inputting boundary conditions in PLAXIS, whatever the head difference that was input, the model never seemed to fail, even with a water head difference of 28.5 cm.

On the other hand, when the calculation was made using the time-dependent simulator, despite the numerous attempts for the soil to fail, this revealed itself a lengthy process and it was never achieved. However, when the displacements were analysed, they appeared to be very large, so a safety factor calculation was made, using the PLAXIS's *phi-c reduction* feature. Once again a strange thing happened, since the safety factor gave a final value of 0.09, which is impossible, and so, nothing could be concluded from this result.

A lot of attempts were made to try to solve this problem but all in vain. It was tried to lower the friction angle, the Young's modulus, the interface angle, to a plausible value of course, but nothing

seemed to work, and once again this was a lengthy process, which means that a lot of time was wasted in this part of the work. Finally, there was no other way than to leave this matter aside.

In Fig. 47 it can be observed, once again, that despite the model resistance is kept, the safety factor is way below one. This example presents the soil with a fine layer of fine soil positioned at a height of 7.6 cm above the bottom of the model.

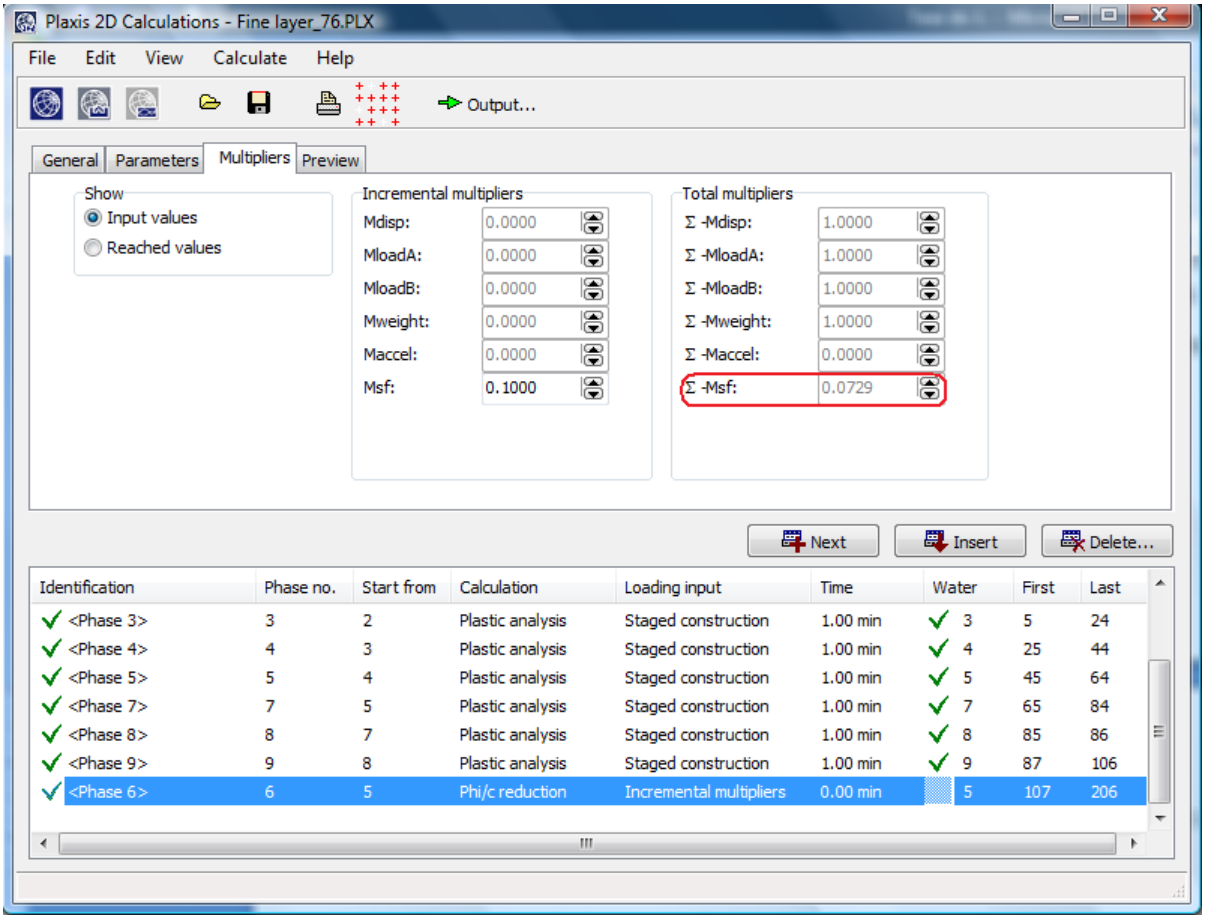

Fig. 47 – PLAXIS calculations program when the soil has a fine layer of fine soil positioned at a height of 7.6 cm above the bottom of the model.

Once again, the figure shows the water head lowering phases are all OK, with the green checkmarks, and the safety factor calculation is equal to 0.07, which is incomprehensible. The same thing happens with all the other fine layer cases.

4.3.5 Manual calculation

After getting to no conclusion about the reasons why the soil did not achieve failure in the PLAXIS calculation, it was decided to make a manual calculation of the safety factor to see if the predictions were right and the soil should have failed, or if , on the contrary, the software was right and the model was stable.

The hydraulic gradient, *i*, is defined as the ratio of the difference in hydrostatic potential between two points on a connecting flow line to the length of this flow path. If the hydraulic gradient is zero, hydrostatic groundwater conditions exist, no flow occurs and the pressure varies linearly with depth. The hydraulic gradient is calculated by the equation:

$$i = \frac{\Delta h_{total}}{N_e a} \quad (5.20)$$

Being Δh_{total} the total difference in hydrostatic potential, between upstream and downstream, N_e the number of equipotential lines between upstream and downstream, and a the distance between two equipotential lines measured in the flux lines.

In the next figure it can be seen a volume of soil in a hydrodynamic condition. The water flow is vertical and it moves upwards.

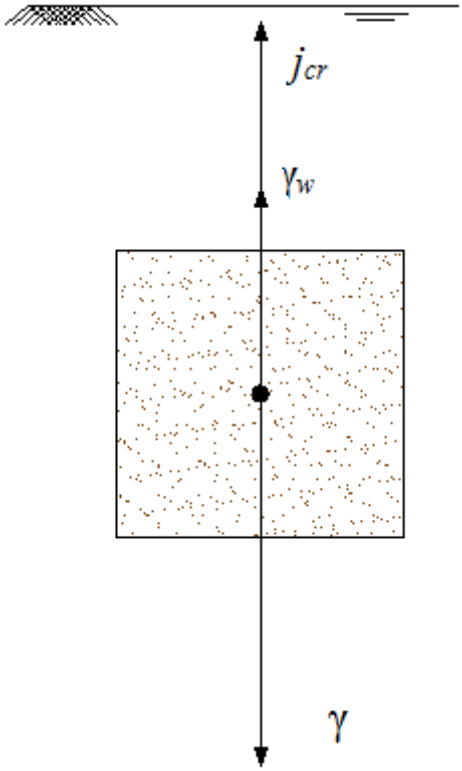

Fig. 48 – Volume of soil in a hydrodynamic condition

As it can be seen, the weight of the soil is couter balanced by the water momentum and the seepage force per unit volume. In this specific situation the water momentum and the seepage force are equal to the soil weight, and this is called critical situation and the respective hydraulic gradient is called the critical hydraulic gradient, i_{cr}.

Therefore from the equation

$$i_{cr}\gamma_w + \gamma_w = \gamma \quad (5.21)$$

results

$$i_{cr} = \frac{\gamma - \gamma_w}{\gamma_w} = \frac{\gamma'}{\gamma_w} \quad (5.22)$$

The critical situation represents a condition where the water forces balance the gravity forces, so the effective stress gets cancelled and failure occurs.

The majority of the authors considers more correct to calculate the safety factor of the heaving condition by the ratio of the submerged weight, *W'*, and the sum of the seepage forces, *J*, which is given by the equation,

$$SF = \frac{W'}{J} = \frac{\gamma' V}{i_{mean} \gamma_w V} = \frac{i_{cr}}{i_{mean}} \quad (5.23)$$

being the i_{mean}, the mean hydraulic gradient of the amount of potentially heaved soil.

4.3.6. HOMOGENEOUS CASE

As it was said, the results in PLAXIS were not the expected ones, so a manual calculation will be done to see what effectively should have happened: if the soil should have failed in those conditions or not.

Using only PLAXFLOW, it is easy to get the equipotential lines of the model using the *Groundwater head* mode in the *Output* program. In Fig. 49 it is represented a model of the homogeneous case, with an excavation width of 15.2 cm and a wall penetration of 7.6 cm, explained before. The geometric dimensions represented in the Fig. 48 are in millimetres, because it was easier to input such a small model in those units. In this specific phase, the total difference in hydrostatical potential is 232 mm.

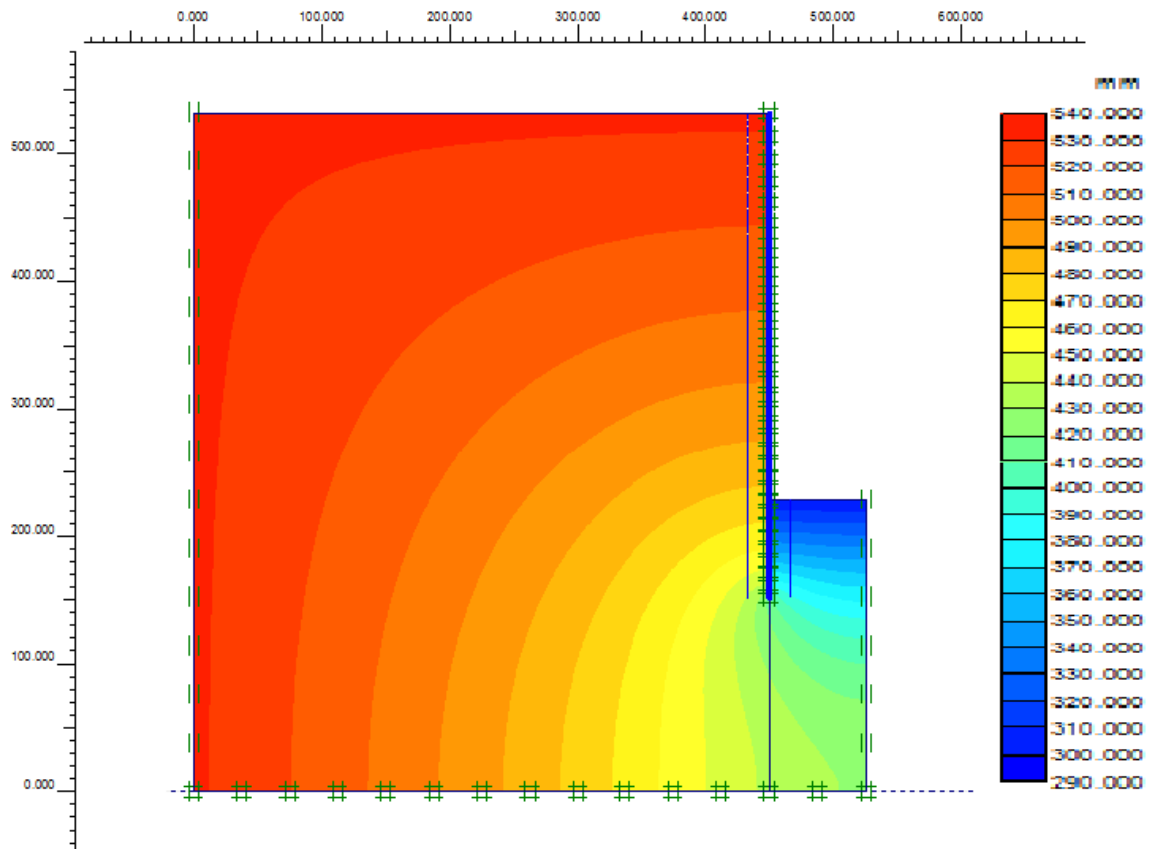

Fig. 49 – Equipotential lines of the homogeneous case

Now, the value of the critical hydraulic gradient, i_{cr}, is easy to calculate, since the specific weight of the water, γ_w, was considered 10 kN/m^3 in the software, and the soil unit weight below phreatic level, $\gamma_{sat,}$ is 20 kN/m^3, so the i_{cr} is equal to the unit.

On the other hand, the calculation of the i_{mean} is a bit more complex, but since it is only to have a general view of the problem nothing will be completely accurate, because the calculation of the safety factor is not the issue, but only to see if it is higher or lower than the unit.

Since the distances between the equipotencial lines next to the wall, on the excavation side, are approximately the same, it will be measured one random distance of those lines in that part and the calculation will be made. Furthermore, the lines are almost horizontal which makes easier the measurement of those distances. These distances are presented in the next table, Table 12.

Table 13 – Parameters for the calculation of the i_{mean} of the homogeneous case

Δh_{total} (mm)	232
N_e	24
a (mm)	8

Therefore the i_{mean} will be,

$$i_{mean} = \frac{\Delta h_{total}}{N_e a} = \frac{232}{24 \times 8} = \frac{232}{192} = 1.2 \quad (5.24)$$

and the safety factor will be,

$$SF = \frac{i_{cr}}{i_{mean}} = \frac{1}{1.2} = 0.83 \quad (5.25)$$

This result means that the model should have indeed failed for this difference of hydrostatical potential, so is not understandable why it does not.

4.3.7. FINE LAYER IN AN HOMOGENEOUS MASS

In this part, the process of manually calculating the safety factor of the previously studied models continues. This time it is going to be studied the non-homogeneous cases, more specifically the case where a fine horizontal layer of very fine soil is inside a mass of homogeneous coarse soil.

4.3.7.1. Height of the layer: 7.6 cm

In Fig. 50 it can be seen the equipotential lines attained by PLAXFLOW, which are used for the manual calculation. In this case the difference of hydraulic potential is higher, 302 mm, and even so, in PLAXIS's calculation, the rupture of the soil did not happen. The data for the manual calculation of the safety factor is in Table 13. The height of the layer in this case is 7.6 cm above the bottom of the model.

Table 14 - Parameters for the calculation of the i_{mean} of the fine layer case when the height of the layer is 7.6 cm

Δh_{total} (mm)	302
N_e	16
a (mm)	14

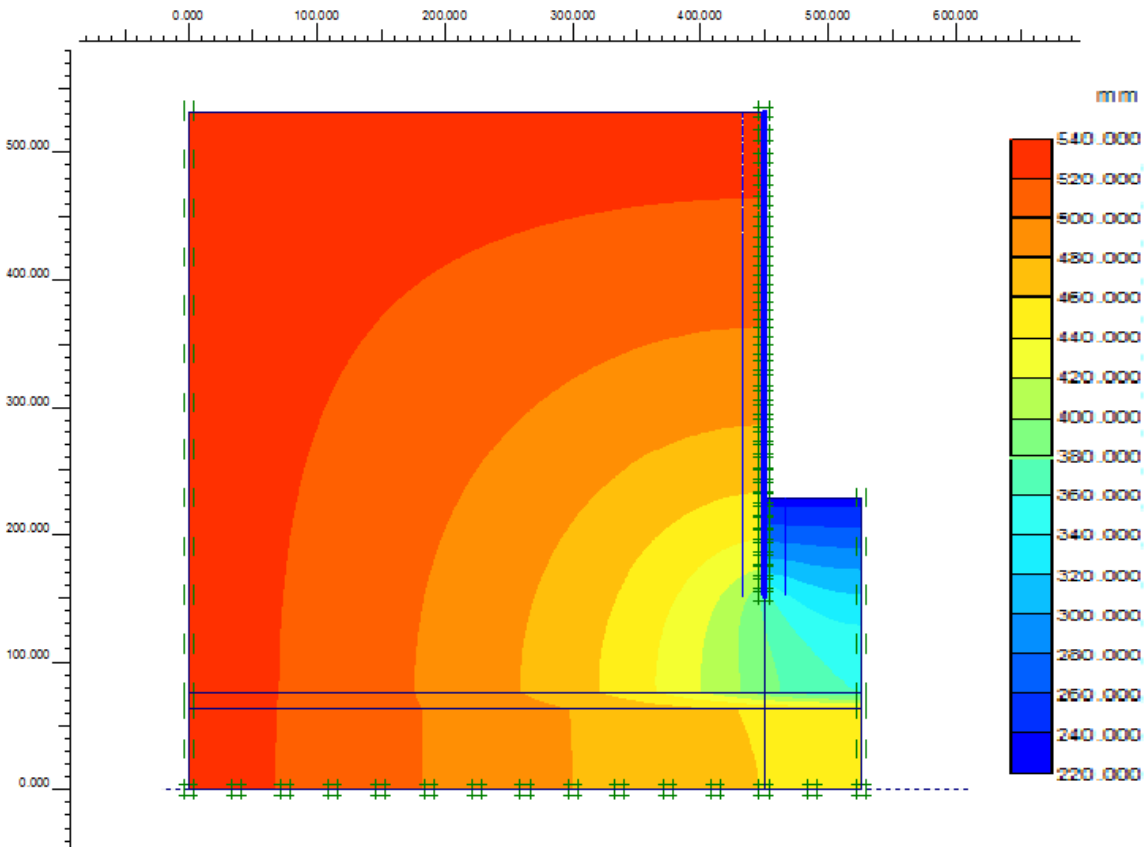

Fig. 50 - Equipotential lines of the fine layer case when the height of the layer is 7.6 cm

The hydraulic critical gradient, i_{cr}, is still the same, because the unit weight of the soil did not change, and the i_{mean} will be,

$$i_{mean} = \frac{\Delta h_{total}}{N_e a} = \frac{302}{16 \times 14} = \frac{302}{224} = 1.35 \quad (5.26)$$

and the safety factor,

$$SF = \frac{i_{cr}}{i_{mean}} = \frac{1}{1.35} = 0.74 \quad (5.27)$$

Once again, the safety factor lies below the unit, which means that the model should have failed when the lowering of the ground water head was happening in the excavation. Even though the safety factor calculated by PLAXIS was also below one, the fact is that the rupture did not happen as it should have.

4.3.7.2. Height of the layer: 3.8 cm

The same calculation will be done for the case when the fine layer of fine soil is located 3.8 cm above the bottom of model. In Marsland (1953)'s paper the failure of the model occurs with a difference of hydraulic potential of 175 mm. In this case, the calculation was made for a difference of 232 mm.

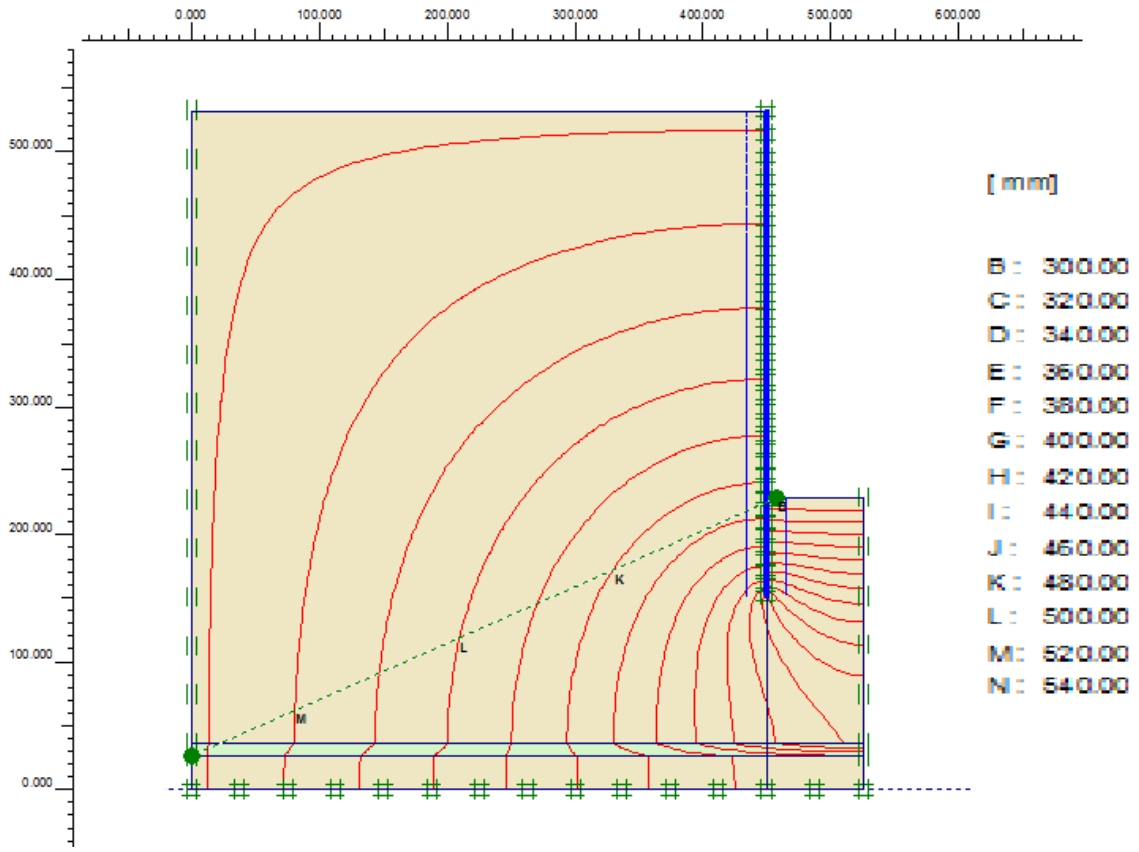

Fig. 51 - Equipotential lines of the fine layer case when the height of the layer is 3.8 cm

In Fig. 51 it can be seen the equipotential lines of the model explained before. As it can be observed in the legend, the line represented by the letter *B*, at the bottom of the excavation, has a hydraulic potential of 300 mm, while the outside of the excavation, on the top, has a groundwater head of 532 mm. Once more, the i_{cr} is equal to one and the i_{mean} will be calculated next with the obtained data of Fig. 50.

Table 15 - Parameters for the calculation of the i_{mean} of the fine layer case when the height of the layer is 3.8 cm

Δh_{total} (mm)	232
N_e	24
a (mm)	8

With this data, the i_{mean} is ready to be obtained, so,

$$i_{mean} = \frac{\Delta h_{total}}{N_e a} = \frac{232}{24 \times 8} = \frac{232}{192} = 1.21 \quad (5.28)$$

and the safety factor,

$$SF = \frac{i_{cr}}{i_{mean}} = \frac{1}{1.21} = 0.83 \quad (5.29)$$

As it was predictable, the safety factor is lower than 1 which means that the soil should have failed in the process of the ground water lowering in the excavation. This was predicted by the *phi-c reduction* feature, despite the previous phases did not originate rupture in the model.

4.3.7.3. Height of the layer: 9 cm

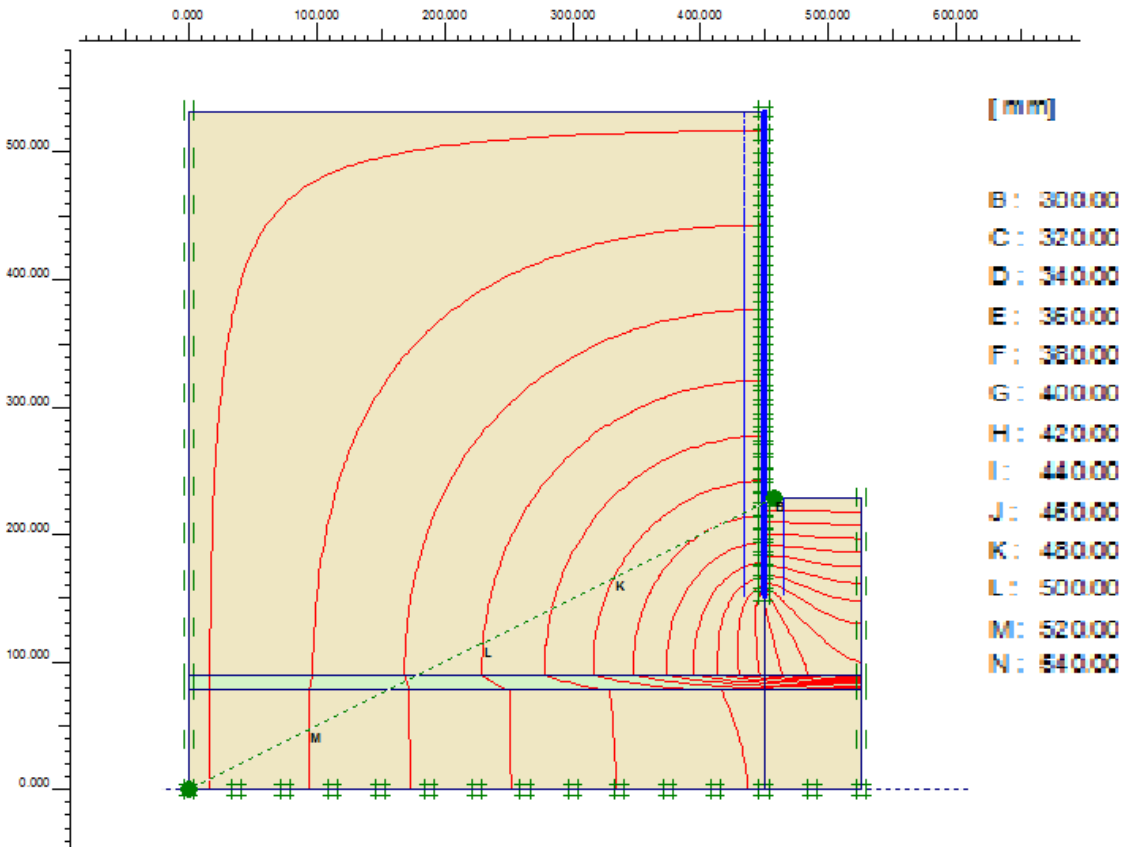

Fig. 52 - Equipotential lines of the fine layer case when the height of the layer is 3.8 cm

Table 16 - Parameters for the calculation of the i_{mean} of the fine layer case when the height of the layer is 9 cm

Δh_{total} (mm)	232
N_e	24
a (mm)	8

With the data acquired from the figure and the tables above, it can now be done the same procedure as before. Knowing that the i_{cr} is always the same, with the value of 1, the next step is the calculation of the i_{mean}, obtained by the next equation,

$$i_{mean} = \frac{\Delta h_{total}}{N_e a} = \frac{232}{24 \times 8} = \frac{232}{192} = 1.21 \quad (5.30)$$

and the safety factor,

$$SF = \frac{i_{cr}}{i_{mean}} = \frac{1}{1.21} = 0.83 \quad (5.31)$$

The same thing happened with this case: PLAXIS's safety factor calculation was right in obtaining a value below one, although in the previous steps failure did not occur.

4.3.7.4. Conclusions

The study of model experiments to analyse the influence of seepage in sands is not an easy task. It is very hard to work without specified material properties, so one has to input some characteristics with plausible values, but without really knowing if they are really correct.

There are a whole range of plausible explanations for this problem, and some of them are going to be nominated:

- the type of soils used in Marsland (1953)'s investigation was not the same characterized in Bolton (1986)'s article;
- the input data in the software is not correct, because only a few parameters were given or could be obtained in Bolton (1986)'s paper;
- the program probably has an error, because it is very strange to attain a safety factor lower than the unit and still not have soil rupture.

5

CONCLUSIONS

After the various analysis and comparisons made in the previous chapters, the main conclusions are going to be presented in this part.

Regarding the part of the undrained excavation in soft soils, it was studied the influence of the ratio of the depth to the width, the thickness of the soft soil layer between the excavation base and the hard stratum. This part was accomplished with a significant success, since the use of PLAXIS revealed even better results than the ones made by other software. It was effectively proven that the stability of this type of excavations is deeply connected to the parameters stated above. However, it was also observed that although the interface angle of the wall was not so significant, as the other parameters, in the final value of the safety factor, that influence is not so negligible as to be disregarded. In terms of attaining the value of the safety factor, PLAXIS revealed to be very powerful, and because its *mesh generator* is so easy to use, the mesh can be easily refined wherever it is necessary and, consequently, more reliable data is obtained. In the study of the safety factor it was concluded, as in previous literature, that when the depth of the wall is null, the normalized value of the safety factor, N_c, increases almost linearly with the relation H/B. On the other hand, one important issue was observed. In previous literature, it was stated that to obtain good results in 2D base stability using FEM the horizontal distance from the wall to the outer boundary has to be at least 2 times the height of the wall, and this statement was proven insufficient, because, actually, the volume of displaced soil in the upstream part of the wall is related to the thickness of the soft soil layer existent between the pile tip, and the hard stratum. A formula to set up that distance has been proposed to summarise the observations made in this respect.

In the part concerning the deep excavation in sands subjected to seepage forces the results were not always satisfactory. Comparison with precedenting numerical analysis was good only for a restricted set of parameters. For certain specific conditions, for example, when the friction angle was higher than 30º and the interface ratio, δ/ϕ, was equal to 2/3 the results were outstanding with a very well defined failure prism.

An attempt was made to reproduce physical models of sands subject to seepage forces in PLAXIS. The models required a more complex set of boundary conditions and the combination of PLAXFLOW and PLAXIS for their correct specification. The lack of important data regarding the original sand's characteristics made difficult to choose the right input values for the model. Although the manual calculations using general definitions about soil stability always resulted in soil failure, the results obtained using PLAXIS were hard to conciliate with this. Despite the soil never appearing to fail in the program calculation, the safety factor calculations revealed a very different result, since it was always lower than the unit and therefore suggesting that the model should have ruptured.

In conclusion, PLAXIS is a very powerful geotechnical tool, but when used with PLAXFLOW for the analysis of coupled flow-deformation problems a lot of caution and patience is needed, adding the fact that the final results have to be carefully analysed.

BIBLIOGRAPHY

Benmebarek, N., Benmebarek, S., Kastner, R., *Numerical studies of seepage failure of sand within a cofferdam*, Computers and Geotechnics, 32 (2005), 264–273

Bjerrum L, Eide O. *Stability of strutted excavations in clay*. Geotechnique 1956;6(1):32–47.

Bolton, M. D., *The strength and dilatancy of sands*, Géotechnique 36, Nº 1, 1986, 65-78

Davidenkoff RN, *Zur berechnung des hydraulischen grundbruches*, Wasserwirtschaft 1954(46):298–307.

Ergun, M. U., *Deep Excavations*, EJGE

Faheem, H., Cai, F., Ugai, K., Hagiwara, T., *Two-dimensional base stability of excavations in soft soils using FEM*, Computers and Geotechnincs, 30 (2003), 141–163

Gebreselassie, B., *German Recommendation for Excavation in Soft Soils (EAB, 2006)*

Kaiser, P. K., Hewitt, K. J., *The effect of groundwater flow on the stability and design of retained excavations*, Can. Geotech. J., Vol. 19, 1982

Lam, L., Fredlunda, D. G., Barbour, N. D. S. L., *Transient seepage model for saturated-unsaturated soil systems: a geotechnical engineering approach*, Can. Geotech. J. Vol. 24, 1987

Marsland, A., *Model experiments to study the influence of seepage on the stability of a sheeted excavation in sand*, Géotechnique, Volume 3, Issue 6, 06/03/1953, 223 –241

Matos Fernandes, M., *Mecânica dos Solos*, FEUP, Porto, 2006

McNamee J. *Seepage into a sheeted excavation*, Géotechnique, The Institution of Civil Engineers, London 1949;4(1):229–41.

German recommendations of the Committee for Waterfront Structures Harbours and Waterways (EAU 2004), Arbeitsausschu Ufereinfassungen der HTG e. V.

German recommendation for excavations in soft soils (EAB 2006)

Soubra A-H, Kastner R, Benmansour A, *Passive earth pressures in the presence of hydraulic gradients*. Géotechnique, The Institution of Civil Engineers, London 1999;3(49):319–30.

Tanaka, T., Kusaka, T., Nagai, S., Hirose, D., *Characteristics of Seepage Failure of Soil under Various Flow Conditions*, Proceedings of the Nineteenth International Offshore and Polar Engineering Conference, June 21-26, 2009, Osaka, Japan

Terzaghi K. *Theoretical soil mechanic*, 1943, New York: Wiley

Thansnanipan, N., Maung, A. W., Aye, Z. Z., Submaneewong , C., Boonyarak, T., *Construction of Diaphragm Wall for Basement Excavation Adjacent to Tunnels in Bangkok Subsoil*, International Symposium on Underground Excavation and Tunnelling, 2-4 February 2006, Bangkok, Thailand

Van Mieghem, J., Aerts, F., Thues, G.J.L., De Vlieger, H., Vandycke, S., *Building on Soft Soils*, Terra et Aqua, Nº 75, June 1999

Wudtke, R. H., *Failure Mechanisms of Hydraulic Heave at Excavations*, 19th European Young Geotechnical Engineers' Conference, 3-5 September 2008, Győr, Hungary